Central European University
Department of Mathematics and its Applications

Irena Matkovič

Tight and Fillable Contact Structures on Seifert Fibered Manifolds

Doctoral Thesis

Supervisor: Professor András Stipsicz

Budapest, 2018

I hereby declare:

- that the dissertation contains no materials accepted for any other degrees in any other institution, and
- that the dissertation contains no materials previously written and/or published by another person, except where appropriate acknowledgement is made in the form of bibliographical reference, etc.

Budapest, 10 April 2018 Irena Matkovič

Abstract

The fundamental question of contact topology is to classify contact structures. Since overtwisted structures respect homotopy principles, we restrict the question to tight structures, and among them to the fillable ones, which bound in symplectic or holomorphic category. First to be understood are prime atoroidal manifolds, which are either hyperbolic or small Seifert fibered.

This thesis deals with small Seifert fibered manifolds, which are obtained from circle bundles over the sphere by performing Dehn surgery along (at most) three of the fibers. For many of these manifolds, the complete classification is known, and all tight structures are also fillable. We review these results from various perspectives: convex decompositions along with contact surgery, the dual presentation by open books, and in Heegaard Floer theory by means of the Ozsváth-Szabó contact invariant. Our main focus are zero-twisting structures on small Seifert fibered spaces of the form $M(-1; r_1, r_2, r_3)$, which are special as they include non-fillable tight structures. We classify them by the Ozsváth-Szabó contact invariant and characterize which of them are (Stein) fillable. The crucial properties of these contact manifolds are the possibility to view the underlying manifold as the boundary of a negative definite plumbing and the planarity of the contact structures. For classification of tight structures, we use a specific description of Heegaard Floer homology by equivalence classes of characteristic cohomology elements on the bounded plumbing; we single out the elements which correspond to the contact invariants and give a contact interpretation to the equivalence relations between them. In order to characterize fillability, we study positive factorizations of the planar monodromy.

Math. Subj. Class. (2010): 57R17, 57R57, 57M50

Keywords: Seifert fibered manifolds, tight contact structures, (Stein) fillable contact structures, convex surface theory, contact surgery, open book decompositions, Ozsváth-Szabó contact invariant

Vse poti so večno stare,
vsak korak je večno nov.

All the ways are old forever,
every step is always new.

Kajetan Kovič

To those who went before me,
to those who have walked with me

– thanks and respect.

Contents

$$0 = \infty$$

1

Introduction

A *contact* 3*-manifold* is a smooth 3-manifold endowed with an additional geometric structure. The ultimate goal of contact topology is to understand (classify) contact manifolds, up to certain equivalence relations. For low dimensional topology such classifications are useful as the behavior of contact structures often reveals subtle properties of the underlying manifold, which are hidden to more algebraic methods. On the other hand, contact structures naturally arise as induced boundary structures on holomorphic and symplectic domains, and are thus essentially involved in various gluing constructions of 4-manifolds. When approaching them, we are usually trying to understand compatibly embedded submanifolds or we are looking at their dual counterpart, open book decompositions; whereas the gauge theory (in particular, Heegard Floer homology) enters the subject by providing obstructions for certain phenomena. Looking backwards, classification results then help us to understand what these (in spirit) analytical invariants actually see about manifolds.

At large, contact structures fall into two significantly different classes. Overtwisted structures are everywhere existing and homotopically classified [11]. Tight structures are geometric, they resemble some rigidity of complex manifolds [14]; they might bound in the symplectic category, in which case we say they are fillable. Therefore, the classification problem reduces to tight structures and in particular to the fillable ones. Furthermore, we usually stick to prime atoroidal manifolds; the first because tight contact structures respect connected sum decomposition of 3–manifolds [8], the second because an embedded essential torus is a known source of infinitely many non-isotopic tight structures [6]. Small Seifert fibered manifolds, beside hyperbolic ones, share these properties.

Seifert fibered manifolds borrow their name from their decomposition into disjoint simple closed curves (called fibers) such that each fiber has a tubular neighborhood which forms a standard fibered torus (that is, a solid torus foliated into the core and the curves of the same rational slope on all concentric tori). Throughout, we will think of them as circle bundles over a surface with isolated singular fibers, along which Dehn surgery is performed. This description directly

corresponds to a surgery diagram, and after applying inverse slam-dunks, also to the plumbings of disk bundles which the Seifert manifolds bound. Simplifying the drawings, these plumbings are given by weighted star-shaped graphs whose vertices are decorated by pairs recording the genus of the base and the Euler number of the corresponding disk bundle. In fact, all but the central vertex belong to disk bundles over the sphere and in this case, we omit 0 for the genus. Specially, by *small Seifert fibered space* we mean a Seifert fibration over the sphere S^2 with three singular fibers, standardly (after normalization by applying Rolfsen twists) given as $M(e_0; r_1, r_2, r_3)$ where $e_0 \in \mathbb{Z}$ and $r_i \in \mathbb{Q} \cap (0,1)$ with $r_1 \geq r_2 \geq r_3$. By reversing its orientation, we get $-M = M(-e_0 - 3; 1 - r_1, 1 - r_2, 1 - r_3)$. Regarding algebraic topology, we observe that a small Seifert fibered space M is a rational homology sphere if and only if $e(M) = e_0 + r_1 + r_2 + r_3 \neq 0$, and that the corresponding 4-dimensional plumbing is negative definite when $e(M) < 0$, and has $b_2^+ = 1$ when $e(M) > 0$. Finally, *L-spaces* (by definition, Heegaard Floer homology lens spaces) among Seifert fibered manifolds are geometrically characterized by the absence of transverse contact structures [51]. The restriction for small Seifert fibered spaces which are rational homology spheres, can simply be described in terms of the Seifert invariants: L-spaces are all manifolds with $e_0 \geq 0$ and with $e_0 \leq -3$, while for $e_0 = -1, -2$ some explicit numerical inequalities are imposed on the triple (r_1, r_2, r_3).

As the aim of this thesis is to present what is known about the classification of tight and fillable structures on small Seifert fibered spaces, we conclude the introduction by citing the existence results, due to Lisca and Stipsicz [52] for tight structures and due to Lecuona and Lisca [46] for the fillable ones. To have some tight structure, we need to avoid the one-parameter family of $(2n-1)$–surgeries on the torus knot $T_{2,2n+1}$ (equivalently, the manifolds which are orientation preserving diffeomorphic to $M(-1; \frac{1}{2}, \frac{n}{2n+1}, \frac{1}{2n+3})$ for some $n \in \mathbb{N}$). The manifolds of special type, which do not admit any fillable structure, are characterized as L-spaces for which $r_i + r_j < 1$ for all pairs of legs; this family of course contains the non-tight family listed previously. Roughly, classification of tight contact structures then arises from the comparison of bounds: the lower bound is obtained constructively by contact surgery complemented with the use of invariants, and for the upper bound convex surface theory is applied; whereas fillability can usually be proven only by exhibiting the appropriate filling, which in turn is most tractable by studying the supporting open books.

Chapter 2 Contact three-manifolds are introduced. We focus on constructive aspects, contact surgery along with convex decompositions, and supporting open books. The two example sections tackle contact structures on Seifert fibered spaces.

Chapter 3 After generalities of Heegaard Floer theory, we discuss its behavior in the presence of two special structures, when the underlying manifold arises as the boundary of a negative definite plumbing, and for contact manifolds. Example complements the presentation of Seifert fibered spaces from the previous chapter.

Chapter 4 The discussion is targeted at the classification of tight contact structures on small Seifert fibered spaces. The main subject are zero-twisting structures on $M(-1; r_1, r_2, r_3)$, and we approach them through the study of their Ozsváth-Szabó contact invariants. The first part is based on a yet unpublished note, the second part follows the article [54].

Chapter 5 The upshot is a characterization of fillability for tight contact manifolds discussed in the previous chapter. We analyze the supporting open books, specifically positive factorizations of their monodromy. The chapter covers the preprint [55].

2

Contact three-manifolds

A *contact structure* on a smooth oriented 3-manifold is a nowhere integrable 2-plane field $\xi \subset \mathrm{T}Y$; when it is positive cooriented, it is globally described as $\xi = \ker \alpha$ for some 1-form $\alpha \in \Omega^1(Y)$ which satisfies $\alpha \wedge \mathrm{d}\alpha > 0$. The 1-form is determined up to multiplication by a positive function $Y \to \mathbb{R}^+$, and hence endows the plane bundle with a conformal symplectic structure. The basic equivalence relation for pairs (Y, ξ) is given by a *contactomorphism* which is a diffeomorphism between the underlying manifolds $f : Y \to Y'$ whose differential connects the two contact structures $f_*(\xi) = \xi'$.

Locally, contact manifolds are homogeneous. According to Darboux's Theorem, around any point p in any contact manifold (Y, ξ) we can set a local chart U_p in which the contact structure $\xi|_{U_p}$ is described by the standard contact form of the 3-dimensional Euclidean space, $\alpha_{\mathrm{std}} = \mathrm{d}z + x\,\mathrm{d}y$.

Globally, we wish to classify contact structures up to contact isotopy. On compact 3-manifolds this is – according to Gray's Stability Theorem – the same as to determine the connected components of the space of contact structures. The underlying topological question is the classification of oriented 2–plane fields $\xi \in \Xi$ up to homotopy. Recall that $\pi_0(\Xi)$ can be identified with homotopy classes of maps $[Y, S^2]$, which can be through Pontryagin-Thom construction given by framed links in Y. Here a link up to oriented cobordism represents the class in $\mathrm{H}_1(Y; \mathbb{Z})$, equivalently the Spin$^{\mathrm{c}}$ structure $\mathbf{t}_\xi$, while the framing corresponds to the Hopf invariant as a 3–dimensional obstruction for homotopies between plane fields. So, the homotopy type is given by the pairs of the induced Spin$^{\mathrm{c}}$ structure $\mathbf{t}_\xi$ and the 3–dimensional invariant $d_3(\xi) \in \mathbb{Z}_{\mathrm{div}(c_1(\mathbf{t}_\xi))}$ where $\mathrm{div}(c_1(\mathbf{t}_\xi))$ is the divisibility of $c_1(\mathbf{t}_\xi) \in \mathrm{H}^2(Y; \mathbb{Z})$. In fact, there is a subclass of *overtwisted* contact structures which – according to Eliashberg [11] – completely respects homotopy principles; the flexibility is ensured by inclusion of certain submanifold (as specified in Section 2.1.1). All other structures are called *tight*. Their classification is much more subtle – they tend to contain geometric information. Particularly, due to adjunction type inequalities [14], there are only finitely many homology classes realized as Euler classes of tight contact structures, also they are (in general) not

distinguished by homotopic invariants [48].

In one direction, the rigidity is explained by the theorem of Eliashberg [12] and Gromov, saying that contact manifolds which are null-cobordant in the holomorphic or symplectic category (in the sense below), are tight. The notions of fillability are from the 4-dimensional viewpoint complemented by convexity; they are all weaker versions of geometrically convex domains. A contact manifold (Y, ξ) is *Stein fillable* when Y is given as Levi pseudoconvex boundary of a compact complex manifold (X, J) with ξ equal to the complex tangent bundle $\mathrm{T}^{\mathbb{C}}Y = \mathrm{T}Y \cap J(\mathrm{T}Y)$. The plurisubharmonic (exhaustion) function $\phi : X \to \mathbb{R}$ endows a Stein domain with an exact symplectic form $\omega_\phi = -\mathrm{d}\mathrm{d}^{\mathbb{C}}\phi$ whose primitive (contraction by the gradient field) gives the contact form $\alpha = -\mathrm{d}^{\mathbb{C}}\phi$. A contact manifold (Y, ξ) is *(strongly) symplectically fillable* when it bounds a compact symplectic domain (X, ω) which is exact along the boundary with the primitive which defines the contact structure ξ (in other words, when there is an outward pointing transverse Liouville field along the boundary). Finally, we say that (Y, ξ) is *weakly symplectically fillable* if Y bounds X and ω is a symplectic form for ξ. Stein fillability implies strong fillability, strong fillability implies weak fillability, but all the notions are distinct, as first observed by Ghiggini ([24]; on certain Brieskorn spheres, by the means of Heegaard Floer theory) and Eliashberg ([15]; on T^3, building on the work of Giroux), respectively. Still, they are all very restrictive: none of the overtwisted structures bound, and not all tight structures do. For the latter, the first examples were obtained by Etnyre and Honda [21]. More generally, we can talk about a *symplectic cobordism*, a compact symplectic manifold (W, ω) whose boundary ∂W can be written as a disjoint union of two components Y_- and Y_+, along which ω is exact with its primitive defining a negative and a positive contact form on Y_- and Y_+, respectively. Finally, a symplectic cobordism from (Y, ξ) to $\emptyset$ is called a *cap*. In contrast to the fillings, existence of caps is non-restrictive [16, 18], however their topological and symplectic properties restrain the contact manifold [47].

2.1 Special submanifolds

Similarly to the usual topological setting, we can extract a lot of information out of embedded submanifolds, and here also out of the way their position relates to the neighboring contact planes. There are some preferred positions of knots and surfaces in contact 3-manifolds with prescribed neighborhoods, which is especially important for construction of manifolds.

2.1.1 Legendrian knots

Knots can arise in two special positions: as integral submanifolds (Legendrian), which are interesting as cores for surgeries (Weinstein handles), or with inherited contact structure (transverse), which come into play as bindings of open books.

A knot $K \subset (Y, \xi)$ is called *Legendrian* if it is everywhere tangent to ξ, that is $\mathrm{T}K < \xi$ or equivalently $\alpha(\mathrm{T}K) = 0$. Every knot can be $\mathcal{C}^0$-approximated by a Legendrian one, but equivalence given by Legendrian isotopy is much finer than the smooth isotopy of knots. Particularly, it contains information about neighboring contact structure. The preferred framing of a Legendrian knot is given by the direction positively transverse to the contact planes, it is called the *contact framing*. The number describing its relative twisting with respect to some fixed framing $\mathcal{F}$ is denoted by $\mathrm{tw}(K, \mathcal{F})$, and in the null-homologous case with $\mathcal{F}$ being the Seifert framing it is called the *Thurston-Bennequin invariant* $\mathrm{tb}(K)$. On the other hand, the *rotation number* $\mathrm{rot}_\Sigma(K)$ gives the winding of the knot tangents in a trivialization of the contact structure over a Seifert surface Σ, or in other words, the relative Euler class of the contact structure over Σ (when $\mathrm{H}_2(Y; \mathbb{Z}) \neq 0$ it might depend on the relative homology class of the surface). Legendrian knots in the standard $(\mathbb{R}^3, \xi_{\mathrm{std}} = \ker(\mathrm{d}z + x\,\mathrm{d}y))$ are usually presented by their front projection to the yz-plane, whose characteristic feature are cusps in the place of vertical tangencies; from it the two invariants can be read off as $\mathrm{tb}(K) = \mathrm{writhe} - \frac{1}{2}\#\mathrm{cusps}$, and $\mathrm{rot}(K) = \frac{1}{2}(\#\text{down-cusps} - \#\text{up-cusps})$.

Dichotomy between overtwisted and tight contact structures is, by definition, based on the containment of an unknot with $\mathrm{tb} = 0$ in overtwisted structures, and its absence in the tight ones. Equivalently (as shown by Eliashberg [14]), tight contact structures can be characterized by satisfying the adjunction inequality $\mathrm{tb}_\Sigma(K) + |\mathrm{rot}_\Sigma(K)| \leq -\chi(\Sigma)$ for every Legendrian knot $K \subset (Y, \xi)$ and its Seifert surface Σ. Similarly, in tight contact manifold (Y, ξ) there is a genus bound $\langle c_1(\xi), [\Sigma] \rangle \leq \max\{0, -\chi(\Sigma)\}$ for closed oriented surfaces Σ.

Stabilization is a simple deformation of a Legendrian knot type, which is intimately connected to several other basic blocks of contact topology: bypasses from the point of view of convex surface theory, basic slices (and thickenings) in the convex decompositions, and positive Dehn twists in the monodromy factorizations of open books. It consists of a local twisting change: in the front projection (inside a Darboux chart) we replace a straight segment with a pair of upward or downward cusps, resulting in a negative K^- or positive K^+ stabilization of the Legendrian knot K. Hence, the invariants change to $\mathrm{tb}(K^\pm) = \mathrm{tb}(K) - 1$ and $\mathrm{rot}(K^\pm) = \mathrm{rot}(K) \pm 1$. A knot $K \subset (Y, \xi)$ is called *transverse* when it is positively transverse to the contact structure, that is $\alpha(\mathrm{T}K) > 0$. They appear as push-offs of Legendrian knots in the direction transverse to the contact structure. Since their Legendrian approximation is unique up to negative stabilizations [17], we think of their theory as a stable Legendrian theory.

2.1.2 Convex surfaces

Nonintegrability prevents surfaces from being tangent to the contact distribution. Therefore, contact planes always carve into an embedded surface. In the following, let Σ denote a compact oriented surface, possibly with Legendrian boundary.

Characterictic foliation Σ_ξ is a 1-dimensional singular foliation which integrates the line field arising in the intersection $\mathrm{T}\Sigma \cap \xi|_\Sigma$. If we write out the contact form $\alpha = \beta_t + f_t \,\mathrm{d}t$ in a vertical neighborhood of the surface $\Sigma \times \mathbb{R}_t$, it is given by $\ker \beta_0$. We say (in analogy with symplectic convexity) that Σ is *convex* if there is a transverse contact vector field V (such that $L_V \alpha = \lambda\alpha$ for a positive function λ) in its neighborhood, or equivalently, when Σ admits a vertically invariant neighborhood (in which $\alpha = \beta + f \,\mathrm{d}t$ with t-independet β and f). On a convex surface Σ a *dividing set* Γ_Σ is a non-empty set of (properly embedded) curves $\{p; V(p) \in \xi(p)\} = \{p; f(p) = 0\}$; notice that Γ_Σ is transverse to Σ_ξ, dividing Σ into alternating positive and negative regions $\Sigma_\pm = \{p; \pm \mathrm{d}\beta(p) > 0\}$. The convex placement of surfaces in contact 3-manifolds is generic (provided the twisting of boundary components is non-positive), their importance stems from the Giroux's Flexibility Theorem [33] which says that the germ of the surrounding contact structure can be discretized into their dividing set. In particular, Giroux's Criterion [33] gives a complete characterization of neighboring tightness in terms of the dividing set: Γ_Σ should contain no contractible components for $\Sigma \neq S^2$, and should be connected when $\Sigma = S^2$.

We present dividing sets and characteristic foliations on surfaces which are related to standardized neighborhoods of certain submanifolds [37].

1. *Boundary of the Darboux ball.* Since, according to Giroux, $\#\Gamma_{S^2} = 1$, the characteristic foliation on a convex sphere in tight ambient has two singularities and S^1-family of lines flowing between them. Explicitly, for $\alpha_{\mathrm{std}} = \mathrm{d}z + r^2 \,\mathrm{d}\varphi$, it is described by $(xz - y, yz + x, -x^2 - y^2)$ with $\Gamma_{S^2} = \{z = 0\}$.

2. *Overtwisted disk.* A contact structure in a neighborhood of an overtwisted disk Δ is described by $\alpha_{\mathrm{ot}} = r \sin r \,\mathrm{d}\varphi + \cos r \,\mathrm{d}z$. On $\Delta = \{z = 0, r \leq \pi\}$, the boundary $\partial\Delta$ with $\mathrm{tb}(\partial\Delta) = 0$ is a closed orbit of the characteristic foliation which has an elliptic singularity in the center; the two are separated by a single dividing circle.

3. *Boundary of the Legendrian standard neighborhood.* First, by Giroux's Criterion, the dividing set Γ_{T^2} on a convex torus in tight ambient consists of an even number of parallel homotopically essential curves; after identifying $T^2 \cong \mathbb{R}^2/\mathbb{Z}^2$, they are described by the boundary slope s. The characteristic foliation can be perturbed into S^1 family of closed curves of slope $r \neq s$, called Legendrian rulings, and the tangencies between dividing curves

are called Legendrian divides. Concretely, for the standard neighborhood $V^n_{\text{std}} = (S^1 \times D^2, \alpha = -\sin(2\pi n\vartheta)\,\mathrm{d}x + \cos(2\pi n\vartheta)\,\mathrm{d}y)$ of a Legendrian curve $S^1 \times 0$ with twisting $-n$, the boundary dividing curves are parallel to the contact framing; hence in the trivialization by the meridian (ϑ_0, x, y) and the longitude (ϑ, x_0, y_0) the slope equals $-\frac{1}{n}$.

4. *The collar neighborhood of the Legendrian boundary component.* As in the previous example we are in the standard Legendrian neighborhood V^n_{std}, but looking at the collar annulus $A = S^1 \times [0,1]$ bounded by the core Legendrian curve K. The characteristic foliation again consists of Legendrian rulings, circles parallel to the boundary, and as the contact planes twist along the knot, we alternatively hit dividing arcs and Legendrian divides which cross the annulus. In particular, $\mathrm{tw}(K, A) = -\frac{1}{2}\#(K \pitchfork \Gamma_A)$.

5. *Edge-rounding.* Looking at two annuli as above which intersect transversely at K, the dividing arcs appear alternatively along K. Concretely, if we align and orient them as $A_x = \{x = 0, 0 \le y \le 1\}$ with positive normal ∂_x and $A_y = \{y = 0, 0 \le x \le 1\}$ with positive normal ∂_y, then $\Gamma_{A_x} = \{\frac{2k}{4n}\} \times [0,1]$ and $\Gamma_{A_y} = \{\frac{2k-1}{4n}\} \times [0,1]$, respectively. After rounding the edge, the dividing arcs at the height $\frac{2k}{4n}$ get connected to the dividing arcs at $\frac{2k-1}{4n}$.

As we move a convex surface Σ inside (Y, ξ) we hit (according to Giroux, discrete) singular levels, at which the characteristic foliation changes by a bifurcation. In terms of dividing sets, Honda [37] has described an equivalent operation combinatorially. A *bypass* D is a half of an overtwisted disk attached to a convex surface Σ along a Legendrian arc α which intersects the dividing set Γ_Σ in three points; its boundary ∂D is the union of two Legendrian arcs $\alpha \cup \beta$ with $\mathrm{tw}(\alpha, D) = -1$ and $\mathrm{tw}(\beta, D) = 0$. We say that the bypass is positive or negative if such is the sign of the middle singularity on α. A *bypass attachment* isotopes the convex surface Σ across a bypass disk to obtain a new convex surface Σ', locally changing the dividing curves as depicted: 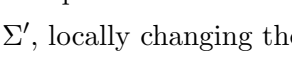 .

Finding a bypass usually consists of finding a bounded convex surface with a boundary-parallel dividing arc (which intersects same boundary component twice and cuts off a disk without further dividing curves); it embraces one singularity, and flowing out along characteristic foliation we cover a disk with Legendrian boundary. Particular case of this is the Imbalance Principle, used in tight ambient for a convex annulus with different (and negative) twisting number at the two boundary components. Finally, from the knot perspective [20], adding a bypass increases the twisting of the Legendrian curve, more, a bypass disk cuts off a stabilization disk from a Seifert surface (studying a local picture we can see that half-elliptic singularities of the characteristic foliation occur at cusps).

2.2 Cut and paste

Understanding of compatibly embedded submanifolds is essential to perform constructive techniques known from smooth manifold theory. These are based on understanding some simple basic blocks and the study of how they are glued together.

2.2.1 Convex decomposition

The main idea is to cut a contact manifold along properly embedded convex surfaces to obtain simpler pieces (and eventually balls); if the initial structure was tight, all the pieces need to be tight as well. To cut along a chosen surface we only need flexibility, first to Legendrian realize the boundary curves, and then to perturb the surface into convex position. More interesting is the retrograde process, starting with tight pieces, how to glue them together to preserve tightness, and moreover, whether different gluings give us different results.

The fundamental result is Eliashberg's uniqueness of the tight contact structure on a ball B^3 [14], more precisely, a unique extension of the contact structure which induces connected dividing set on $S^2 = \partial B^3$ from the neighborhood of the sphere to the ball B^3. Further cases of particular interest are the simplest pieces with the toric boundary, that is $S^1 \times D^2$ and $T^2 \times I$ [37]. Throughout, we limit the vertical twisting of the contact structure around the embedded tori, requiring that there is no stack of convex tori on which the slope of dividing curves would change for more than π. We call such structures *appropriate*, and in particular case of $T^2 \times I$ *minimally twisting*.

Theorem 2.2.1 (Honda)**.** *Let $T^2 \times I$ have convex boundary with 2-component dividing curves of slopes $s(\Gamma_{T_1}) = -\frac{p}{q}$ with $p \geq q > 0$ and $\gcd(p, q) = 1$, and $s(\Gamma_{T_0}) = -1$. Then there are exactly $|(a_0 - 1)(a_1 - 1) \cdots (a_{k-1} - 1)(a_k)|$ tight minimal twisting contact structures on $T^2 \times I$, up to isotopy fixing the boundary, for $a_0, \ldots, a_k$ the coefficients of the continued fraction expansion of $-\frac{p}{q}$.*

We review the main ideas behind this theorem. The complete classification is based on the layering of $T^2 \times I$ into *basic slices*. A basic slice is $T^2 \times I$ with minimal twisting tight contact structure and convex boundaries whose 2-component dividing curves take, up to $\mathrm{SL}_2(\mathbb{Z})$-displacement, the slopes 0 and -1. For fixed boundary slopes, there are exactly two such contact manifolds, distinguished by the sign. Notable is the relation of the basic slices to the bypasses: a basic slice $(T^2 \times I, s_0 = 0, s_1 = -1)$ is the trace of the isotopy which a convex torus T, with $\#\Gamma_T = 2$ and $s(\Gamma_T) = 0$, describes when it is slid over a bypass attached to its front along a linear arc of slope $r, -\infty < r \leq -1$. The sign agrees with the sign of the bypass attached. The possible $\mathrm{SL}_2(\mathbb{Z})$-transformations are neatly presented by the Farey tessellation of the hyperbolic disk $\mathbb{H}$: its geodesics

connect exactly the pairs of boundary points which correspond to the pairs of vectors forming basis of $\mathbb{Z}^2$, hence the pairs of boundary slopes of a basic slice. In this language, having a convex torus with 2-component dividing curve of slope s, and a bypass attached to it along a Legendrian ruling curve of slope $r \neq s$, the other slope equals s', a point on the arc $[r, s] \subset \partial\mathbb{H}^2$ which is closest to r and connected to s.

Every contact $T^2 \times I$ can be sliced into basic slices, but not all sequences of basic slices are different, neither they are all tight. The continued fraction expansion of $-\frac{p}{q} = [a_0, \ldots, a_k]$ with $a_i > 1$ determines a minimal sequence of basic slices into which $(T^2 \times I, s_0 = -1, s_1 = -\frac{p}{q})$ factors. The boundary slopes of the factorization can be obtained in order by decreasing the last entry of the continued fraction. Any other slicing of this thickened torus is a subfactorization of the described one. In the case of the minimal factorization the glued together contact structure is tight regardless how the signs of basic slices are chosen, while in any refinement all subslices of a single basic slice from the minimal factorization should share the same sign (Gluing Lemma). Still, even in the minimal factorization, not all the slices are equal. This is a consequence of the fact that bypasses to which they correspond are not all attached with the same slope. Concretely, starting with the convex torus of slope -1, the bypasses for the zeroth continued fraction block, up to the boundary slope $-a_0 + 1$, are attached with slope ∞; the bypasses for the first continued fraction block, up to the boundary slope $[a_0, a_1 - 1]$, are attached with the slope $-a_0$; the bypasses for the second continued fraction block, up to the boundary slope $[a_0, a_1, a_2 - 1]$, are attached with the slope $[a_0, a_1]$, etc. The distinguished property of the slices which belong to the same continued fraction block is, that they can be shuffled within themselves without changing the glued-together structure.

A topologically assigned invariant of contact structures on manifolds with boundary is their *relative Euler class* $e(\xi, s) \in \mathrm{H}^2(Y, \partial Y; \mathbb{Z})$, relative to a non-zero section s of ξ along ∂Y. If Legendrian boundary of a convex embedded surface Σ is aligned with s, we can compute its evaluation on Σ as $\langle e(\xi, s), \Sigma\rangle = \chi(\Sigma_+) - \chi(\Sigma_-)$. In fact, since $\mathrm{H}_1(T^2 \times I; \mathbb{Z}) \cong \mathbb{Z}^2$, the evaluation on two annuli, interpolating between Legendrian rulings of two different slopes, completely determines the Euler class. What is more, the minimally twisting tight contact structures on $T^2 \times I$ with $\#\Gamma_{T_i} = 2$ and boundary slopes $s_0 = -1$ and $s_1 = -\frac{p}{q} < -1$ are classified by their relative Euler class, even less, by the value their relative Euler class takes at a horizontal annulus A with Legendrian boundary. Writing out

$$\begin{aligned}\langle e(\xi, s), [A]\rangle &= \mathrm{PD}(e(\xi, s)) \cdot [A] = \left(\textstyle\sum_{b \text{ basic slice}} \pm(v_1^b - v_0^b)\right) \begin{pmatrix} 0 & 1 \\ 1 & 0 \end{pmatrix} \begin{pmatrix} 1 \\ 0 \end{pmatrix} \\ &= \chi(A_+) - \chi(A_-)\end{aligned}$$

we observe that the dividing set on A consists of two arcs which cross from one

boundary to the other, and $p-1$ one-sided arcs which cut off (possibly nested) bypass disks. Concretely, for each ε-signed basic slice in the i^{th} continued fraction block there are as many ε-signed disk regions as the numerator of $[a_0,\dots,a_{i-1}]$, or 1 for $i=0$.

For the solid torus with convex boundary with $\#\Gamma_T = 2$ and $s(\Gamma_T) = -\frac{p}{q}$ for $p \geq q > 0$, the number of tight contact structures is the same as the number of tight minimally twisting contact structures on $T^2 \times I$ with slopes $s_0 = -1$ and $s_1 = -\frac{p}{q}$. We get them by gluing the toric annulus to the standard neighborhood of the Legendrian knot. Additionally, solid tori of any other boundary slope can be by a change of framing, multiplication by a Dehn twist, transformed into a unique one as above. In particular, the boundary of the standard neighborhood of the twisting $-n$ Legendrian curve has slope $-\frac{1}{n}$. Inside this neighborhood we can find tori of slope $-\frac{1}{m}$ for any $m > n$, and indeed, by inserting stabilizations we decrease the twisting of the core Legendrian curve. On the other hand, a thickening of the standard neighborhood is possible only in the presence of bypasses (and is precisely described by the Twist Number Lemma).

Finally, we consider appropriate contact structures on $\Sigma \times S^1$ where Σ stands for the pair of pants. We define *maximal twisting number* to be the difference between the contact framing and the fibration framing, maximized in the smooth isotopy class of the (vertical) fiber. By standardization of the dividing set on the section, cutting along carefully embedded vertical annuli and using the above classification for the thickened torus, Ghiggini [26] obtained the following uniqueness (in the zero-twisting case with ∞ boundary slopes, the result is due to Honda [38]).

Theorem 2.2.2 (Honda, Ghiggini)**.** *Up to an isotopy not necessarily fixed on the boundary, there is a unique tight contact structure on $\Sigma \times S^1$ with maximal twisting number $-q$ inducing the standard characteristic foliations on $-\partial(\Sigma \times S^1) = T_1 \cup T_2 \cup T_3$ of slope $-\frac{p_1}{q}$, $-\frac{p_2}{q}$ and $\frac{p_1+p_2+1}{q}$, respectively.*

In general [39], we call a collection of compact pieces after cutting along a properly and essentially embedded convex surface, with inherited contact structure, a *state* $(Y \backslash W, \xi|_{Y\backslash W})$, and the cutting surface a *wall* W. A *state traversal* then describes an isotopy of W inside Y, hence it changes Γ_W by a bypass attachment. Analysis of the states and their transitions allows complete classification of tight structures.

Theorem 2.2.3 (Honda)**.** *Provided we are able to describe all the states reached from any given state in a finite number of state traversals, a contact structure ξ on Y is tight if and only if all of these states are tight, and two structures ξ_1 and ξ_2 are isotopic if and only if their associated sets of states are the same.*

The most studied state traversal is performed along the essential torus in a toric annulus. Since we are applying it in a circle bundle over the pair of pants, we

will first need a standardization of the annulus cutting between two of the three boundary tori. With some further restrictions this is given in Section 4.2.3.

2.2.2 Four-dimensional viewpoint

At first glance, the study of symplectic fillings and caps presents a different sort of cut and paste, in which the convex (and here not equivalent, concave) attaching role is played by contact manifolds. But the changes in the induced boundary structure can be described by cut and paste on the 3-dimensional level, as shown in the next section.

Analyzing its plurisubharmonic Morse function, it is easy to see that a Stein manifold has a homotopy type of a half-dimensional CW-complex. Eliashberg [13] has proved the reverse, namely, for $n > 2$ every $2n$-dimensional manifold which admits an almost complex structure and can be built only by handles of dimension at most n, admits a Stein structure; for $n = 2$ there is an additional obstruction in terms of the framing of the critical handles. Gompf [35] gives a handle description of Stein surfaces.

Theorem 2.2.4 (Gompf)**.** *Every Stein surface is built from some handlebody* $\#^g S^1 \times D^3$ *(with its unique Stein structure) by attaching* 2*-handles along a Legendrian link with all framings one less than the contact framing.*

For the cobordism, corresponding to a handle attachment, to bridge the contact information we need it to be symplectic. The attaching sphere of the handle is Legendrian; this follows from the fact that the stable manifolds of the gradient flow in the metric, defined by ω (that is, $g(\cdot,\cdot) = \omega(\cdot, J\cdot)$), are isotropic, and so the same holds for their intersection with the regular value level set. The symplectic structure on the handle is the standard one $\omega_{\text{std}} = \mathrm{d}x_1 \wedge \mathrm{d}y_1 + \mathrm{d}x_2 \wedge \mathrm{d}y_2$, and on the collar of Y it is given by the symplectization $(I \times Y, \mathrm{d}(\mathrm{e}^t \alpha))$. The Liouville vector fields, which get identified by gluing, are given by the gradient field ∇f of the Morse function $f = x_1^2 + x_2^2 - \frac{1}{2}(y_1^2 + y_2^2)$ along the concave end $\{f = -1\} = \{x_1 = x_2 = 0, y_1^2 + y_2^2 = 2\} = S$ of the handle, and by ∂_t along Y. Finally, we determine the gluing framing in the standard model of the handle: the attaching sphere S spans a disk in $y_1 y_2$-plane, its normal direction being trivialized by ∂_{x_1}, while the contact form restricted to S takes the form $\alpha|_S = \iota_{\nabla f}\omega|_S = y_1\,\mathrm{d}x_1 + y_2\,\mathrm{d}x_2$ and gives the contact framing $y_2\partial_{x_1} - y_1\partial_{x_2}$, which twists once positively compared to ∂_{x_1}. Reversed, the handle framing with respect to the contact framing is -1, and so the same has to be the gluing framing. Finally, note that attaching along the convex end of the handle gives the framing $+1$ with respect to the contact framing, but since in this case the Liouville fields are not coherently oriented, the symplectic structure does not extend over the handle.

At the 3-dimensional level, the symplectic handle attachment corresponds to the Legendrian surgery. It is a Dehn surgery along K with framing -1 compared to the contact framing. If we trivialize $-\partial(Y\backslash\nu K)$ and $\partial\nu K$ as $\mathbb{R}^2/\mathbb{Z}^2$ with $\binom{1}{0}$ the meridional direction and $\binom{0}{1}$ the direction of the slope (given by the pair of dividing curves), then the resulting manifold is $Y\backslash\nu K \cup_f \nu K$ with $f : \partial\nu K \to -\partial(Y\backslash\nu K)$ given by $\left(\begin{smallmatrix} 1 & 0 \\ -1 & 1 \end{smallmatrix}\right) \in \mathrm{SL}_2(\mathbb{Z})$, and the contact structures are glued together along the tori with matching dividing sets.

A question arises, when the Legendrian surgery can be done in a given topological type. Though for any given knot we have a homotopic Legendrian knot, not all topological framings can be realized as -1 framings for some Legendrian embedding in the given homotopy class. In fact, it is always possible only to lower the contact framing (by stabilizations), to increase it we are in tight contact manifolds limited by the maximal Thurston-Bennequin invariant of a knot, while in overtwisted manifolds we can still achieve it by connect summing with the boundary of the overtwisted disk. On the other hand, from the above we have that the Legendrian surgery preserves fillability of contact structures, even more, by the result of Wand [72] it preserves also tightness in the class of closed contact manifolds.

From the handle description we can directly read off the first Chern class of the Stein structure. When the Stein surface (X, J) is given by attaching -1-framed 2-handles to (D^4, J_{std}) along the Legendrian link L, the first Chern class evaluates on the homology generators (the capped-off Seifert surfaces Σ_{L_i}) as $\langle c_1(X, J), [\Sigma_{L_i}]\rangle = \mathrm{rot}(L_i)$ [35]. (It describes how the $\mathbb{C}$-trivialization of the handle structure, given by the inward normal and the tangents of the attaching circle, compares to the standard $\mathbb{C}$-trivialization of $\mathrm{T}D^4$, given by the outward normal and $\partial_x \in \xi$.) The significance for the contact topology stems from the theorem of Lisca and Matić [48], which allows us to distinguish (homotopy equivalent but) non-isotopic fillable contact structures.

Theorem 2.2.5 (Lisca-Matić)**.** *If different Stein structures induce isotopic contact structures on the boundary, then their* $\mathrm{Spin}^{\mathrm{c}}$ *structures (and in particular, Chern classes) are isomorphic.*

2.2.3 Contact surgery

Rational contact surgery is performed along a Legendrian link $L \subset (Y, \xi)$ and the surgery coefficient is measured with respect to the contact framing. In addition to ordinary surgery, it prescribes for the contact structure to be preserved in the complement of a tubular neighborhood of the core link, while the extension to glued-up tori needs to be tight. The possible contact structures on every solid torus are determined by the boundary slope, given by the surgery coefficient. They are listed in the Honda's classification in terms of the continued fraction

decomposition, and in particular, there is no tight extension if and only if the surgery coefficient is zero.

Moreover, Ding and Geiges [7] have shown that:

Theorem 2.2.6 (Ding-Geiges)**.** *Any (closed) contact* 3*-manifold can be obtained from the standard contact structure on* S^3 *by a sequence of contact* ± 1*-surgeries.*

Their conversion of contact r-surgery into successive $+1$- and -1-surgeries encodes the convex decomposition of glued up tori in a form of the surgery diagram.

Let us first recall that in the smooth category [36] we can replace rational surgery coefficients by the chains of integral surgeries (along meridians of meridians) using the inverse slam dunks. Essentially this means that we factorize the gluing diffeomorphism. Namely, we are repeatedly taking out thinner and thinner tubular neighborhoods of always the same core knot, successively approaching the surgery coefficient. Explicitly, if the surgery coefficient is $r = \frac{p}{q}$, and $n \in \mathbb{N}$ is the minimal such that $-\frac{P}{Q} = \frac{p}{q-np} < 0$, and $-\frac{P}{Q} = [a_0, \dots, a_k]$, then we can factorize

$$\mathrm{SL}_2(\mathbb{Z}) \ni \begin{pmatrix} p & p' \\ q & q' \end{pmatrix} = \begin{pmatrix} 1 & 0 \\ n & 1 \end{pmatrix} \begin{pmatrix} -a_0 & 1 \\ -1 & 0 \end{pmatrix} \cdots \begin{pmatrix} -a_k & 1 \\ -1 & 0 \end{pmatrix}.$$

Recalling that ± 1-surgery correspond to $\left(\begin{smallmatrix} 1 & 0 \\ \pm 1 & 1 \end{smallmatrix}\right) = T^{\pm 1}$ and denoting $S = \left(\begin{smallmatrix} 0 & 1 \\ -1 & 0 \end{smallmatrix}\right)$, we have $T^n \cdot ST^{-a_0} \cdot \ldots \cdot ST^{-a_k}$. Here, the initial T^n corresponds to the change of framing, T^{a_i} are the successive surgeries, and S rotates the basis.

In the contact setting, the slicing can be described on Legendrian push-offs of the surgered knot K. First we perform contact $+1$-surgery along n push-offs of K, then for each successive i^{th} continued fraction block we do -1-surgery along K_i where K_i is obtained from K_{i-1} by Legendrian push-off and additional $a_i - 1$ stabilizations, and $K_0 = K$ stabilized $a_0 - 1$ times. All possible contact structures on glued-up torus are then covered by all possible choices of positive or negative stabilizations. Note that, since there is a Legendrian isotopy between the push-off and the meridian of a -1-surgery curve [9], the obtained surgery diagram is equivalent to the legendrianized smooth picture.

After the initial change of framing (the $+1$-surgeries), we have direct correspondence between the surgery diagram and the Honda's decomposition of the glued-up solid torus, whose boundary slope is $-\frac{P}{P'} = [a_k, \dots, a_0]$, the pull-back of the ∞-slope by $\left(\begin{smallmatrix} P & P' \\ -Q & -Q' \end{smallmatrix}\right) \in \mathrm{SL}_2(\mathbb{Z})$. Explicitly, in the layering of this solid torus

$$(S^1 \times D^2, \eta) = \bigcup_{i=0}^{k} \bigcup_{j=1}^{a_i - 1} (T^2 \times I, \eta(i,j)) \cup V^1_{\text{std}},$$

the continued fraction blocks $(T^2 \times I, \eta(i))$ are arranged from outside in, and they are cut out by pairs of tori of slopes $[a_k, \dots, a_{j+1} - 1]$ and $[a_k, \dots, a_j - 1]$ (the

outermost being $[a_k, \dots, a_0]$, and the innermost -1). In a surgery diagram, they are represented in a chain of pushed-off knots K_i, and the successive slopes are captured by their Thurston-Bennequin invariants. The distribution of signs of the basic slices $(T^2 \times I, \eta(i,j))$ within the i^{th} continued fraction block is reflected in the choice of signs for stabilizations of the Legendrian knot K_i (in other words, in its rotation number). The loss of basic slice ordering in the transition is explained by the shuffling property of basic slices within a single block.

An advantage of having a surgery description over the convex decomposition is, that we can directly read off the homotopy invariants of the contact structure [10]. As described at the end of the previous section, the Spin^c structure induced by a Stein structure is given by $\langle c_1(X,J), [\Sigma_{L_i}]\rangle = \mathrm{rot}(L_i)$. In case there are some $+1$-surgeries, the almost complex structure J does not spread throughout the manifold, but it can still be extended to the complement of a ball in each $+1$-handle. So, it induces a Spin^c structure $\mathbf{s}_J$ on X, equivalently $c(X, \mathbf{s}_J) \in \mathrm{H}^2(X;\mathbb{Z})$, an integral lift of $w_2(X)$, and it evaluates on all homology generators as before $\langle c(X, \mathbf{s}_J), [\Sigma_{L_i}]\rangle = \mathrm{rot}(L_i)$. The $\mathbf{s}_J$ restricts to the boundary $Y = \partial X$ as $\mathbf{t}_\xi = \mathbf{s}_J|_Y$ which is the induced Spin^c structure of the contact structure ξ. When $c_1(\xi)$ is torsion, the three-dimensional invariant also has numerical expression (due to Gompf [35]); the information is essentially contained in the almost complex structure J, together with the topology of X (its intersection form). It is given as an obstruction for gluing Stein domains (along (Y,ξ)) into closed almost complex 4-manifold, thus $d_3(\xi) = \frac{1}{4}(c_1^2(X,J) - 3\sigma(X) - 2\chi(X)) \in \mathbb{Q}$. In the presence of $+1$-surgeries it is for each $+1$-handle corrected by d_3 of the plane bundle induced by J on the boundary ∂B^3, which cumulates in $d_3(\xi) = \frac{1}{4}(c^2(X, \mathbf{s}_J) - 3\sigma(X) - 2\chi(X)) + \#(+1\text{-surgeries})$.

2.2.4 Example

We give surgery presentation of many contact structures mostly on Seifert fibered manifolds. First, the tight contact structure on the 3-sphere is given by the empty diagram; recall that its uniqueness follows from the uniqueness of the tight ball, observed by Eliashberg. Similarly, we have a unique tight structure on $S^1 \times S^2$ and it is described by Stein 1-handle, or equivalently [9], by contact $+1$-surgery on a Legendrian unknot with $\mathrm{tb} = -1$.

To construct overtwisted structures (on any 3-manifold Y) we may rely on the homotopic classification [10]. It suffices to find a surgery diagram for a single contact structure on Y, which we then alter in a neighborhood of an embedded $S^1 \times S^2$ and along some S^3, topologically trivially but changing the Spin^c structure and the 3-dimensional invariant, respectively. For the single structure, we change the smooth surgery by successive blow-ups so that all surgery coefficients (except for each last blowing-up unknot) are smaller than the maximal Thurston-Bennequin invariant of the corresponding knot, and then

legendrianize and stabilize so that all coefficients are -1 (and replace -1-framed unknots with $+1$-surgery on the unknot with $\mathrm{tb} = -2$). For the alterations, we need diagrams for all overtwisted structures on S^3 and $S^1 \times S^2$. See the paper of Ding, Geiges and Stipsicz [10] for details.

We take up tight structures on small Seifert fibered spaces. On a lens space, we get a number of tight structures by putting the unknots in the chain (whose coefficients are all at most -2) into Legendrian position and introducing stabilizations until all surgery coefficients are equal to -1. For the general $M(e_0; r_1, r_2, r_3)$ the plumbing graph is star-shaped with three legs, with central coefficient e_0 and all others at most -2. When $e_0 \leq -2$, we can do the same as above. And for $e_0 \geq 0$, we can blow-up the central vertex until its coefficient becomes 1, and then blow-down the central vertex, resulting in five -1-linked unknots with coefficients $0, -\frac{e_0-1}{e_0}$ and the three $-\frac{1+r_i}{r_i}$. After legendrianization and appropriate stabilizations we are left with some Legendrian surgery on the tight $S^1 \times S^2$, a single $+1$-surgery along a $\mathrm{tb} = -1$ unknot. All the above structures are fillable, also all of them are distinct (which is easiest to see by applying Theorem 2.2.5, or more elementary by comparing Spin^c structures). What is more, using the classification of tight structures on tori and the uniqueness of tight $\Sigma \times S^1$ with fixed maximal twisting, we get that these tight structures are all tight structures – on lens spaces due to Honda [37] and Giroux, when $e_0 \neq -2$ due to Wu [75] and Ghiggini, Lisca and Stipsicz [29], and for L-spaces with $e_0 = -2$ due to Ghiggini [26]. When $e_0 = -1$ we can anti blow-up the central vertex twice and then blow it down, resulting again in five -1-linked unknots, now with coefficients $0, 0$ and $-\frac{1+r_i}{r_i}$. The associated contact surgery diagram is some Legendrian surgery on an overtwisted S^3, given by $+1$-surgery along two once linked unknots of $\mathrm{tb} = -1$. In this case, Lisca and Stipsicz [51] showed, again using the uniqueness of appropriate $\Sigma \times S^1$, that all tight zero-twisting structures (all tight structures for L-spaces) are of this form. Notice however, that the structures described by this presentation are not necessarily (and indeed, they are not) all tight, also they are not all distinct. We achieve a complete characterization of tightness and fillability for these structures in Chapters 4 and 5. Finally, let us emphasize that L-space restriction in the cases $e_0 = -1, -2$ ensured fixed maximal twisting, which is 0 and -1, respectively.

2.3 Open books

Contact manifolds can be alternatively approached by looking at their dual counterpart – open book decompositions.

An *open book decomposition* of a 3-manifold Y is given by a fibered link $B \subset Y$, the link B is called the *binding* and a fiber F of the fibration $\pi : Y \backslash B \to S^1$, which is a Seifert surface for B, is called a *page*. The fibration can be described

by its monodromy $\phi : (F, \partial F) \to (F, \partial F)$, and we refer to the pair (F, ϕ) as an *abstract open book*. Given two 3-manifolds with open book decompositions, their connected sum has an open book decomposition whose page is a Murasugi sum of the pages of the original open books. In particular case, when one of the two is an open book decomposition of S^3 with positive or negative Hopf bands as pages, we get a new open book for $Y \cong Y \# S^3$ called the *positive or negative stabilization*. Notice that the new page F' is built from F by adding a 1-handle, and the new monodromy is given as $\phi \circ D_\gamma^{\pm 1}$ for D_γ the positive (right-handed) Dehn twist along a simple closed curve $\gamma \subset F'$ which intersects the cocore of the new 1-handle once.

We say that the open book decomposition *supports* the contact structure when the contact planes are almost tangent to the interior of the pages ($\mathrm{d}\alpha$ is a volume form on each page), and are positively transverse to the binding, oriented as the boundary of a page ($\alpha(\mathrm{T}B) > 0$). The contact manifold supported by the Murasugi sum open book is equivalent to the connected sum of the originally supported contact manifolds. Because the positive Hopf open book on S^3 supports the standard tight contact structure, positive stabilizations do not change the contact structure the open book supports. Thurston and Winkelnkemper [70] showed that any open book decomposition supports a contact structure, Giroux [34] proved the converse, and established that:

Theorem 2.3.1 (Giroux)**.** *Contact structures on* 3*-manifolds up to contact isotopy are in one to one correspondence with open book decompositions up to positive stabilization.*

In particular, starting from a surgery presentation of the contact manifold (Y, ξ) we can built an open book (with a torus knot binding) which supports $(S^3, \xi_{\mathrm{std}})$, and for which the surgery link sits on a single page; the supporting open book of (Y, ξ) has the same page and the monodromy given as product of positive and negative Dehn twists along curves corresponding to cores of -1- and $+1$-surgeries, respectively.

In the light of Giroux's correspondence, there arises a need for a geometric characterization of various algebraic and combinatorial properties of open books [23]. A well-known open question in the area is, whether all contact structures can be supported by open books of some bounded genus (in particular, genus-one). Etnyre [19] proved that all overtwisted structures are planar. On the other hand, there are obstructions for planarity of several other contact manifolds in terms of the topology of their fillings [19, 27]. A general belief is that contact structures whose Stein fillings admit arbitrarily large topology can not be supported by genus-one open books. Such structures were found by Baykur and Van Horn-Morris [4] via constructing arbitrarily long factorizations of corresponding monodromies on genus-g, $g > 1$, surfaces. On the other hand, it is known that such factorizations

of genus-one monodromies do not exist, but the problem is that the properties of open books are not stabilization invariant.

Conversely, we wish to understand how contact properties (fillability, tightness) manifest in the open book decompositions. It is a result of Giroux (building on handle decomposition) that a contact 3-manifold (Y, ξ) is Stein fillable if and only if it admits a supporting open book decomposition whose monodromy factorizes into positive Dehn twists only (along homotopically nontrivial simple closed curves). Moreover, according to Loi and Piergallini [53] (also Akbulut and Özbağcı[1]), every Stein manifold admits the structure of an *allowable Lefschetz fibration*. Recall that a Lefschetz fibration on a compact, oriented 4-manifold X is a smooth surjective map to a compact, oriented surface (for us, a disk D) $\pi : X \to D$ which is a fiber bundle except at finitely many (interior) singular points, around which π takes the form $(z_1, z_2) \mapsto z_1^2 + z_2^2$ in some local chart. The topology of the underlying 4-manifold is determined by the fiber, which gives 0- and 1-handles of $F \times D$, and the vanishing cycles (isotopy classes of simple closed curves in the nearby fiber which collapse to a point in the singular fiber), which describe attaching circles of -1-framed 2-handles. The boundary $Y = \partial X$ consists of two parts: a fibration over the circle $\pi^{-1}(\partial D)$, and solid tori from the boundary components of all fibers $\partial F \times D^2$. So, it comprises the open book decomposition (F, ϕ) with F the fiber of the Lefschetz fibration and the monodromy ϕ given by a product of positive Dehn twists, one along each vanishing cycle. This (F, ϕ) supports the same contact structure which is induced on the boundary by the Stein structure, as shown by Plamenevskaya [66]. In general, a problem is that not every open book, which supports a Stein fillable structure, admits a positive factorization [2, 73]. A theorem of Wendl confirms this for planar contact structures, even more, in this case all Stein fillings arise as positive factorizations of the same planar open book. (More in Section 5.1.)

The study of Stein fillings brings to our attention the study of positive factorizations in the mapping class groups. We briefly recall that the group $\Gamma_{g,r}$ is generated by Dehn twists along finitely many non-separating simple closed curves and a Dehn twist along a simple closed curve parallel to each boundary component. The group is (in general) not commutative, still the Dehn twists along disjoint curves commute. Important non-trivial relations among generators are the lantern relation (relating boundary and pairwise twists in the 4-punctured sphere), and its repeated generalization, the daisy relation; which in 4-dimensional world, as monodromy substitution for the Lefschetz fibration, correspond to the rational blow-down.

On the other hand, according to Honda, Kazez and Matić [40], a contact 3-manifold (Y, ξ) is tight if and only if all of its open book decompositions (F, ϕ) have *right-veering* monodromy ϕ. In contrast to positive factorization, this is a local property which describes how the monodromy acts on properly embedded

arcs in a page. The mapping class ϕ is said to be right-veering if every arc is mapped to the right at its endpoints (after we isotope the image so that it has minimal intersection with its original). This approach allows us to detect overtwistedness, but we need to find a supporting open book which contains an arc which is mapped to the left, and not all open books supporting an overtwisted structure are like that.

From an open book decomposition we can built a particular Heegaard splitting of the (contact) 3-manifold (Y, ξ). If we write out Y as $F \times [0,1]/\sim$ where $\sim$ identifies $(p,1) \sim (\phi(p),0)$ for every $p \in F$, and $(p,t) \sim (p,s)$ for $p \in \partial S$ and $t, s \in [0,1]$, the two handlebodies are $H_\alpha = F \times [0, \frac{1}{2}]$ and $H_\beta = F \times [\frac{1}{2}, 1]$, and the Heegaard surface is $\Sigma = \partial H_\alpha = F_{\frac{1}{2}} \cup -F_0$. If $F = \Sigma_{g,r}$ a connected orientable surface of genus g with r boundary components, then Σ has genus $n = 2g + r - 1$. Using convex surface theory, Torisu [71] showed that on the handlebodies H_α and H_β there is a unique tight contact structure with dividing curves $\Gamma_\Sigma = B = \partial F$. This means that the contact information is also completely contained in the gluing map, and we rewrite it in form of the Heegaard diagram as follows. With $\{a_1, \dots, a_n\}$ pairwise disjoint, properly embedded and homologically independent arcs in F, and $\{b_1, \dots, b_n\}$ their displacements, moving the endpoins in the direction of ∂F and intersecting original arcs transversely once, we describe the α- and β-attaching curves as $\alpha_i = a_i \times \{\frac{1}{2}\} \cup a_i \times \{0\}$ and $\beta_i = b_i \times \{\frac{1}{2}\} \cup \phi(b_i) \times \{0\}$.

2.3.1 Example

Here, we directly complement the discussion in Section 2.2.4. As already mentioned, the simplest open book for (S^3, ξ_{std}) has disk pages and trivial monodromy, though we mostly use its positive stabilization, which has annular pages and monodromy given by positive (right-handed) Dehn twist along the core. Note however that not every open book for (S^3, ξ_{std}) is a positive stabilization of the disk one [22]. To get $S^1 \times S^2$, we perform $+1$-surgery on an unknot with $\text{tb} = -1$, which is exactly the core of the annular page of the Hopf open book for S^3_{std}. The positive Dehn twist of the initial S^3-monodromy and the negative Dehn twist representing $+1$-surgery cancel each other, resulting in an open book for tight $S^1 \times S^2$ with annular page and trivial monodromy.

As observed by Etnyre [19], all overtwisted structures are supported by planar open books. This again rests on the homotopic classification. We take a planar open book for the underlying manifold, then we realize all Spin^c structures by performing Lutz twists along homologically independent curves, and realize 3-dimensional invariants by Murasugi summing with a planar open book for overtwisted 3-spheres. We refer to the original paper [19] for the planar realization of the Lutz twist, as well as for overtwisted structures on S^3.

We exhibit planar open books for all tight contact structures constructed in Section 2.2.4 on small Seifert manifolds, except the ones on $M(-2; r_1, r_2, r_3)$. To

conclude, all contact structures on lens spaces, on small Seifert fibered spaces with $e_0 \neq -1, -2$, and the zero-twisting ones on $M(-1; r_1, r_2, r_3)$, are planar. For this, we need a contact surgery presentation whose core Legendrian link sits on a union of pages of some planar open book for S^3_{std}. For lens spaces and when $e_0 \leq -3$ such presentations were given by Schönenberger [68]; he calls them rolled-up diagrams, and they are reminiscent to Ding-Geiges's surgery presentation by Legendrian push-offs. Concretely, instead of taking the plumbing graph and legendrianize all unknots, we start at one end of the chain (for lens spaces), realize first unknot and take its Legendrian push-off in place of the meridian (the two being Legendrian isotopic after -1-surgery on the first unknot [9]), then we proceed analogously, always taking the push-off of the previous unknot in the chain. For $M(e_0; r_1, r_2, r_3)$ with $e_0 \leq -3$, we take the above presentation for the lens space described by two legs and the central vertex, then we look for a meridian of the central unknot which is once linked also with all the following unknots in the chain, and insert a rolled-up diagram of the third leg in its place. Finally, for $e_0 \geq -1$ we take surgery diagrams described in Section 2.2.4. In the following, we explain how to build a planar open book from such surgery presentations. In all the cases we start with the Hopf open book for S^3_{std} which we then stabilize. Concretely, we insert a hole, encircled by one positive Dehn twist, for every stabilization of every unknot in the surgery diagram; the stabilization holes which correspond to positive stabilizations lie between the inner boundary of the annulus and its core, the negative ones between the core and the outer boundary. For lens spaces and when $e_0 \leq -3$ we add positive Dehn twists in the same order as how we have described the surgery curves. From the first unknot we get a positive Dehn twist along a push-off of the core (that is, the Dehn twist which remained from the initial Hopf open book) modified by encircling an additional stabilization hole for each negative stabilization, and avoiding a stabilization hole for each positive stabilization. The twists corresponding to the subsequent unknots are obtained by described modification on a push-off of the twist corresponding to the previous unknot. When $e_0 \geq -1$ we start with $+1$-surgeries, when there is one it eliminates the positive Dehn twist along the core, when there are two we have a negative Dehn twist along the core instead. We then proceed with each leg from the center out in the same manner as we described in the case of lens spaces. At the end, let us remark that on many L-spaces of the form $M(-2; r_1, r_2, r_3)$ no tight contact structure admits a planar open book, due to obstructions which restrict possible intersection forms for Stein fillings of planar contact manifolds (spotted by Etnyre [19], and Ghiggini, Golla and Plamenevskaya [27]).

3

Heegaard Floer homology

Defined by Ozsváth and Szabó [61, 62, 65], Heegaard Floer homology (in its initial form) is an invariant of a closed, oriented 3-manifold. Following its two-fold name, it combines the topology of pointed Heegaard diagram $(\Sigma_n, \boldsymbol{\alpha}, \boldsymbol{\beta}, z)$ with the analysis of Lagrangian intersection Floer homology. Out of the first, capturing the intersection data of stable and unstable manifolds associated with a self-indexing Morse function, it keeps $\mathrm{H}_*(Y)$, and additionally, paired with the chosen base-point assigns $\mathrm{Spin}^{\mathrm{c}}$ structures to intersection points. Rewriting the input in the symmetric product

$$(\mathrm{Sym}^n(\Sigma), \mathbb{T}_\alpha = \alpha_1 \times \cdots \times \alpha_n, \mathbb{T}_\beta = \beta_1 \times \cdots \times \beta_n, V_z = \{z\} \times \mathrm{Sym}^{n-1}(\Sigma)),$$

$\mathrm{HF}^\infty(Y)$ (basically) arises as the homology of a suitable $\mathbb{Z}$-covering of the path space $\mathcal{P}(\mathbb{T}_\alpha, \mathbb{T}_\beta)$, layered by V_z-intersections, which gives it $\mathbb{F}[U, U^{-1}]$-module structure with U corresponding to a generator of deck translations.

Concretely, the chain groups are freely generated by the intersection points $\mathbf{x} \in \mathbb{T}_\alpha \cap \mathbb{T}_\beta$, paired with integers $i \in \mathbb{Z}$. The grading and the boundary map are defined as follows. Given intersection points $\mathbf{x}, \mathbf{y} \in \mathbb{T}_\alpha \cap \mathbb{T}_\beta$, we consider the moduli spaces $\mathcal{M}(\mathbf{x}, \mathbf{y}) = \bigcup \mathcal{M}(\phi)$ of pseudoholomorphic representatives of a Whitney disks ϕ from $\mathbf{x}$ to $\mathbf{y}$, that is, $\phi \in \pi_2(\mathbf{x}, \mathbf{y}) = \{u : \mathbb{D} \to \mathrm{Sym}^n(\Sigma), \partial\mathbb{D} \cap \{\mathrm{Re}\, z < 0\} \mapsto \mathbb{T}_\alpha, \partial\mathbb{D} \cap \{\mathrm{Re}\, z > 0\} \mapsto \mathbb{T}_\beta, (\mathrm{i}, -\mathrm{i}) \mapsto (\mathbf{x}, \mathbf{y})\}$. The maps u in $\mathcal{M}(\mathbf{x}, \mathbf{y})$ lift to holomorphic maps $\widetilde{u} : \widetilde{\mathbb{D}} \to \Sigma$ where $\widetilde{\mathbb{D}} \to \mathbb{D}$ is a suitable n-fold branched cover; thus the disks u can be understood by looking at the image of $\widetilde{u}$ which is a union of domains in $\Sigma \backslash (\boldsymbol{\alpha} \cup \boldsymbol{\beta})$ with boundary alternating between segments of α- and β-curves. The expected dimension of $\mathcal{M}(\phi)$ is given by the Maslov index $\mu(\phi)$. Now, the relative grading on the generators of $\mathrm{CF}^\infty(Y)$ is defined by $\mathrm{gr}([\mathbf{x}, i], [\mathbf{y}, j]) = \mu(\phi) - 2n_z(\phi) + 2i - 2j$ (for admissible Heegaard diagram independently of the choice of $\phi \in \pi_2(\mathbf{x}, \mathbf{y})$), and the boundary map counts the 0-dimensional components of $\mathcal{M}(\mathbf{x}, \mathbf{y})/\mathbb{R}$ by the formula

$$\partial^\infty[\mathbf{x}, i] = \sum_{\mathbf{y} \in \mathbb{T}_\alpha \cap \mathbb{T}_\beta} \sum_{\substack{\phi \in \pi_2(\mathbf{x}, \mathbf{y}) \\ \mu(\phi) = 1}} \#(\mathcal{M}(\phi)/\mathbb{R}) \cdot [\mathbf{y}, i - n_z(\phi)].$$

Here, the function $n_z(\phi)$ is given by the transverse intersections of $u(\mathbb{D})$ with V_z. Additionally, the chain complex admits an $\mathbb{F}[U]$-modul structure where U acts by $U \cdot [\mathbf{x}, i] = [\mathbf{x}, i-1]$, reducing grading by two.

Fixing the basepoint z, each intersection point $\mathbf{x} \in \mathbb{T}_\alpha \cap \mathbb{T}_\beta$ defines a Spin^c structure $\mathbf{t_x}$ on the 3-manifold Y. Since there is a Whitney disk between $\mathbf{x}$ and $\mathbf{y}$ only if the two Spin^c structures $\mathbf{t_x}$ and $\mathbf{t_y}$ agree, the chain complex splits as a direct sum $\oplus_{\mathbf{t}\in \mathrm{Spin}^c(Y)}(\mathrm{CF}^\infty(Y,\mathbf{t}), \partial^\infty)$. Furthermore, since the submanifold V_z is a complex hypersurface, any pseudoholomorphic disk meets it positively; hence $n_z(\phi) > 0$ whenever $\mathcal{M}(\phi)$ is nonempty. Therefore the subset CF^- generated by the elements $[\mathbf{x}, i]$ with $i < 0$ forms a subcomplex of CF^∞. We define CF^+ to be the quotient $\mathrm{CF}^\infty / \mathrm{CF}^-$, that is the complex generated by $[\mathbf{x}, i]$ with $i \geq 0$. The corresponding homology groups are related by an exact sequence $\cdots \to \mathrm{HF}^- \xrightarrow{\iota} \mathrm{HF}^\infty \xrightarrow{\pi} \mathrm{HF}^+ \xrightarrow{\delta} \cdots$, giving rise to a group $\mathrm{HF}_{\mathrm{red}} = \mathrm{coker}(\pi)$. Finally, we define $\widehat{\mathrm{CF}}$ to be the complex generated by the kernel of the U-action on CF^+; we may think of it as a chain complex generated by $\mathbf{x} \in \mathbb{T}_\alpha \cap \mathbb{T}_\beta$ with the boundary map counting only the disks which do not meet V_z. We have an exact sequence $\cdots \to \widehat{\mathrm{HF}} \to \mathrm{HF}^+ \xrightarrow{U\cdot} \mathrm{HF}^+ \to \cdots$. All the chain groups and the homology groups split according to Spin^c structures and carry a relative $\mathbb{Z}_{\mathrm{div}(c_1(\mathbf{t}))}$-grading where $\mathrm{div}(c_1(\mathbf{t}))$ is the divisibility of $c_1(\mathbf{t}) \in \mathrm{H}^2(Y;\mathbb{Z})$.

An oriented cobordism of 3-manifolds induces homomorphism between their Heegaard Floer groups HF°. It splits according to the Spin^c structures on the cobordism: for each $\mathbf{s}$ on W, which restricts to $\mathbf{t}_i$ on Y_i, we have an induced map $F^\circ_{W,\mathbf{s}} : \mathrm{HF}^\circ(Y_1, \mathbf{t}_1) \to \mathrm{HF}^\circ(Y_2, \mathbf{t}_2)$. These maps are defined by looking at the relative handle decomposition of (W, Y_1), using Heegaard triples and counting holomorphic triangles. Most important is the map associated to a 2-handle attachment. Here, the triple $\boldsymbol{\alpha}, \boldsymbol{\beta}, \boldsymbol{\gamma}$ is obtained from the Heegaard diagram $(\Sigma, \boldsymbol{\alpha}, \boldsymbol{\beta}_K)$ for the complement of the knot K along which the handle is attached. The initial manifold Y is presented as $(\Sigma, \boldsymbol{\alpha}, \boldsymbol{\beta})$ with $\boldsymbol{\beta}$ extending $\boldsymbol{\beta}_K$ by the meridian of K, the surgered manifold $Y_n(K)$ is presented as $(\Sigma, \boldsymbol{\alpha}, \boldsymbol{\gamma})$ for $\boldsymbol{\gamma}$ consisting of twice-intersecting push-offs of $\boldsymbol{\beta}_K$ and the $(n,1)$-curve on $\partial(\nu K)$, and $(\Sigma, \boldsymbol{\beta}, \boldsymbol{\gamma})$ is a diagram for $\#^{n-1} S^1 \times S^2$. The boundary map then counts triangles for which one corner goes to the distinguished top generator $\theta \in \mathbb{T}_\beta \cap \mathbb{T}_\gamma$.

The maps behave well under the compositions of cobordisms: if $(W_1, \mathbf{s}_1)$ is a Spin^c cobordism from $(Y_1, \mathbf{t}_1)$ to $(Y_2, \mathbf{t}_2)$, $(W_2, \mathbf{s}_2)$ is a Spin^c cobordism from $(Y_2, \mathbf{t}_2)$ to $(Y_3, \mathbf{t}_3)$, and we denote $W_1 \cup_{Y_2} W_2$ by W, then $F^\circ_{W_2,\mathbf{s}_2} \circ F^\circ_{W_1,\mathbf{s}_1} = \sum_{\{\mathbf{s}\in \mathrm{Spin}^c(W) : \mathbf{s}|_{W_i} = \mathbf{s}_i\}} F_{W,\mathbf{s}}$. An important property of the induced maps $F^\infty_{W,\mathbf{s}}$ is that they vanish for all Spin^c structures $\mathbf{s}$ once $b_2^+(W) > 0$. This allows for W with $b_2^+ > 1$ to define a mixed homomorphism $F^{\mathrm{mix}}_{W,\mathbf{s}} : \mathrm{HF}^-(Y_1, \mathbf{t}_1) \to \mathrm{HF}^+(Y_2, \mathbf{t}_2)$ which factors through $\mathrm{HF}_{\mathrm{red}}(N, \mathbf{t})$ of an admissible cut N (a 3-manifold which splits W into halves W_1, W_2 with $b_2^+(W_i) \geq 1$ and such that $\mathrm{H}^2(W) \to \mathrm{H}^2(W_1) \oplus \mathrm{H}^2(W_2)$ is injective). In particular, when $(W, \mathbf{s})$ is a Spin^c cobordism from $(Y_1, \mathbf{t}_1)$ to $(Y_2, \mathbf{t}_2)$

with $\mathbf{t}_1, \mathbf{t}_2$ both torsion, the map $F^\circ_{W,\mathbf{s}}$ shifts the grading of any homogeneous element by the rational number $\frac{1}{4}(c_1^2(\mathbf{s}) - 3\sigma(W) - 2\chi(W))$. Thus, whenever $c_1(\mathbf{t})$ is torsion, the relative $\mathbb{Z}$-grading on $\mathrm{HF}^\circ(Y,\mathbf{t})$ lifts to an absolute $\mathbb{Q}$-grading, defined through Spin^c cobordisms. We capture it by the *d-invariant* $d(Y,\mathbf{t})$, the absolute degree of the unique nontrivial element $x \in \mathrm{HF}^+(Y,\mathbf{t})$ which is in the image of the map $\mathrm{HF}^\infty(Y,\mathbf{t}) \to \mathrm{HF}^+(Y,\mathbf{t})$ and for which $Ux = 0$.

For a rational homology sphere, the Heegaard Floer homology in any Spin^c structure takes the form $\mathrm{HF}^+(Y,\mathbf{t}) = \mathcal{T}^+_{d(Y,\mathbf{t})} \oplus \mathrm{HF}_{\mathrm{red}}(Y,\mathbf{t})$ for $\mathcal{T}^+_d$ an $\mathbb{F}[U]$-module $\mathbb{F}[U,U^{-1}]/U\mathbb{F}[U]$ with the lowest degree element in degree d. In particular, $\dim \widehat{\mathrm{HF}}(Y) \geq |\,\mathrm{H}_1(Y;\mathbb{Z})|$. A rational homology sphere Y is called an *L-space* if $\mathrm{HF}^+(Y,\mathbf{t})$ is isomorphic to $\mathcal{T}^+$ for all Spin^c structures $\mathbf{t} \in \mathrm{Spin}^c(Y)$, equivalently, $\dim \widehat{\mathrm{HF}}(Y) = |\,\mathrm{H}_1(Y;\mathbb{Z})|$. So, for an L-space the group $\widehat{\mathrm{HF}}(Y,\mathbf{t})$ can be described as the kernel of the U-map on homology, $U : \mathrm{HF}^+(Y,\mathbf{t}) \to \mathrm{HF}^+(Y,\mathbf{t})$, and the d-invariant is characterized as the degree of the unique nontrivial element in $\widehat{\mathrm{HF}}(Y,\mathbf{t})$.

The power of Heegaard Floer theory comes from the fact that it is well adapted to usual geometric constructions in 3-manifold theory. A particular case of this is the *surgery exact triangle*. Let the manifold $Y_n(K)$ be given as an integral n-surgery along a knot K in Y, and $Y_{n+1}(K)$ be defined by an integral surgery along K with the framing one higher. The groups corresponding to these 3-manifolds, together with the maps induced by cobordisms W_1, W_2, W_3, defined by attaching a 2-handle along K with framing n, along its meridional circle M with framing -1, and along the meridian N of M with framing -1, respectively, fit into an exact triangle:

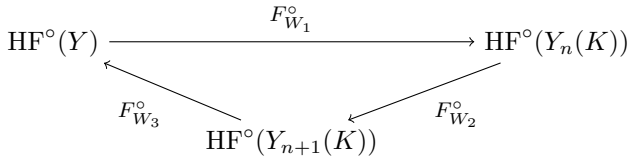

where $F^\circ_{W_i} = \sum_{\mathbf{s} \in \mathrm{Spin}^c(W_i)} F^\circ_{W_i,\mathbf{s}}$.

Finally, the determination of Heegaard Floer invariants often uses the special way in which a particular manifold is constructed. Specifically, in the cases below, we have negative definite plumbings, for which HF^+ can be isomorphically described by some equivalence classes of characteristic cohomology elements, and contact structures, where the supporting open book decompositions are utilized.

3.1 Negative definite plumbings

For many graph 3-manifolds, a combinatorial description of HF^+ in terms of characteristic cohomology elements on the bounded 4-dimensional plumbings

has been achieved [60, 56], based on the functorial behavior of Heegaard Floer homology with respect to cobordisms.

Let Γ stand for a weighted tree which has at most one bad vertex (that is, a vertex which has more neighbors than the negative of its weight) and such that its intersection matrix is negative definite. We denote the associated plumbing of disk bundles (over spheres) and its boundary, by X_Γ and Y_Γ, respectively. Homology of these manifolds is described by three groups: $\mathrm{H}_2(X_\Gamma;\mathbb{Z})$, generated by the sections (vertices $v \in \Gamma$) of the disk bundles, $\mathrm{H}_2(X_\Gamma, Y_\Gamma;\mathbb{Z})$ and $\mathrm{H}_1(Y_\Gamma;\mathbb{Z})$, related by the exact sequence

$$\mathrm{H}_2(Y_\Gamma;\mathbb{Z}) = 0 \to \mathrm{H}_2(X_\Gamma;\mathbb{Z}) \xrightarrow{\mathrm{PD}} \mathrm{H}_2(X_\Gamma, Y_\Gamma;\mathbb{Z}) \to \mathrm{H}_1(Y_\Gamma;\mathbb{Z}) \to 0 = \mathrm{H}_1(X_\Gamma;\mathbb{Z}).$$

In particular, Y_Γ is a rational homology sphere. The Spin^c structures on X_Γ can be equivalently described by the characteristic cohomology elements $\mathrm{Char}(\Gamma) = \{K; \langle K, v\rangle + v\cdot v \equiv 0 \bmod 2 \ \text{ for all } v\} \subset \mathrm{H}^2(X_\Gamma;\mathbb{Z}) \cong \mathrm{H}_2(X_\Gamma, Y_\Gamma;\mathbb{Z})$. The Spin^c structures on Y_Γ, which are in one to one correspondence with $\mathrm{H}_1(Y_\Gamma;\mathbb{Z})$, agree with the $\mathrm{H}_2(X_\Gamma;\mathbb{Z})$-orbits in $\mathrm{Char}(\Gamma)$, inducing a partition $\mathrm{Char}(\Gamma) = \uplus\, \mathrm{Char}_{\mathbf{t}}(\Gamma)$.

Denote by $\mathbb{K}^+_{\mathbf{t}}(\Gamma)$ the equivalence classes $\mathbb{Z}^{\geq 0} \times \mathrm{Char}_{\mathbf{t}}(\Gamma)/\sim$ where the equivalence relation $\sim$ for $K \in \mathrm{Char}_{\mathbf{t}}(\Gamma)$ with $2n = \langle K, v\rangle + v\cdot v$ means $U^{m+n} \otimes (K + 2\,\mathrm{PD}(v)) \sim U^m \otimes K$ if $n \geq 0$, and $U^m \otimes (K + 2\,\mathrm{PD}(v)) \sim U^{m-n} \otimes K$ if $n < 0$. Ozsváth and Szabó [60] establish the following isomorphism, describing $\mathrm{HF}^+(-Y_\Gamma)$.

Theorem 3.1.1 (Ozsváth-Szabó)**.** *With the above notation, there is an isomorphism*

$$\Phi_l : \Big(\ker U^{l+1} \subset \mathrm{HF}^+(-Y_\Gamma, \mathbf{t})\Big) \to \mathrm{Hom}\left(\frac{\mathbb{K}^+_{\mathbf{t}}(\Gamma)}{\mathbb{Z}^{\geq l} \times \mathrm{Char}_{\mathbf{t}}(\Gamma)}, \mathbb{F}\right) \ \textit{for every } l \in \mathbb{Z}_{\geq 0}.$$

The maps Φ_l for all l fit together into an isomorphism

$$\Phi : \mathrm{HF}^+(-Y_\Gamma, \mathbf{t}) \to (\mathbb{K}^+_{\mathbf{t}}(\Gamma))^*.$$

The isomorphism Φ (and similarly its restrictions Φ_l) is given by the pairing

$$\mathrm{HF}^+(-Y_\Gamma, \mathbf{t}) \times \mathbb{K}^+_{\mathbf{t}}(\Gamma) \to \mathbb{F} \text{ which sends } \ (x, U^m \otimes K) \mapsto \Big(U^m \cdot F^+_{X_\Gamma, K}(x)\Big)_0$$

where we regard X_Γ as cobordism from $-Y_\Gamma$ to S^3, and $(\ \cdot\ )_0$ denotes the 0-degree level of $\mathcal{T}^+_0 \cong \mathrm{HF}^+(S^3)$. In fact, if we set the grading on $\mathbb{K}^+(\Gamma)$ to assign $\deg(U^m \otimes K) = 2m - \frac{K^2 + |\Gamma|}{4}$, then Φ gives a grading preserving isomorphism.

In particular, characteristic classes which present generators of $\ker U$ can be recognized through the behavior of their full paths. A sequence of characteristic covectors $\{K_i\}$ on W_Γ is said to be a *full path* if its elements satisfy the bounds $v\cdot v \leq \langle K_i, v\rangle \leq -v\cdot v$ for all $v \in \Gamma$, and are connected by the following 2 PD

steps: for some vertex v with $\langle K_i, v\rangle = -v \cdot v$, the vector K_{i+1} is given by $K_{i+1} = K_i + 2\,\mathrm{PD}(v)$. The path either reaches the proper ends in the *initial vector* K_1 satisfying $v \cdot v + 2 \leq \langle K_1, v\rangle \leq -v \cdot v$ for all $v \in \Gamma$ and the *terminal vector* K_t satisfying $v \cdot v \leq \langle K_t, v\rangle \leq -v \cdot v - 2$ for all $v \in \Gamma$ – a full path with such ending determines a non-trivial element of $\ker U$. Otherwise, the path ends by some characteristic vector K which exceeds the bounds $v \cdot v \leq \langle K_i, v\rangle \leq -v \cdot v$ at some $v \in \Gamma$ – we say that the path drops out, and its elements are equivalent in $\mathbb{K}^+(\Gamma)$ to $U^m \otimes K'$ for some $m > 0$ and $K' \in \ker U$. The following properties establish full paths as an algorithm to determine $\ker U$. Two characteristic covectors are equivalent in $\mathbb{K}^+(\Gamma)$ if and only if there is a full path containing both of them. If any full path which crosses a covector K properly ends (or drops out), then all full paths through K behave the same. This means that we have a bijective correspondence between a set of generators for $\ker U$ and connected components defined by full paths with proper ends (equivalently, initial vectors starting a full path which leads to a terminal vector). Finally, from the U-equivariance of the maps $F^+_{X_\Gamma,K}$, induced by the negative definite cobordism, we derive that the d-invariant corresponds to the Spin^c structure on X_Γ which decreases the absolute grading the least, thus $d(-Y_\Gamma, \mathbf{t}) = \min \frac{-K^2-|\Gamma|}{4}$ where minimum is taken over covectors K which admit properly ending full paths.

Némethi's lattice cohomology [56] reinterprets and generalizes (to a wider class of graphs) the above isomorphism Φ. He establishes it as an invariant for links of normal surface singularities [57], in particular, he observes the following.

Theorem 3.1.2 (Némethi)**.** *The set $\mathbb{K}^+(\Gamma)$ depends only on the 3-manifold Y and is independent of the choice of the negative definite plumbing graph Γ which provides Y (that is, independent of the plumbed 4-manifold that Y bounds).*

Essentially this means that blowing up induces a degree preserving isomorphism between characteristic covectors of different plumbings.

Let us remark that the negative definite graphs naturally arise in singularity theory as resolution graphs where vertices correspond to exceptional divisors and edges represent their intersections. Lately, some relations between the bad vertices and the support genus of the canonical contact structures on links of singularities have been established (obstructions for planarity due to Ghiggini, Golla and Plamenevskaya [27], and construction of genus-one open books by Choi and Park [5]). In another direction, in Chapter 4 we find for a larger set of characteristic covectors but for a very particular set of star-shaped plumbings a contact interpretation for the steps in the full path associated to the bad vertex.

3.2 Contact invariant

The Ozsváth-Szabó contact invariant [64] is defined using the Giroux's correspondence between contact structures and open book decompositions. The definition rests on the fact that every contact structure is supported (possibly after positive stabilizations) by an open book with connected binding and with pages of genus $g > 1$. By capping off the one boundary component, we obtain a closed surface. If we denote by Y_0 the corresponding fibered 3-manifold and by $\mathbf{t}_0$ the Spin^c structure on Y_0 given by the fibration, then $\mathrm{HF}^+(-Y_0, \mathbf{t}_0)$ is generated by a single element c_0^+. The contact invariant $c^+(Y,\xi) \in \mathrm{HF}^+(-Y)$ is the image of this element c_0^+ under the map F^+_V, induced by the capping cobordism V turned upside-down. In particular, $c^+(Y,\xi)$ lies in $\ker U$; when we consider it as an element of $\widehat{\mathrm{HF}}(-Y)$ we denote it $c(Y,\xi)$. (The capping homomorphism was generalized to open books with disconnected binding by Baldwin [3].) As elucidated by Plamenevskaya [66] and Ghiggini [25], we can actually find a symplectic cap (W',ω') of (Y,ξ) with $b_2^+(W') > 1$ for which the contact invariant can be expressed as $c^+(\xi) = F^{\mathrm{mix}}_{W',\mathbf{k}'}(\theta^-)$ with $\mathbf{k}'$ the canonical Spin^c structure on (W',ω') and θ^- the generator of $\mathrm{HF}^-_{-2}(S^3)$. Alternatively, Honda, Kazez and Matić [41] later gave a reformulation of the Ozsváth-Szabó contact invariant in terms of the Heegaard diagram $(\Sigma, \boldsymbol{\alpha}, \boldsymbol{\beta})$ described at the end of Section 2.3. If we place the basepoint into the complement of the thin strips between a_i- and b_i-arcs on $F_{\frac{1}{2}}$, the unique intersection point of α- and β-curves on $F_{\frac{1}{2}}$ gives rise to a cycle $[\mathbf{x}, 0] \in \mathrm{CF}^+(-Y)$ whose homology class agrees with $c^+(Y,\xi)$.

The contact invariant $c^+(\xi) \in \mathrm{HF}^+(-Y)$ is an isotopy invariant of the contact structure ξ, and it contains information about its homotopy type by lying in $\mathrm{HF}^+_{-d_3(\xi)}(-Y, \mathbf{t}_\xi)$ for $\mathbf{t}_\xi$ the Spin^c structure induced by ξ and (if $c_1(\mathbf{t}_\xi)$ is torsion) $d_3(\xi)$ its 3-dimensional invariant. Additionally, the contact invariant captures a lot of geometric information; in particular, it vanishes for all overtwisted structures, and it is non-vanishing for strongly fillable ones. It behaves naturally with respect to Legendrian surgeries; moreover [25]:

Theorem 3.2.1 (Ghiggini)**.** *There exists a unique, canonical,* Spin^c *structure* $\mathbf{k}$ *on a Stein cobordism* W *from* (Y_1,ξ_1) *to* (Y_2,ξ_2) *for which* $F^+_{W,\mathbf{k}}(c^+(\xi_2)) = c^+(\xi_1)$*, while* $F^+_{W,\mathbf{s}}(c^+(\xi_2)) = 0$ *for any other* $\mathbf{s} \in \mathrm{Spin}^c(W)$*.*

In particular, Legendrian surgery preserves non-vanishing of the contact invariant. Also, because of the U-equivariance of the induced homomorphisms, the U-depth $\sigma(Y,\xi) = -\max\{d; c^+(\xi) \in U^d \cdot \mathrm{HF}^+(-Y)\}$ of the contact invariant behaves monotonically with respect to the ordering by Stein cobordisms; the invariant σ was first introduced by Karakurt [44].

Although the contact invariant vanishes for many tight structures (in particular, in the presence of Giroux torsion [28], or its higher genus generalizations

[45]), it has proved to be useful in recognizing tightness of contact structures which are not (or not obviously) fillable, notably in the work of Lisca and Stipsicz [49, 50, 51, 52]. In most cases (including the ones we explore in Chapter 4) where it is known to be a complete classification invariant for tight contact structures, however, these structures can be set apart using only the homotopy type. Distinctively, in the case of Brieskorn spheres $-\Sigma(2,3,6n-1)$ the classification (due to Ghiggini and Van Horn-Morris [32]) of homotopic (non-isotopic) structures was resolved using contact invariants. For Stein fillable structures, Plamenevskaya [66] obtained the Heegaard Floer analogue of Theorem 2.2.5 of Lisca and Matić.

Theorem 3.2.2 (Plamenevskaya)**.** *If the* Spin^c *structures of the Stein structures* J_1 *and* J_2 *on the bounded compact* 4*-manifold* X *are not isomorphic, then the induced contact structures* ξ_1 *and* ξ_2 *on the boundary* $Y = \partial X$ *have distinct contact invariants* $c^+(\xi_1) \neq c^+(\xi_2) \in \mathrm{HF}^+(-Y)$*.*

This result basically follows from Theorem 3.2.1 applied on the Stein cobordism W from S^3 to Y. In the case of negative definite Stein plumbings, the fact that $F^+_{W,\mathbf{s}}(c^+(\xi))$ is non-trivial only for the canonical Spin^c structure, together with the definition of the isomorphism from the previous section, implies the following proposition (first observed by Karakurt [44]).

Proposition 3.2.3 (Karakurt)**.** *Let* (Y,ξ) *be a contact boundary of Stein negative definite plumbing* (X,J)*. Then the contact invariant* $c^+(\xi)$ *is mapped to the dual of the first Chern class* $c_1(J) \in \mathrm{H}^2(X;\mathbb{Z})$ *via the isomorphism* Φ *between* $\ker U \subset \mathrm{HF}^+(-Y)$ *and* $\mathrm{Hom}\Big(\frac{\mathbb{K}^+(\Gamma)}{\mathbb{Z}^{>0}\times \mathrm{Char}(\Gamma)}, \mathbb{F}\Big)$*.*

Finally, we look at how some properties of supporting open books reflect in the Heegaard Floer setting. First, the Heegaard diagram reformulation of the contact invariant (due to Honda, Kazez and Matić [41]) was in fact introduced parallel to the right-veeringness. The arc which is mapped to the left instantly gives rise to a disk in the differential of the Heegaard Floer complex which causes vanishing of the contact invariant. Higher-genus differentials have been closer studied only recently, in work of Kutluhan, Matić, Van Horn-Morris and Wand [45]. On the other hand, the planarity of contact structures is in the Heegaard Floer homology captured in the U-action, as noticed by Ozsváth, Stipsicz and Szabó [59]. Since any planar open book can be by adding positive Dehn twists only transformed into an open book for a lens space with its canonical contact structure, or alternatively because the capping off always brings us to a disk open book of (S^3,ξ_{std}), the U-equivariance of the induced maps gives the following.

Theorem 3.2.4 (Ozsváth-Stipsicz-Szabó)**.** *For a planar contact structure* ξ *on* Y *the contact invariant* $c^+(\xi) \in \mathrm{HF}^+(-Y)$ *is contained in* $U^d \cdot \mathrm{HF}^+(-Y)$ *for all* $d \in \mathbb{N}$*.*

3.2.1 Example

Once again we follow the exposition of Sections 2.2.4 and 2.3.1. The contact invariant of the standard contact structure on the 3-sphere is non-zero and lies in degree zero, it generates $\mathcal{T}^+_{(0)} \cong \mathrm{HF}^+(S^3)$. The contact invariant of the tight $S^1 \times S^2$ is non-zero, it belongs to the torsion Spin^c structure and has degree $\frac{1}{2}$, it generates $\mathcal{T}^+_{(\frac{1}{2})} \subset \mathcal{T}^+_{(\frac{1}{2})} \oplus \mathcal{T}^+_{(-\frac{1}{2})} \cong \mathrm{HF}^+(S^1 \times S^2, \mathbf{t}_0)$.

The contact invariant of an overtwisted structure (Y, ξ) vanishes. This can be seen directly using an open book which is not right-veering, or we can (again relying on the classification) build a Stein cobordism W on (Y, ξ) which contains a sphere of self-intersection -1 and hence induces $F^+_W = 0$.

Before looking into tight contact structures on small Seifert fibered spaces, we recall that most of these manifolds are actually L-spaces, in fact if $e_0 \neq -1$ or -2, all of them are. Now, if the contact invariant of some ξ on an L-space is non-vanishing, then its 3-dimensional invariant necessarily agrees with the d-invariant of the induced Spin^c structure. Since all tight structures on lens spaces and on small Sefert fibered spaces with $e_0 \neq -1$ (with additional assumption of being an L-space when $e_0 = -2$) are actually fillable, we have for all of them $d_3(\xi) = d(M, \mathbf{t}_\xi)$ and $c^+(M, \xi)$ generates $\mathcal{T}^+_{(d_3(\xi))} \cong \mathrm{HF}^+(Y, \mathbf{t}_\xi)$. For a zero-twisting structure ξ on $M = M(-1; r_1, r_2, r_3)$, the non-vanishing $c^+(M, \xi) \neq 0$ implies $d_3(\xi) = d(M, \mathbf{t}_\xi)$ even if M is not an L-space, because we have observed that all these structures are planar and so Theorem 3.2.4 applies to them. Recall that such ξ is given by five -1-linked Legendrian unknots of $\mathrm{tb} = -1$, performing $+1$-surgery along two of them, and contact $-\frac{1}{r_i}$-surgery along the other three. Lisca and Stipsicz [51] established the reverse implication.

Theorem 3.2.5 (Lisca-Stipsicz)**.** *If for ξ as above on $M(-1; r_1, r_2, r_3)$ with $r_1 + r_2 + r_3 - 1 > 0$ the equality $d_3(\xi) = d(M, \mathbf{t}_\xi)$ holds, then its contact invariant $c^+(M, \xi) \in \mathrm{HF}^+(-M, \mathbf{t}_\xi)$ does not vanish.*

We summarize their argument. According to Theorem 3.2.1, the contact invariant $c^+(M, \xi)$ equals $F^+_{-W,\mathbf{k}}(c^+(M', \xi'))$ for the canonical Spin^c structure $\mathbf{k}$ on the cobordism W induced by one $+1$-surgery. Since ξ' is a Stein fillable structure on $M' = M(0; r_1, r_2, r_3)$, its contact invariant $c^+(M', \xi')$ does not vanish and it satisfies $d_3(\xi) = d(M, \mathbf{t}_\xi)$. The result now follows from the injectivity of $F^+_{W,\mathbf{k}}$, which in turn is a consequence of negative definiteness of W (inducing an isomophism on the HF^∞-level), taking into account $\mathbb{F}[U]$-equivariance and the degree-shift by $-d_3(\xi) + d_3(\xi')$, which by assumption equals to $d(-M, \mathbf{t}_\xi) - d(-M', \mathbf{t}_{\xi'})$. In the case of L-spaces, Lisca and Stipsicz [52] actually gave a geometric realization of the equality $d_3(\xi) = d(M, \mathbf{t}_\xi)$ which allows us in Chapter 4 to systematically analyze tightness of zero-twisting structures on $M(-1; r_1, r_2, r_3)$.

4

Tight contact structures on $M(-1; r_1, r_2, r_3)$

The existence question for tight contact structures on Seifert manifolds has been completely answered by Lisca and Stipsicz [52]: only the ones which belong to the one-parameter family of $(2n-1)$-surgeries on the torus knot $T_{2,2n+1}$ (equivalently, which are orientation preserving diffeomorphic to $M(-1; \frac{1}{2}, \frac{n}{2n+1}, \frac{1}{2n+3})$ for some $n \in \mathbb{N}$) do not admit any tight structure. Classification then arises from the comparison of bounds: the lower bound is obtained constructively by contact surgery complemented with the use of invariants, and for the upper bound convex surface theory is used.

The main invariant in the classification of tight Seifert fibered manifolds is the maximal twisting number (of a regular fiber; as defined in Section 2.2.1) – applied in convex surface theory, it allows one to give upper bounds on the number of tight structures. By the results of Wu [75] all tight contact structures when $e_0 \leq -2$ have negative maximal twisting, while for $e_0 \geq 0$ they are all zero-twisting; in the work of Ghiggini [25] the negative maximal twisting is further related to the existence of transverse contact structures. This, in the case of L-spaces, results in a simple division: maximal twisting is equal to zero when $e_0 \geq -1$, and has value -1 when $e_0 \leq -2$. The fixed maximal twisting of a regular fiber in all the cases gives some unique contact structure on the complement of singular fibers relative to boundary (see Theorem 2.2.2), pushing the classification into tubular neighborhoods of the three singular fibers.

As presented in Section 2.2.4, the classification whenever $e_0 \neq -1$ is then finished by Legendrian surgery construction – the diagrams are simply given by legendrianization of the standard presentation of a Seifert manifold; this has been done by Wu [75] for $e_0 \neq -2, -1, 0$, by Ghiggini, Lisca and Stipsicz [29] for $e_0 \geq 0$, and by Ghiggini [25] for L-spaces with $e_0 = -2$. In particular, all these tight structures are Stein fillable, and are classified by the first Chern class of their fillings (according to Lisca and Matić, Theorem 2.2.5), or closer to the present context by their contact Ozsváth-Szabó invariants (according to Plamenevskaya, Theorem 3.2.2).

In the following, we will explore the remaining case of $M(-1; r_1, r_2, r_3)$ which

are rational homology spheres ($e(M) \neq 0$). Note that the family of Seifert manifolds which do not admit fillable contact structures, as well as the family of Seifert manifolds without tight contact structures, are of this type. Also, as we will see in Chapter 5, some of these manifolds admit both fillable and non-fillable tight structures. Remember that tight structures when $e_0 = -1$ are essentially of two flavors: zero-twisting and negative twisting. Negative twisting structures are conjecturally characterized as surgeries on transverse contact structures. As such, their contact class is never vanishing in reduced Heegaard Floer homology; they are expected all to be symplectically fillable. A complete classification of (mainly) negative twisting structures was achieved on Brieskorn spheres $-\Sigma(2,3,6n-1)$ by Ghiggini and Van Horn-Morris [32]; note also that the examples (due to Ghiggini) of strongly but not Stein fillable contact structures are on these manifolds [24]. Our goal here is to understand the zero-twisting structures. As mentioned in Section 2.2.4, Lisca and Stipsicz gave the following uniform surgery description of them. Since they are all planar (see Section 2.3.1), their contact invariant (if non-vanishing) always lies in the tower $\mathcal{T}^+_{d(-M,\mathbf{t}_\xi)} \subset \mathrm{HF}^+(-M,\mathbf{t}_\xi)$.

Proposition 4.0.1. [51, Proposition 6.1] *Each tight contact structure with maximal twisting equal to zero on the small Seifert fibered space $M(-1;r_1,r_2,r_3)$ is given by one of the surgery presentations of Figure 4.1 left.* □

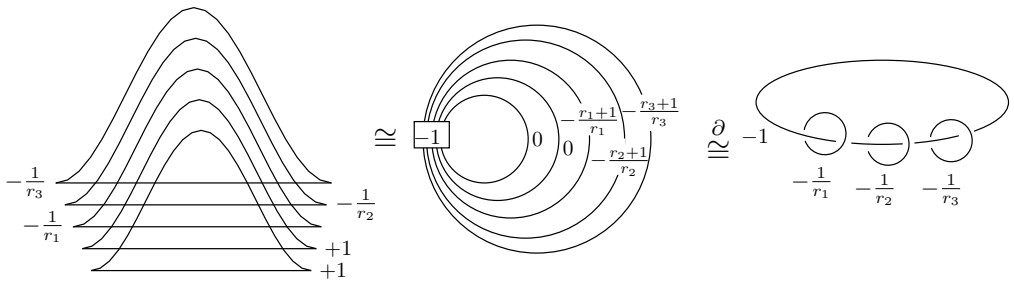

Figure 4.1: Contact structures on $M(-1;r_1,r_2,r_3)$, followed by the smoothened surgery diagram of the underlying 3-manifold and its standard presentation; when referring to them as 4-manifolds, we assume inverse slam-dunks to be done and we denote them X and W.

By means of Section 2.2.3, this reduces the classification problem to the recognition of tightness and isotopies between the finite collection of structures, listed by the associated Thurston-Bennequin and rotation numbers. We devote this chapter to the study of their Ozsváth-Szabó contact invariants.

4.1 Contact invariant in lattice homology

Let the initial setting of this section be slightly more general; we consider Seifert manifolds M of the form $M(-1; r_1, \dots, r_n)$ with $e(M) = -1 + r_1 + \cdots + r_n > 0$, together with the contact structures ξ as in Figure 4.2.

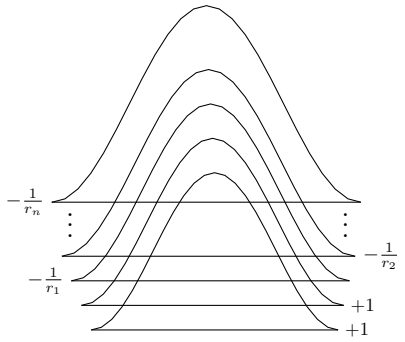

Figure 4.2: Contact structures on $M(-1; r_1, \dots, r_n)$.

A characteristic property of these 3-manifolds is that their orientation reversals bound negative definite star-shaped plumbings. Recall from Section 3.1, that for the latter, Ozsváth and Szabó give a combinatorial description of their Heegaard Floer homology in terms of characteristic cohomology elements of the plumbing they bound. Specifically, for $-M = \partial W_{\Gamma'}$ we have an isomorphism Φ from Theorem 3.1.1 identifying $\mathrm{Hom}\left(\frac{\mathbb{K}^+(\Gamma')}{\mathbb{Z}^{>0}\times \mathrm{Char}(\Gamma')}, \mathbb{F}\right) \cong \ker(U) \subset \mathrm{HF}^+(-M)$.

We focus on the pair of star-shaped plumbed 4-manifolds W_Γ and $W_{\Gamma'}$ which arise as complementing parts in $R = \mathbb{C}P^2 \# N\overline{\mathbb{C}P}^2$ when cut along a hypersurface M. The configurations of the two intersection graphs Γ, Γ' are obtained by blowing-up the initial lines $l_1, \dots, l_n \subset \mathbb{C}P^2 : l_1 \cap \cdots \cap l_n = \{p\}$, and $l \subset \mathbb{C}P^2 : p \notin l$, as shown in Figure 4.3 (see [52, Lemma 4.2]).

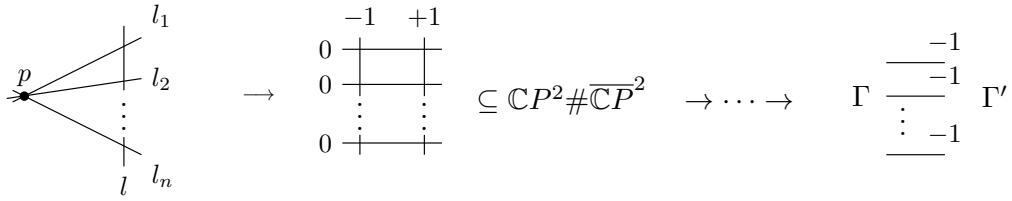

Figure 4.3: $R \backslash \nu(M) = W_\Gamma \cup W_{\Gamma'}$.

Via the embedding $W_\Gamma \cup W_{\Gamma'} \hookrightarrow R$ (as given in Figure 4.3) the vertices of the intersection graphs Γ and Γ' can be expressed in the standard generators of $\mathrm{H}_2(R; \mathbb{Z})$:

- $\{z = \text{ center of } \Gamma\} \mapsto e_1$

- $\{z' = \text{ center of } \Gamma'\} \mapsto h - e_2 - \cdots - e_{n+1}$
- $\{x_i = \text{ first vertex of the leg } L_i \subset \Gamma\} \mapsto h - e_1 - e_{i+1} - \sum e_j$ for $i = 1, \ldots, n$
- $\{v \text{ vertex}, v \neq z, z', x_i\} \mapsto e_j - \sum e_l$, for example
  $\{x_i' = \text{ first vertex of the dual leg } L_i' \subset \Gamma'\} \mapsto e_{i+1} - \sum e_l$ for $i = 1, \ldots, n$.

We will refer to Γ as the manifold side and Γ' as the dual side. Throughout, we will follow the convention that primed notation belongs to the dual graph: apart from the special vertices denoted above, let v_j^i be the j^{th} vertex of L_i and $v_j^{i'}$ the j^{th} vertex of L_i'.

Motivated by the geometric realization of the condition $d_3(\xi) = d(M, \mathfrak{t}_\xi)$ given by Lisca and Stipsicz in [52, Theorem 3.3] (see also the end of Section 3.2.1), we pick a specific characteristic class in $\mathrm{H}^2(W_{\Gamma'}; \mathbb{Z})$ which we name contact covector in the light of the theorem stated below.

Definition 4.1.1. Denote by h and e_i the standard generators of $\mathrm{H}_2(R; \mathbb{Z})$ and define a class $c \in \mathrm{H}^2(R; \mathbb{Z})$ through its Poincaré dual by $\mathrm{PD}(c) := \alpha h + \sum \alpha_i e_i$ where $\alpha, \alpha_i \in \{\pm 1\}$ are constrained by the surgery presentation on W_Γ as follows: $c|_{W_\Gamma}$ corresponds through the central blow-up to the Spin^c structure whose first Chern class evaluates as rotation numbers on surgery generators (see Figure 4.4). Let us call the restriction $c' := c|_{W_{\Gamma'}}$ the *contact covector*.

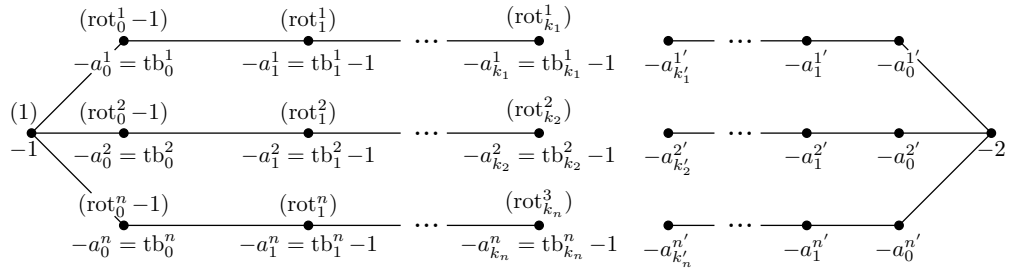

Figure 4.4: Plumbing graph Γ (left) and its dual Γ' (right) with denoted self-intersections and evaluations of characteristic covector c, $(\cdot) = \langle c, v \rangle$, on the manifold side; the central and the first vertices on legs are given in generating classes of $\mathrm{H}_2(R; \mathbb{Z})$.

Although c, and hence the contact covector, is not uniquely determined, different classes specify the same element in $\mathbb{K}^+(\Gamma')$ (see Lemma 4.1.6).

Theorem 4.1.2. *Let (M,ξ) be any of the contact Seifert fibered 3-manifolds given by Figure 4.2 for which $e(M) = -1+r_1+\cdots+r_n > 0$. Then the contact invariant $c^+(\xi)$ is mapped to the dual of the contact covector c' via the isomorphism Φ between $\ker U \subset \mathrm{HF}^+(-M)$ and $\mathrm{Hom}\Big(\frac{\mathbb{K}^+(\Gamma')}{\mathbb{Z}^{>0}\times \mathrm{Char}(\Gamma')}, \mathbb{F}\Big)$.*

In the remaining of the section we study the Heegaard Floer behavior of the contact covector which eventually leads to the verification that it plays a role of the contact invariant (proof of Theorem 4.1.2).

Notice that any class c as in Definition 4.1.1 satisfies $c^2 = \sigma(R)$. Since c restricts to c_Γ, corresponding to $c(X, \mathbf{s}_J)$, on W_Γ, it satisfies

$$d_3(\xi) = \frac{1}{4}(c_\Gamma^2 - 3\sigma(W_\Gamma) - 2b_2(W_\Gamma)) + 1 = \frac{1}{4}(c_\Gamma^2 - \sigma(W_\Gamma));$$

and since the degree of c' in $\mathbb{K}^+(\Gamma')$ is defined to be

$$\deg(c') = \frac{1}{4}(c'^2 + |\Gamma'|) = \frac{1}{4}(c'^2 - \sigma(W_{\Gamma'})),$$

the equality $c^2 = \sigma(R)$ is equivalent to $-d_3(\xi) = \deg(c')$. When M is an L-space [52, Theorem 3.3], properly ending full path of c' (that is, c' being non-trivial in $\ker U \subset \mathrm{HF}^+(-Y)$) suffices to conclude that $-d_3(\xi) = d(-M; \mathbf{t}_\xi)$, hence by Theorem 3.2.5 also $c^+(M,\xi) \neq 0$, and also that c' represents $c^+(M,\xi)$ in $\mathbb{K}^+(\Gamma')$. In general however, even if the full path ends properly, the degree $\deg(c')$ might be different from $d(-M, \mathbf{t}_\xi)$, in which case $c^+(M,\xi)$ (of a planar structure) vanishes, or even if $\deg(c') = d(-M, \mathbf{t}_\xi)$, the element c' might not lie in the tower $\mathcal{T}^+_{(-d_3(\xi))}$.

4.1.1 Full path of contact covector

We study full path of the contact covector on the level of homology generators of $\mathrm{H}^2(R;\mathbb{Z})$. This allows us to follow the corresponding changes on the manifold side. Proofs in this section are straightforward but technical.

Notation 4.1.3. We describe a characteristic cohomology element $c \in \mathrm{H}^2(R;\mathbb{Z})$ as $\mathrm{PD}(c) = \alpha h + \sum \alpha_i e_i$ where $\alpha, \alpha_i \in \{\pm 1\}$. In the following, vectors of signs correspond to parts of the coefficient-vector (α, α_i), covering generators of (usually) a single Γ- or Γ'-vertex.

We often refer to a single vertex by its self-intersection. When a vertex is written out in generating classes, these are called starting, middle and last, according to the position; explicitly, if $v = e_s - \sum_{j=s+1}^{l} e_j$, then e_s is starting, e_l is last, and all others are middle. On legs, the starting generator of a vertex and the last generator of the previous vertex coincide.

Presentability will be assigned to dual vectors $c|_{\Gamma'}$ and it means that the corresponding manifold side arises from a contact presentation, that is, $c|_{\Gamma'}$ is a contact covector of some presentation.

Let our starting point be a characteristic vector $c \in \mathrm{H}^2(R;\mathbb{Z})$ which comes from a contact presentation, and which satisfies $v \cdot v \leq \langle c, v\rangle \leq -v \cdot v$ (otherwise the full path has already dropped out). We will follow the path only in one direction – towards the initial vector. Recall that the corresponding step is given by $c \mapsto c - 2\,\mathrm{PD}(v)$ for some v with $\langle c, v\rangle = v \cdot v$, and the vector we aim at satisfies $v \cdot v + 2 \leq \langle c, v\rangle \leq -v \cdot v$. Everything could be verbatim repeated with opposite signs in the direction of the terminal vector.

Steps on legs

First, we observe that steps taken for $v \neq z'$ never change the surgery presentation considered, nor does the path drop out at any of these vertices.

Lemma 4.1.4. *Characteristic vectors c and $c - 2\,\mathrm{PD}(v)$ for $v \neq z'$ with $\langle c, v\rangle = v \cdot v$, always belong to the same surgery presentation.*

Proof. As these vertices ($v \in \Gamma', v \neq z'$) are described by $v = e_i - \sum e_j$, the evaluation of the characteristic covector c reaches the self-intersection when presenting generators all admit the same sign as in the vertex. So, $-2\,\mathrm{PD}(v)$ changes their signs from $(+ - \cdots -)$ to $(- + \cdots +)$. But this change has no effect on the evaluation of c on any of the Γ-vertices.

Indeed, from the way how the exceptional classes are chosen we see that each e_j starts some new vertex, either one on the manifold side or one on the dual side. So, the starting and the last generator of v are non-starting on the manifold side, while all its middle generators are starting (and last) generators of manifold vertices. Hence, the restriction of c to the generators of v evaluates trivially on Γ, that is, $\langle c|_v, \Gamma\rangle = 0$, and is therefore independent of sign.

Since these (manifold-side) evaluations directly correspond to rotation numbers, with neither of these moves do we switch between presentations. □

Lemma 4.1.5. *All drop-outs occur in the center $z' = h - e_2 - \cdots - e_{n+1}$ of the dual star.*

Proof. We notice that all the vertices in legs of Γ' are formed by exactly as many generators (e_j's) as the value of their self-intersections. Hence, there is no way to drop out at any of them. So, the only possible drop-out happens at z' when the signs of generators h and $e_2, \ldots, e_{n+1}$ are all the same, and $\langle c, z'\rangle = \pm(n+1)$. □

In sum, we may assume the initial condition $v \cdot v + 2 \leq \langle c, v\rangle \leq -v \cdot v$ is violated only at the central vertex z' – such a vector can be easily reached by finishing all possible $-2\,\mathrm{PD}$-steps on legs, which either sweep out the problem or transfer it to the center. (As each $-2\,\mathrm{PD}$-step pushes the problem to the neighboring vertices, we are successively completing the steps, as long as we do not run into a vertex v which despite of the -2-change does not evaluate as $v \cdot v$,

or we reach the end of the leg.) In particular, neither non-central vertex is of the form $(+ - \cdots -)$.

Contact covector is well-defined

We check that the contact covector c' is well-defined as an element of $\mathbb{K}^+(\Gamma')$.

Lemma 4.1.6. *Any two contact covectors associated to ξ (via Definition 4.1.1) are related by a sequence of full path steps.*

Proof. Contact covectors are restrictions to $W_{\Gamma'}$ of characteristic vectors $c \in \mathrm{H}^2(R;\mathbb{Z})$ for which $c^2 = \sigma(R)$ (ensured by expansion of $\mathrm{PD}(c)$ as $\{\pm 1\}$-linear combination of generators), and whose evaluations on all the manifold vertices agree. So, once we connect any two characteristic vectors $c \in \mathrm{H}^2(R;\mathbb{Z})$ which have the same evaluations on the manifold side, by full path steps (not necessarily a path) we are done.

Let us successively turn both of them into the same characteristic vector applying only $-2\,\mathrm{PD}$ steps which do not change the presentation. First, we apply steps on legs to both of them.

Observe a simple consequence of the above reduction.

Lemma 4.1.7. *After all steps on legs (in the initial direction) are done, a presentable covector on no dual vertex takes the form $(+ - \cdots - +)$.*

Proof. Suppose on the contrary, there is such a dual vertex; it is not the last vertex of the dual leg, because it would give the last vertex on the manifold side with self-intersection -2 and c-evaluation $+2$. But then, every non-(-2) dual vertex further on the dual leg needs to have again negative middle signs (otherwise we have found a manifold vertex, starting in the negative sign of the previous non-(-2) with all following generators positive) and positive last one (because of $(+ - \cdots -)$ exclusion). After all, we end in the impossible last dual vertex. □

Therefore, since the middle generators of dual vertices are same-signed and because of the rotation number constraints on the manifold side, the dual non-central vertices need to be of one of the following forms $(- - \cdots - -), (- + \cdots + -), (- + \cdots + +), (+ + \cdots + -)$ or $(+ + \cdots + +)$. If the two vectors (after steps on legs are applied) disagree on the generators of some dual leg L'_i, they disagree already on x'_i, taking the form $(+ \cdots + -)$ on one and $(- \cdots -)$ on the other. But then c-evaluations on x_i disagree unless the sign of h is different in the two configurations. But this in turn requires that the signs on the generators of all dual legs are related in the same way as the ones on L'_i, and after adding $-2z'$ to the covector with positive h-sign the two vectors coincide. □

Central step

After finishing all steps on legs, covector c either drops out at z', presents the initial vector or, it reaches self-intersection at z'. For the latter, the generators forming $z' = h - e_2 - e_3 - \cdots - e_{n+1}$ take values: either $(+ - - \cdots -)$ or $(- + - \cdots -)$, up to reordering the legs. The -2 PD-step taken next changes exactly these generators by twice $(- + + \cdots +)$. In the first, trivial, case we stay in the same presentation, as the step only switches the signs in the pairs $(h, e_i), i = 2, \ldots, n+1$, preserving the evaluation on all the influenced manifold vertices, $x_1, \ldots, x_n$. In the second case, we can (on the level of generators) instead of simply adding $-2z'$ to the given description of $\mathrm{PD}(c)$, first change the sign configuration, without changing the dual $c|_{\Gamma'}$ and with controlled (seen later) change on the manifold side $c|_\Gamma$, and then do the -2 PD-step as above, not influencing the manifold side.

Algorithm 4.1.8 (Central step or turn)**.** Whenever we arrive, after possibly renumbering the legs, at c with $(h, e_2, e_3, \ldots, e_{n+1}) = (- + - \cdots -)$ and $\langle c, v\rangle \neq v \cdot v$ for all $v \neq z'$, the next step in the full path is given by the characteristic covector $\bar{c}$ as follows. Denoting vertices of L'_1 by $\{v'_0, \ldots, v'_{k'_1}\}$ and their generators as $v'_i = e^i_1 - \sum_{j=2}^{l_i} e^i_j$ with $e^i_{l_i} = e^{i+1}_1$ and $e^0_1 = e_2$, define $\mathrm{PD}(\bar{c}) = \mathrm{PD}(c) + 2h - 2e_2$ and modify it as follows:

$$\begin{array}{lll} \text{for } i \in \{0, \ldots, k'_1\} & \text{if } \langle \bar{c}, e^i_1\rangle \neq \langle c, e^i_1\rangle : & \text{for } j \in \{2, \ldots, l_i\} \\ & & \quad \text{if } \langle c, e^i_j\rangle = +1 : \\ & & \quad \mathrm{PD}(\bar{c}) := \mathrm{PD}(\bar{c}) - 2e^i_j \text{ \& endfor} \\ & \text{if } \langle \bar{c}, e^i_1\rangle = \langle c, e^i_1\rangle : & \text{stop.} \end{array}$$

Then add $-2z'$ to the so obtained sign configuration $\mathrm{PD}(\bar{c})$.

To prove well-definedness, we need that this reformulation always exists (the inner loop in our Algorithm always stops; see Lemma 4.1.9) and that uniqueness, ensured by always taking the first positive generator (chosen ordering of the inner loop), can be explained by the independence of order, at least as far as contact presentations are concerned (Lemma 4.1.10).

Lemma 4.1.9. *Every characteristic vector $c_{\Gamma'}$ with $\mathrm{PD}(c|_{z'}) = (- + - \cdots -)$ can be achieved by another distribution of signs, with positive sign on h; it is associated to a different manifold vector (possibly non-presentable).*

Proof. Starting at the center z', the two distributions are given by $(- + - \cdots -)$ and $(+ - - \cdots -)$. The switch of the h-sign with the opposite sign of e_2, does not impose any change into dual legs other than the first. For the first leg, the appropriate adaptation of signs, which results in the same dual evaluation, exists because of the exclusion of any $(+ - \cdots -)$-configurations (that is, the assumption $\langle c, v\rangle \neq v \cdot v$ for any $v \neq z'$). □

Lemma 4.1.10. *If a sign on one middle generator of a dual vertex is changed, all of them need to be changed (independent of order) before we get back into presentable. A turn of the last generator can result in a presentable vector only when all prior middle generators are negative.*

Proof. For a covector to be presentable, all dual vertices have to have same-signed middle generators, because these generators on the manifold side are forming a chain of -2's, zero being their only possible rotation number.

For the second claim, suppose on the contrary the middle signs on some v' are positive. Changing the sign of its last generator (from positive to negative) forces a switch of all the signs in the following chain (if any) of dual -2's (to preserve dual evaluations). Then, this influences the evaluation on the next non-(-2) dual vertex w', which can be corrected by changing one of its later generators from positive to negative. If the middle generators of w' are already negative or if we get them all negative by the current turn, we have found (independent of further changes) a manifold-side vertex which starts at positive (second last) generator in v' and has all further signs negative. If by the change of one middle generator not all of them are negative, the vector is non-presentable by the first part. If all generators of w' are positive, and we turn the last one, we need to repeat the same argument with w' in place of v'. It remains to check whether we could get presentable result by correcting only starting and last generators of all following (necessarily, fully positive) dual vertices. But if not before, the process ends in non-presentable, giving $(+ - \cdots -)$ on the last manifold vertex. □

To sum up, the central turns are the only significant steps in following possible changes on manifold vectors, and by that, in presentations. We may assume that after each central turn also all -2 PD-steps on legs are finished.

Necessary for proper ends

Lemma 4.1.11. *If after a central step, the covector c on the starting dual vertices evaluates as their self-intersection, that is, $\langle c, x'_i\rangle = x'_i \cdot x'_i$:*

- *on at most $n-2$ legs, we have arrived at the initial end;*
- *on $n-1$ legs, the full path continues;*
- *on all n legs, this causes a drop-out.*

Proof. The maximal starting dual evaluations tell us on how many legs we need further -2 PD-steps. The evaluation $\langle c, z'\rangle$ on z' right after a central turn is $n-1$. If further turns are needed for $n-2$ legs only, we do not reach a $1-n$ central evaluation again and the corresponding vector is initial; with $n-1$ we get back to $\langle c, z'\rangle = 1-n$ and we continue with another central turn; n gives a drop-out in $(h, e_2, \ldots, e_{n+1}) = (- - \cdots -)$. □

Corollary 4.1.12. *A presentation ξ, whose contact covector has a full path with proper ends, admits a leg, starting in a fully positive vertex. (If the presentation corresponds to the initial vector, there are at least two fully positive starting vertices.)*

Proof. For PD(c) take a sign configuration which evaluates on manifold vertices according to the rotation numbers of ξ, which takes minus sign on h, and for which $\langle c, v' \rangle \neq v' \cdot v'$ for all $v' \in \Gamma' \backslash \{x'_i; i = 1, \dots, n\}$. (This is the stage right after a central turn.) As in Lemma 4.1.11 above, there is a leg, say L_1, for which $\langle c, x'_1 \rangle \neq x'_1 \cdot x'_1$. We prove that on this leg $\langle c, x_1 \rangle = a^1_0 - 2$ holds, that is, the generators of x_1 (apart from h, e_1) are positive.

Write out x_1 as $h - e_1 - e_2 - e_5 - \cdots - e_J$. The signs on the generators up to e_{J-1} are positive as otherwise we would have shuffled the negative sign to e_5 by -2 PD-steps on consecutive dual vertices of square -2 (resulting in $\langle c, x'_1 \rangle = -2$ for $x'_1 = e_2 - e_5$). The positivity of e_J follows from presentability, as it is a middle generator of a dual vertex starting in positive e_{J-1}. Indeed, the middle generators of any dual vertex are same-signed, and the $(+ - \cdots -)$-configuration as well as $(+ - \cdots - +)$-configuration are excluded; the first by assumption $\langle c, v' \rangle \neq v' \cdot v'$ for $v' \neq x'_i$, the second by Lemma 4.1.7. □

4.1.2 Contact covector represents contact invariant

We prove Theorem 4.1.2, first for some overtwisted structures, then for some fillable structures, and finally for the general case. Sufficient conditions for overtwistedness and fillability which we use in this section are for $M(-1; r_1, r_2, r_3)$ special cases of conditions we obtain in Section 4.2.3 and Section 5.2.

Overtwisted structures We consider a convex decomposition of the manifold $M(-1; r_1, \dots, r_n)$ with a zero-twisting structure (Figure 4.2) into a product of the n-punctured sphere with the circle $\Sigma \times S^1$ (the background), and the neighborhoods of the n singular fibers. We trivialize the separating tori by the section and the fiber in the background basis, and by the meridian and a longitude in the standard toric basis, so that the gluing maps are described by $A_i = \left(\begin{smallmatrix} \alpha_i & \alpha'_i \\ -\beta_i & -\beta'_i \end{smallmatrix}\right) \in \mathrm{SL}_2(\mathbb{Z})$ where $\frac{\beta_i}{\alpha_i} = r_i$ (or $r_1 - 1$ for the first leg). In particular, the infinite boundary slope of the thickened neighborhoods of singular fibers correspond to $-\frac{\alpha_i}{\alpha'_i} = [a^i_{k_i}, ..., a^i_0]$ in the toric basis. The boundary slopes in the basic slice decomposition of the considered neighborhoods (that is, the factorizations of the solid tori) are given – in order from outside in – by decreasing the last entry of the continued fraction. (Recall Section 2.2.1 for details.)

Proposition 4.1.13. *Necessarily for tightness, the presentation admits a leg i starting in the unknot with* $\mathrm{rot}^i_0 = \mathrm{tb}^i_0 + 1 = -a^i_0 + 1$ *or a leg starting in the unknot with* $\mathrm{rot}^j_0 = -\mathrm{tb}^j_0 - 1 = a^j_0 - 1$.

Proof. (The proof builds on its special case [30, Proposition 6.3].) Conditions say that the presentation should contain a fully positively stabilized or a fully negatively stabilized starting unknot. Equivalently, in the light of convex decompositions, signs of all slices in the basic slice decomposition of the corresponding toric annulus are the same.

Assume the contrary, there is no leg satisfying either condition. This means, that all neighborhoods of singular fibers admit a positive as well as a negative basic slice in their outermost continued fraction blocks. We start with the first two singular fibers F_1 and F_2, we shuffle the basic slices of their outermost continued fraction blocks so that the outermost basic slices have the same sign. Peeling off these slices from the singular tori, we hit the tori of slope 0 and -1 in the background basis. Connecting their rulings by an annulus (which admits no one-sided dividing curves) and edge-rounding, we obtain a torus surrounding both fibers, and of 0-slope. By adding a bypass to its back (which exists because the background is zero-twisting) we obtain a basic slice around F_1 and F_2 together, with boundary slopes 0 and ∞. Then we successively expand this toric annulus so that it contains more and more singular fibers, by always cutting between its 0-slope boundary and the -1-slope torus which peels off the outermost basic slice of F_i we are including; since we have both, positive and negative, outer basic slices around each F_i, we can always shuffle them so that the outermost sign agrees with the sign of the joint basic slice. Eventually, we obtain a torus of slope 0 around the (last remaining) singular fiber F_n. The toric annulus between this torus and the ∞-slope boundary of the neighborhood of F_n, forms a basic slice. Pulled-back (in the toric basis of F_n) the 0-slope equals $[a^n_{k_n}, ..., a^n_1]$, which means that the outermost continued fraction block of F_n together with this additional basic slice gives a glued-together basic slice (having subsequent boundary slopes $[a^n_{k_n}, ..., a^n_1 - 1], [a^n_{k_n}, ..., a^n_1]$), and by Gluing Lemma it is tight exactly when all its subslices have the same sign. In particular, all the signs in the outermost continued fraction block of F_n are the same, contradicting our assumption. □

Corollary 4.1.14. *Theorem 4.1.2 holds for (M, ξ) which admits neither any starting unknot with $\mathrm{rot}^i_0 = \mathrm{tb}^i_0 + 1 = -a^i_0 + 1$ nor with $\mathrm{rot}^j_0 = -\mathrm{tb}^j_0 - 1 = a^j_0 - 1$.*

Proof. According to Proposition 4.1.13, (M, ξ) is overtwisted, in particular $c^+(M, \xi) = 0$. According to Corollary 4.1.12, the full path of its associated contact covector drops out. □

Fillable structures

Proposition 4.1.15. *Contact surgery diagram as in Figure 4.2 with $n = 2$, with surgery coefficients equal to $r_1 = \frac{1}{p}$ and $r_2 = \frac{p-1}{p}$ for $p \in \mathbb{N}$, and stabilizations chosen so that $\mathrm{rot}^1_0 = \pm(p-1)$ and $\mathrm{rot}^2_0 = \mp 1$, describes the tight $S^1 \times S^2$.*

Proof. Described surgery is a special instance of surgery diagrams studied in Section 5.2, where we obtain a positive factorization for the corresponding planar monodromy. We give here an alternative proof in the light of Heegaard Floer theory.

The proof is based on an interpretation of a surgery exact triangle relating orientation reversals of manifolds, smoothly given by four -1-linked unknots with framing coefficients $x, 0, -p-1, -\frac{2p-1}{p-1}$, where x stands for $\infty, 0, -1$, and the underlying manifolds are $-L(p^2, p-1), S^1 \times S^2$, and $L(p,1)\# - L(p,1)$, respectively.

Here cobordism X between $L(p^2, p-1)$ and $S^1 \times S^2$ corresponds to one contact $+1$-surgery. The associated map in Heegaard Floer homology relates contact invariants of the two ends $F_{-X}(c(L(p^2, p-1), \zeta)) = c(S^1 \times S^2, \eta)$. As $c(L(p^2, p-1), \zeta) \neq 0$ (given by Legendrian surgery on the standard tight $S^1 \times S^2$) we wish to prove that for ζ given by $\mathrm{rot}_0^1 = \pm(p-1)$ and $\mathrm{rot}_0^2 = \mp 1$, it is not in the kernel of F_{-X}.

Now, for the purpose of the following consideration we simplify the presentation by Kirby moves of Figure 4.5.

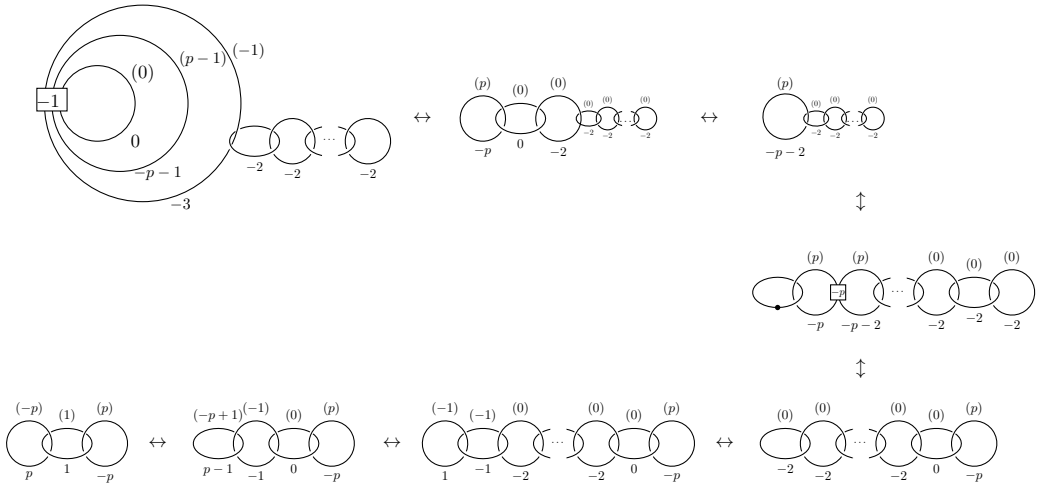

Figure 4.5: Kirby diagrams for $L(p^2, p-1)$ with Spin^c structure $\mathbf{t}_\zeta$.

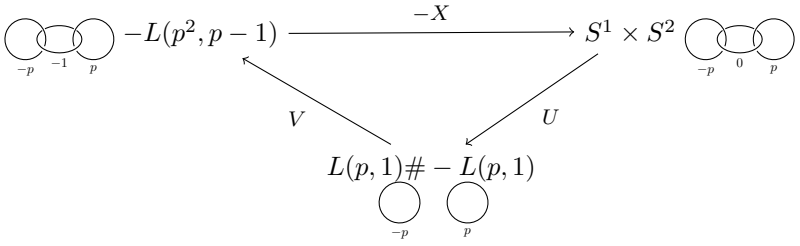

Figure 4.6: Surgery exact triangle.

Consider surgery exact triangle of Figure 4.6. The cobordisms $-X$ and U have zero signature, while V is generated by $(1,p,-1)$ in the given presentation of $W_{-L(p^2,p-1)}$, whose square is $-p^2$, so we have $\chi(V)=1, \sigma(V)=-1$. Associated Heegaard Floer exact triangle takes the following form.

$$\begin{array}{ccc} \mathbb{Z}_2^{p^2} \cong \widehat{\mathrm{HF}}(-L(p^2,p-1)) & \xrightarrow{\quad F_{-X} \quad} & \widehat{\mathrm{HF}}(S^1\times S^2) \cong \mathbb{Z}_2 \oplus \mathbb{Z}_2 \\ & {\scriptstyle F_V} \nwarrow \quad \swarrow {\scriptstyle F_U} & \\ & \widehat{\mathrm{HF}}(L(p,1)\#-L(p,1)) \cong \mathbb{Z}_2^{p^2} & \end{array}$$

Since $\sigma(-X)=\sigma(U)=0$ and all nontrivial components of F_{-X} and F_U are induced by torsion Spin^c structures, the degree-shift of both F_{-X} and F_U is $-\frac{1}{2}$. The degree-shift for F_V at Spin^c structure $\mathbf{s}=(i,k,j)$ is $\frac{c_1^2(\mathbf{s})+1}{4}$ where for 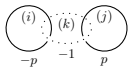

$c_1^2(\mathbf{s}) = \frac{\langle c_1(\mathbf{s}),(1,p,-1)\rangle^2}{-p^2} = \frac{(i+pk-j)^2}{-p^2}$. Furthermore, from the exactness of Heegaard Floer triangle we observe that dimensions of the kernel of F_{-X}, F_U, F_V are $p^2-1, 1, 1$, respectively.

Let us look at the spin structure $\mathbf{t}^{L\#-L}_{(-p,p)} =$ 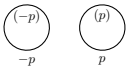

on $L(p,1)\#-L(p,1)$; corresponding Heegaard Floer group is supported in degree 0, $\widehat{\mathrm{HF}}(L\#-L,\mathbf{t}^{L\#-L}_{(-p,p)}) = \mathbb{Z}_{2(0)}$, and we will denote its generator by a.

Since the degree-shift of $F_{(V,\mathbf{s})}$ is non-positive for all $\mathbf{s}\in \mathrm{Spin}^c(V)$ (because of U-equivariance of HF-maps), we can expend $F_V(a) = c(\zeta)+\overline{c(\zeta)}+\sum_{\deg b<0} b$. The contact class $c(\zeta)$ (and its conjugate) are reached by the only degree-zero Spin^c cobordisms, that is for $k=1$ (and 3). Now, as the degree $\deg b<0$, b-elements are all in the kernel of F_{-X} which coincides with the image of F_V; and so, for every b exists b' such that $F_V(b')=b$. We are left with $F_V(a+\sum b') = c(\zeta)+\overline{c(\zeta)}$.

Finally, we need that $c(\zeta)$ itself (thus also $\overline{c(\zeta)}$) is not in the image of F_V. Suppose on the contrary that $F_V(\sum d) = c(\zeta)$, then some of d's must have degree greater than or equal to 0, and some of these needs to be non-spin. Then $F_V(a+\sum b'+\sum(d+\overline{d}))=0$, and thus $a+\sum b'+\sum(d+\overline{d})$ in the image of F_U. But since the degree-shift of the only non-vanishing F_U-component is $-\frac{1}{2}$ and $\widehat{\mathrm{HF}}(S^1\times S^2)$ is supported only in degrees $\pm\frac{1}{2}$, no element in the image of F_U can have degree greater than 0, and hence all d's in the above sum have $\deg d\le 0$. But even so, the sum being in the image of F_U forces each of its summands to be in the image of some Spin^c cobordism, so for some $\mathbf{u}\in\mathrm{Spin}^c(U)$ and $e\in\widehat{\mathrm{HF}}(S^1\times S^2,\mathbf{t}_0)$ we have $F_{U,\mathbf{u}}(e)=a$. But as $\mathbf{t}^{L\#-L}_{(-p,p)}$ and $\mathbf{t}_0$ are both spin, such $\mathbf{u}$ would be spin as well, which is not the case as for 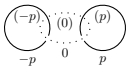

$\langle c_1(\mathbf{u}),(1,p,-1)\rangle = -2p \neq 0.$ □

Proposition 4.1.16. *Assume that (M,ξ) is given by a surgery diagram of Figure*

4.2 and that it contains a surgery link of the tight $S^1 \times S^2$ from Proposition 4.1.15 as a sublink. Theorem 4.1.2 holds for this (M, ξ).

Proof. The complete surgery presentation corresponds to a contact manifold obtained by Legendrian surgery on the tight $S^1 \times S^2$, hence it is Stein fillable. Therefore and since ξ is supported by a planar open book, its contact invariant $c^+(\xi)$ is non-vanishing and lies in the bottom of the tower $\mathcal{T}^+$.

On the other hand, the full path of the associated contact covector c' properly ends. Indeed, as described in Section 4.1.1, we can reduce a full path of any covector to the central steps. Concretely, if contact covector c' is not the initial (the terminal) vector of the full path, we can ensure that violation of the initial (terminal) condition happens on the central vertex with $\mathrm{PD}(c)|_{z'} = -h + e_2 - e_3 - \cdots - e_{n+1}$ (or $+h - e_2 + e_3 + \cdots + e_{n+1}$) or with a drop-out, up to reordering. The special form of the two legs described in Proposition 4.1.15 now ensures that central steps (throughout the path) can be alternatively done with respect to these two legs. Concretely, let us write out the argument for the proper end in the initial direction when $L_1 = (a_0^1)$ with $\mathrm{rot}_0^1 = p - 1$ and $L_2 = (a_0^2, \ldots, a_{p-2}^2)$ with $\mathrm{rot}_0^2 = -1$. First, the path does not drop out at c' because $\mathrm{rot}_0^1 = -\mathrm{tb}_0^1 - 1$ can be reached only when all its generators (apart from h, e_1) are positive, hence the first central turn is done with respect to L_1. This turn changes rotation number on starting vertices of all other legs by $+2$, causing $\mathrm{rot}_0^2 = -\mathrm{tb}_0^2 - 1 = 1$. Now, positivity of generators of a_0^2-unknot and the consequent positivity of generators forming the following chain of -2's, allow us to do the next $p - 1$ turns with respect to L_2 (on the dual side these generators constitute the starting vertex of L_2'). After, the rotation number $-\mathrm{tb} - 1$ is reached on a_0^1-unknot again, and the described sequence of turns can be repeated. Eventually, rotation number $-\mathrm{tb} - 1$ is reached also on the starting vertex of some other leg, and this covector satisfies initial condition (having at least two positive signs in the expansion of $\mathrm{PD}(c')|_{z'}$). Other cases can be handled analogously, in particular, notice that further vertices after a_0^1 on L_1 and after a_{p-2}^2 on L_2 result in less starting -2's on L_1' and lower self-intersection of the starting dual vertex on L_2', which both (at most) stop the path earlier.

So, c' represents a generator of $\ker U \subset \mathrm{HF}^+(-M, \mathbf{t}_\xi)$. Its degree by definition (because of $c^2 = \sigma(R)$) agrees with the negative of the 3-dimensional invariant of the contact structure, which in turn agrees with the degree of the contact invariant in $\mathrm{HF}^+(-M)$, and the last is by the first paragraph of the proof given by $d(-M, \mathbf{t}_\xi)$. Read together:

$$\deg(c') = -d_3(\xi) = \deg(c^+(\xi)) = d(-M, \mathbf{t}_\xi) =: d$$

Note (testing realizability conditions for the Seifert constants) that M is an L-space, hence we have $\mathrm{rk}\,\mathrm{HF}_d^+(-M, \mathbf{t}_\xi) = 1$ and the two generators $c^+(\xi)$ and c' coincide. □

General case Let (M_1, ξ_1) be a given contact manifold, for which we additionally assume that the sign of all stabilizations on the starting a_0^i-unknot is the same, without lost of generality, positive. So, $\mathrm{rot}_0^i = -\mathrm{tb}_0^i - 1 = a_0^i - 1$. Other cases have already been covered by Corollary 4.1.14.

Let (M_2, ξ_2) denote the Stein fillable contact manifold, obtained from (M_1, ξ_1) by adding a new $(n+1)^{\text{th}}$ leg (in the surgery presentation of Figure 4.2) which consists of an unknot with $\mathrm{tb} = -2$ and $\mathrm{rot} = -1$, followed by a chain of non-stabilized unknots, two less than the Thurston-Bennequin invariant tb_0^i of the a_0^i-unknot. By Proposition 4.1.16, this manifold is indeed Stein fillable.

Additionally, write W_1, W_1' and W_2, W_2' for the pairs of plumbed 4-manifolds obtained through the construction of Figure 4.3, which are bounded by $\pm M_1$ and $\pm M_2$, respectively. Finally, for the two structures ξ_1 and ξ_2 denote the contact covectors (defined in Definition 4.1.1) by c_1' and c_2', respectively.

Since (M_2, ξ_2) is constructed from (M_1, ξ_1) by a sequence of Legendrian surgeries, we have a Stein cobordism W from (M_1, ξ_1) to (M_2, ξ_2), such that $W_1 \cup W = W_2$. By Theorem 3.2.1 (of Ghiggini) there is a Spin^c structure $\mathbf{k}$ on W such that $F^+_{\overline{W},\mathbf{k}} : c^+(\xi_2) \mapsto c^+(\xi_1)$, and the degree-shift equals $d_3(\xi_2) - d_3(\xi_1)$. Analogous statement holds for contact covectors.

Lemma 4.1.17. *There is a negative definite* Spin^c *cobordism* $(X, \mathbf{s})$ *from the* Spin^c *manifold* $(-M_2, \mathbf{t}_{\xi_2})$ *to the* Spin^c *manifold* $(-M_1, \mathbf{t}_{\xi_1})$*, whose associated map in Heegaard Floer homology takes* $(c_2')^*$ *to* $(c_1')^*$.

Proof. Look at the negative definite plumbing W_1' bounded by $-M_1$, on which c_1' is defined. According to Theorem 3.1.2 (of Némethi), the lattice cohomology of negative definite plumbings (normal surface singularities) is independent of the graph, that is, blowing up induces a degree preserving isomorphism. Now, blowing up W_1' we get $\bar{W}_1'$ as follows: first blow up the central vertex obtaining a new vertex x (starting the $(n+1)^{\text{th}}$ leg), then blow up x, and further the intersection between x and the last blow-up as long that the self-intersection $x \cdot x$ equals tb_0^i. The resulting plumbing $\bar{W}_1'$ has $n+1$ legs, self-intersection of the central vertex is $-n$, and the new leg consists of tb_0^i vertices, the first one of weight $\mathrm{tb}(K)$, the second one of weight -1, and the other $\mathrm{tb}_0^i - 2$ of weight -2, read from the center out. The contact covector c_1' when described on $\bar{W}_1'$ is changed by -1 on the central vertex, takes value $\mathrm{tb}_0^i - 2$ on x, 1 on -1, and 0 on -2's.

Consider the Spin^c cobordism $(X, \mathbf{s})$ from $(-M_2, \mathbf{t}_{\xi_2})$ to $(-M_1, \mathbf{t}_{\xi_1})$, described on W_2' by adding a chain consisting of a vertex of self-intersection -1 and $\mathrm{tb}_0^i - 2$ vertices of self-intersection -2 with Spin^c evaluations 1 and 0, respectively, to the $(n+1)^{\text{th}}$ leg (a single vertex of self-intersection tb_0^i). By the previous paragraph $(X, \mathbf{s})$ is negative definite, and its associated map in Heegaard Floer homology $F^+_{X,\mathbf{s}}$ takes $(c_2')^*$ to $(c_1')^*$. □

Proof of Theorem 4.1.2. We know from Proposition 4.1.16 that Theorem 4.1.2 holds for (M_2, ξ_2) and c_2'. Thus, since $(c_2')^*$ represents the contact invariant $c^+(\xi_2)$ of a planar Stein structure, it lies in the bottom of the tower $\mathcal{T}^+_{d(-M_2,\mathbf{t}_{\xi_2})}$, and hence its image $(c_1')^*$ can either lie in the bottom of the tower $\mathcal{T}^+_{d(-M_1,\mathbf{t}_{\xi_1})}$ or it vanishes as an element of $\ker U$ (in particular, it is not a generator of $\widehat{\mathrm{HF}}(-M_1)$).

So, if the full path of c_1' properly ends, its degree $\deg(c_1')$, which by definition of the contact covector equals the negative of the 3-dimensional invariant $-d_3(\xi_1)$, agrees with the correction term $d(-M_1, \mathbf{t}_{\xi_1})$. According to Lisca and Stipsicz (see Theorem 3.2.5), this implies that $c^+(\xi_1)$ is also non-zero, and hence $c^+(\xi_1) = (c_1')^*$. If, on the other hand, the full path of c_1' drops out, its degree $\deg(c_1') = -d_3(\xi_1)$ never equals $d(-M_1, \mathbf{t}_{\xi_1})$. If it did, the contact invariant $c^+(\xi_1)$ would be non-zero, and $c^+(\xi_1)$ and $c_1' \sim U^m \otimes h$ (for some $m > 0$ and $h \in \mathrm{Char}(\Gamma_1')$) would be necessarily different elements of $\mathrm{HF}^+_d(-M_1, \mathbf{t}_{\xi_1})$, contradicting the fact that $d(-M, \mathbf{t}_\xi) = \min \frac{-K^2-|\Gamma'|}{4}$ over $K \in \mathrm{Char}_{\mathbf{t}_\xi}(\Gamma')$. But then, as ξ_1 is a planar contact structure with $d(-M_1, \mathbf{t}_{\xi_1}) \neq -d_3(\xi_1)$, its contact invariant $c^+(\xi_1)$ vanishes as well. □

4.2 Complete classification for L-spaces

In the case of L-spaces – where, recall, the zero-twisting tight structures are all tight structures – we give a complete classification.

Theorem 4.2.1. *Let M be a Seifert fibered L-space of the form $M(-1; r_1, r_2, r_3)$. Then a contact structure ξ on M is tight if and only if it is given by a contact surgery presentation of Figure 4.1 and its 3-dimensional invariant $d_3(\xi)$ is equal to the d-invariant $d(M, \mathbf{t}_\xi)$. Moreover, two tight structures ξ_1 and ξ_2 on M are contact isotopic if and only if their induced* Spin^c *structures $\mathbf{t}_{\xi_1}, \mathbf{t}_{\xi_2}$ are isomorphic.*

Our result reduces the classification problem to a well-understood computation of invariants. Although our method does not result in the number of tight structures on a given small Seifert manifold, the problem is translated to a completely combinatorial (so not geometric) count. Indeed, in any special case the number can be easily determined by, say, a computer calculation (as here both d_3 and d are computable, and the Spin^c structure can be given as an element of the first homology). What is more, since there is a surgery presentation of considered contact manifolds, we have a very explicit description of tight structures.

Joint with previously stated results (see beginning of the chapter), all tight structures on small Seifert fibered L-spaces can be characterized in terms of the Ozsváth-Szabó contact invariant.

Corollary 4.2.2. *Let ξ be a contact structure on small Seifert fibered L-space $M = M(e_0; r_1, r_2, r_3)$. Then ξ is tight if and only if its contact invariant $c(\xi) \in$*

$\widehat{\mathrm{HF}}(-M, \mathbf{t}_\xi)$ *is nonzero. Moreover, two tight structures* ξ_1 *and* ξ_2 *are isotopic if and only if their contact invariants* $c(\xi_1), c(\xi_2)$ *coincide, if and only if their induced* Spin^c *structures* $\mathbf{t}_{\xi_1}, \mathbf{t}_{\xi_2}$ *are isomorphic.*

Outline of the proof By Proposition 4.0.1, to construct tight structures on L-spaces of the form $M(-1; r_1, r_2, r_3)$, the contact surgery presentations of Figure 4.1 suffice. This leaves us with a finite collection of contact structures, for which we need a method to detect tightness, and finally a proof that it is complete (that is, a way to recognize overtwistedness and isotopies between possibly different presentations of the same contact structure).

To detect tightness, we essentially use the Ozsváth-Szabó contact invariant, implicitly expecting all tight structures to have non-vanishing one. We think of it in the form of the contact covector, introduced in Definition 4.1.1 and studied in Section 4.1. By Theorem 4.1.2, the non-vanishing of the contact invariant is equivalent to the contact covector having a full path with proper ends. Here, we wish to look closer into the behavior of the full path components of the contact covectors; denote them by $\mathcal{P}_\xi$ according to the contact structure ξ to which they belong. In this language, Theorem 4.2.1 takes the following working form.

Theorem 4.2.3. *The contact structure* ξ *on* $M(-1; r_1, r_2, r_3)$ *given by surgery diagram is tight if and only if its full path* $\mathcal{P}_\xi$ *properly ends in the initial and terminal vector. Two such contact structures* ξ_1, ξ_2 *are isotopic if and only if their paths* $\mathcal{P}_{\xi_1}, \mathcal{P}_{\xi_2}$ *meet (hence, coincide).*

To close our classification we need that the zero elements (drop-outs) correspond to overtwistedness, and for the second part of Theorem 4.2.3 that elements giving the same $\widehat{\mathrm{HF}}(M)$-generator (sharing the same path) are actually contact isotopic. Here, convex surface theory comes in. We need to translate contact surgeries back into convex decomposition. Natural convex decomposition of the manifold M separates the three singular tori from the rest of the manifold. Then the coefficients in the continued fraction expansions of the three surgeries, along with the chosen stabilizations determine basic slice decompositions of the three tori (as explained in Sections 2.2.1 and 2.2.3). What we need is to relate steps in the full path with appropriate state traversals, and drop-outs to non-tight basic slice configurations.

4.2.1 First example

We illustrate our strategy on small Seifert fibered L-spaces $M_p := M(-1; \frac{1}{2}, \frac{1}{2}, \frac{1}{p})$. The classification on these manifolds was first obtained by Ghiggini, Lisca and Stipsicz in [30]; wherever applicable, we use their notation. First we describe tight structures on M_p using Theorem 4.2.1, then we prove Theorem 4.2.1 in this special case.

Claim 4.2.4. *Manifold M_p admits exactly three tight contact structures up to isotopy.*

The finite collection of contact structures, given by Figure 4.1, can be encoded in the following table of invariants:

surgery coefficient	tb	$\mathrm{rot}(\lvert\mathrm{rot}\rvert \leq -\mathrm{tb}-1)$
$+1$	-1	0
$+1$	-1	0
-1	-2	$\mathrm{rot}_1 \in \{-1,1\}$
-1	-2	$\mathrm{rot}_2 \in \{-1,1\}$
-1	$-p$	$\mathrm{rot}_3 \in \{-p+1,-p+3,...,p-1\}$.

As an application of the Theorem, the tightness and isotopies can be recognized solely from the induced Spin^c structures and the two invariants. In our case these are as follows.

$$\begin{aligned} d_3(\xi) &= \tfrac{1}{4}(c^2(X,J)-3\sigma(X)-2b_2(X))+q \\ &= \tfrac{1}{4}((0,0,\mathrm{rot}_1,\mathrm{rot}_2,\mathrm{rot}_3)Q_X^{-1}(0,0,\mathrm{rot}_1,\mathrm{rot}_2,\mathrm{rot}_3)^T-3\cdot(-1)-2\cdot 5)+2. \end{aligned}$$

So, for mixed $(\mathrm{rot}_1,\mathrm{rot}_2)=(\pm 1,\mp 1)$, the d_3 is always zero, as for $(\mathrm{rot}_1,\mathrm{rot}_2)=(\pm 1,\pm 1)$ it runs through the values $\{\frac{2-p}{4},...,\frac{-2+3p}{4}\}$ by the step ± 1 as rot_3 increases.

There are exactly four Spin^c structures for each p (as $|\,\mathrm{H}_1(M_p;\mathbb{Z})|=4$):

$$\begin{aligned} \mathrm{H}_1(-M_p;\mathbb{Z}) &= \left\langle \mu,\mu_a,\mu_b,\mu_c;\begin{pmatrix}1&1&1&1\\1&p&0&0\\1&0&2&0\\1&0&0&2\end{pmatrix}\begin{pmatrix}\mu\\ \mu_a\\ \mu_b\\ \mu_c\end{pmatrix}=0\right\rangle \\ &= \begin{cases} \langle \mu_b; 4\mu_b=0\rangle \cong \mathbb{Z}_4 \text{ for } p \text{ odd} \\ \langle \mu_b,\mu_c; 2\mu_b=2\mu_c=0\rangle \cong \mathbb{Z}_2\oplus\mathbb{Z}_2 \text{ for } p \text{ even.}\end{cases} \end{aligned}$$

They can be given by the set $\{\mathbf{t}_1=\mathbf{t}_4+\mu_b,\mathbf{t}_2=\mathbf{t}_4+\mu_c,\mathbf{t}_3=\mathbf{t}_4+\mu_a,\mathbf{t}_4\}$. And corresponding four characteristic 2-cohomology classes, realizing $d(-M_p,\mathbf{t}_i)$, are on the generators of $\mathrm{H}_2(W_{\Gamma'})$ given by:

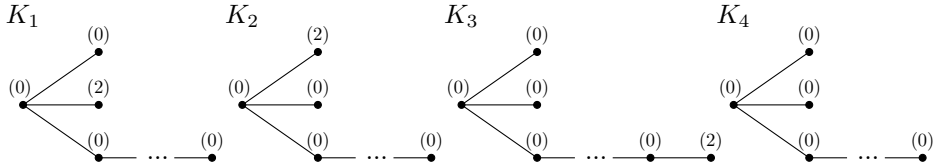

Therefore:

$$d(-M_p,\mathbf{t}_i)=\max\left\{\frac{c_1(\mathbf{s})^2+|\Gamma'|}{4};\mathbf{s}\in \mathrm{Spin}^c(W_{\Gamma'}),\mathbf{s}|_{-M_p}=\mathbf{t}_i\right\}=\begin{cases}0 & i=1,2\\ \frac{p-2}{4} & i=3\\ \frac{p+2}{4} & i=4\end{cases}$$

Applying Theorem 4.2.1, the above computations already give that for distinct $\mathrm{rot}_1, \mathrm{rot}_2$ all structures are tight, and belong to two different isotopy classes, while for equal $\mathrm{rot}_1, \mathrm{rot}_2$ the only tight triples are $(\pm 1, \pm 1, \mp(p-1))$ and they are isotopic to each other. This proves Claim 4.2.4.

Claim 4.2.5. *Theorem 4.2.1 holds for M_p.*

We show this following the two-step analysis described in the outline of the proof.

Detect tightness

The condition we use to recognize tight structures among all (M_p, ξ) presented by surgery diagrams of Figure 4.1 is an existence of the characteristic covector c as in Theorem 4.1.2.

We give c as $\mathrm{PD}(c) = \alpha h + \sum \alpha_i e_i$ where $\alpha, \alpha_i \in \{\pm 1\}$, and such that $(c_i) = \langle c, x_i \rangle = \mathrm{rot}_i - 1$. Concretely, the c-evaluations on Γ belong to one of the following.

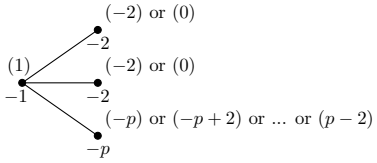

$$z = e_1$$
$$x_1 = h - e_1 - e_2 - e_5$$
$$x_2 = h - e_1 - e_3 - e_6$$
$$x_3 = h - e_1 - e_4 - \textstyle\sum_7^{p+5} e_i$$

Then, for each such (α, α_i) we compute $c|_{\Gamma'}$, and check how its full path ends.

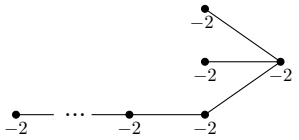

$$z' = h - e_2 - e_3 - e_4$$
$$x'_1 = e_2 - e_5$$
$$x'_2 = e_3 - e_6$$
$$x'_3 = e_4 - e_7, e_7 - e_8, \ldots, e_{p+4} - e_{p+5}$$

Below we list all possible (α, α_i) for each given triple (c_1, c_2, c_3). We will make explicit how some $c|_{\Gamma'}$ drop out, and connect the others to the right initial and terminal vector. Also, we will emphasize the appearance of the same characteristic covectors $c|_{\Gamma'}$ in some pairs of c-triples.

First observe that (on the level of paths) the order of signs on generators of each leg is unimportant, as they can be shuffled using $\pm 2\,\mathrm{PD}(v')$-steps for $\langle c, v' \rangle = \pm 2$. Then there are essentially only two different sign-vectors (α, α_i) for a chosen c-triple, differing in the sign of h. The two are connected by $\pm 2\,\mathrm{PD}(z')$, applied when $\langle c, z' \rangle = \pm 2$. Notice that all these different sign configurations belong to the same surgery presentation.

In the light of the previous paragraph, we record only the number of positive and negative signs on exceptional generators of each leg. Write $\{m+, n-\}_i$ when there are m positive and n negative generators of L_i (counted without h and e_1); not to be confused with vectors of signs which record exact sign configuration on corresponding generators. In addition, let $(h+)_{(c_1,c_2,c_3)}$ and $(h-)_{(c_1,c_2,c_3)}$ denote any of the sign configurations which belongs to (c_1, c_2, c_3) and has positive and

negative sign, respectively, on h. We look separately at the cases with the same, and later with distinct (c_1, c_2).

c_3	$\underline{(-2,-2,c_3)}$		$\underline{(0,0,c_3)}$	
	$(h-)$	$(h+)$	$(h-)$	$(h+)$
	$\{1+,1-\}_1$	$\{0+,2-\}_1$	$\{2+,0-\}_1$	$\{1+,1-\}_1$
	$\{1+,1-\}_2$	$\{0+,2-\}_2$	$\{2+,0-\}_2$	$\{1+,1-\}_2$
$p-2$	$\{p+,0-\}_3$	$\{(p-1)+,1-\}_3$	$\{p+,0-\}_3$	$\{(p-1)+,1-\}_3$
$p-4$	$\{(p-1)+,1-\}_3$	$\{(p-2)+,2-\}_3$	$\{(p-1)+,1-\}_3$	$\{(p-2)+,2-\}_3$
$\vdots$	$\vdots$	$\vdots$	$\vdots$	$\vdots$
$-p$	$\{1+,(p-1)-\}_3$	$\{0+,p-\}_3$	$\{1+,(p-1)-\}_3$	$\{0+,p-\}_3$

For $(-2,-2,c_3)$ with $c_3 \in \{p-4,...,-p\}$, there exists a configuration $(h,e_2,e_3,e_4) = (-,-,-,-)$ which drops out: $\langle c, z'\rangle = \langle -h-e_2-e_3-e_4, h-e_2-e_3-e_4\rangle = -4$. Similarly, $(0,0,c_3)$ with $c_3 \in \{p-2,...,-p+2\}$, drops out at $(h,e_2,e_3,e_4) = (+,+,+,+)$. Therefore, the paths possibly end only for the triples $(-2,-2,p-2)$ and $(0,0,-p)$.

Furthermore, we observe that $(-2,-2,p-2)$ and $(0,0,-p)$ belong to the same full path because the configurations $(h-)_{(-2,-2,p-2)}$ and $(h+)_{(0,0,-p)}$ give the same characteristic vector (zeros on the third leg, and $(h,e_4) : (-,+) \leftrightarrow (+,-)$ with the same evaluation on $z' = h-e_2-e_3-e_4$). This proves also that their (common) path indeed ends, namely at K_3 (given by $(h,e_4,e_7,...,e_{p+4},e_{p+5}) = (-,-,-,...,-,+)$ for $(0,0,-p)$) on the initial side and at $-K_3$ (as $(h,e_4,e_7,...,e_{p+4},e_{p+5}) = (+,+,+,...,+,-)$ for $(-2,-2,p-2)$) on the terminal.

c_3	$\underline{(-2,0,c_3)}$		$\underline{(0,-2,c_3)}$	
	$(h-)$	$(h+)$	$(h-)$	$(h+)$
	$\{1+,1-\}_1$	$\{0+,2-\}_1$	$\{2+,0-\}_1$	$\{1+,1-\}_1$
	$\{2+,0-\}_2$	$\{1+,1-\}_2$	$\{1+,1-\}_2$	$\{0+,2-\}_2$
$p-2$	$\{p+,0-\}_3$	$\{(p-1)+,1-\}_3$	$\{p+,0-\}_3$	$\{(p-1)+,1-\}_3$
$p-4$	$\{(p-1)+,1-\}_3$	$\{(p-2)+,2-\}_3$	$\{(p-1)+,1-\}_3$	$\{(p-2)+,2-\}_3$
$\vdots$	$\vdots$	$\vdots$	$\vdots$	$\vdots$
$-p$	$\{1+,(p-1)-\}_3$	$\{0+,p-\}_3$	$\{1+,(p-1)-\}_3$	$\{0+,p-\}_3$

Sign configurations adapted to any c-triple with distinct c_1 and c_2 build a connected part of (one of the two) full paths. Indeed, let us see how these parts patch together into a path. For $k \in \{1,...,p-1\}$, we have

$$(h+)_{(-2,0,p-2k)} \underset{c|_{\Gamma'}}{=} (h-)_{(0,-2,p-2k-2)} \underset{c|_{\Gamma}}{\equiv} (h+)_{(0,-2,p-2k-2)} \underset{c|_{\Gamma'}}{=} (h-)_{(-2,0,p-2k-4)}$$

where the first and the last equality denote the same characteristic covector on Γ', while the middle equivalence means (different sign distributions of) the same

presentation. This separates all characteristic vectors arising from presentations with mixed (c_1, c_2) into two full paths. One starting at K_1 (as $-h - e_2 + e_5 + e_3 + e_6 + e_4 + e_7 + \cdots + e_{p+5}$ for $(-2, 0, p-2)$) and ending at $-K_2$ (as $+h - e_2 - e_5 + e_3 - e_6 - e_4 - e_7 - \cdots - e_{p+5}$ for $(-2, 0, -p)$) or $-K_1$ (as $+h + e_2 - e_5 - e_3 - e_6 - e_4 - e_7 - \cdots - e_{p+5}$ for $(0, -2, -p)$). The other starting at K_2 (as $-h + e_2 + e_5 - e_3 + e_6 + e_4 + e_7 + \cdots + e_{p+5}$ for $(0, -2, p-2)$) and ending at $-K_1$ (as $+h + e_2 - e_5 - e_3 - e_6 - e_4 - e_7 - \cdots - e_{p+5}$ for $(0, -2, -p)$) or $-K_2$ (as $+h - e_2 - e_5 + e_3 - e_6 - e_4 - e_7 - \cdots - e_{p+5}$ for $(-2, 0, -p)$). The two terminal possibilities depend on the parity of p (odd or even).

In conclusion, translated back into rotation numbers we have obtained the following paths of tight structures, each sharing the same invariants:

- $(-1, -1, p-1)$ and $(1, 1, -p+1)$ ($\mathrm{Spin}^c = \mathbf{t}_4 + \mu_a,\ d_3 = \frac{2-p}{4}$)
- $(-1, 1, p-1)$ and $(1, -1, p-3)$ and $(-1, 1, p-5)$ and ... ($\mathrm{Spin}^c = \mathbf{t}_4 + \mu_b,\ d_3 = 0$)
- $(1, -1, p-1)$ and $(-1, 1, p-3)$ and $(1, -1, p-5)$ and ... ($\mathrm{Spin}^c = \mathbf{t}_4 + \mu_c,\ d_3 = 0$)

Prove overtwistedness and describe contact isotopies

In our (simplest possible) cases with boundary slopes $\frac{1}{k}$ for $k \in \mathbb{Z}$, there is a single continued fraction block for each special fiber. Contact surgery presents a direct translation between positive and negative stabilizations (down- and up-cusps) of core Legendrian unknots and positive and negative basic slices in the decomposition of a continued fraction block with slopes -1 and $-k$. The generators forming the corresponding leg (and by that, the dual vertices) in the plumbings above can be thought of as another way of layering solid torus into k slices.

We need contact topological interpretation for the steps in full paths.

First, the unimportance of sign permutations in the legs coincide with the shuffling of basic slices within a single continued fraction block. Moreover, [30, Section 6] provides sufficient isotopy moves between contact structures presented by different surgery diagrams. Let us spell this out. Since the moves in [30] are given by the matrices of signs whose coefficients are q^i_j, the number of positive basic slices in the j^{th} continued fraction block of the i^{th} leg, in our case only (q^1_0, q^2_0, q^3_0), we rewrite the previously obtained paths of tight structures in this language, changing rotation numbers to the q^i_0:

- $(0, 0, p-1)$ and $(1, 1, 0)$
- $(0, 1, p-1)$ and $(1, 0, p-2)$ and $(0, 1, p-3)$ and ...
- $(1, 0, p-1)$ and $(0, 1, p-2)$ and $(1, 0, p-3)$ and ...

Now, we notice that the conditions which caused a full path to drop out, and so prevented our tightness criterion from working, exactly agree with the condition for which overtwistedness can be proved. And finally, there are contact isotopies between pairs of surgery presentations which share the same path. Let us compare.

Proposition 4.2.6. [30, Propositions 6.3, 6.1 and 6.4] *Let a contact structure on M_p be given by (q_0^1, q_0^2, q_0^3) as above. Then the triples $(1, 1, q_0^3)$ with $q_0^3 \neq 0$ and $(0, 0, q_0^3)$ with $q_0^3 \neq p-1$ present overtwisted structures. Between other presentations, there are the following contact isotopies:*

$$(1,0,q_0^3) \simeq \begin{cases} (0,1,q_0^3+1) \text{ when } q_0^3 < p-1 \\ (0,1,q_0^3-1) \text{ when } q_0^3 > 0 \end{cases} \quad \text{and} \quad (1,1,0) \simeq (0,0,p-1). \qquad \square$$

Problems in general

The examples shown above are special in several ways. In general, it can happen that the full path associated to some presentation $(c_v)_{v\in\Gamma}$ drops out, although all characteristic covectors computed from (α, α_i)-configurations which restrict to $(c_v)_{v\in\Gamma}$ satisfy the bounds $v \cdot v \leq \langle c, v\rangle \leq -v \cdot v$ for all $v \in \Gamma'$. Also, not all the steps in a full path need to be presentable, that is, arising from some tuple of rotation numbers. (For examples of such paths, look at the two "applications" in [52].) That said, we need to find out how the (subsequent) presentations of the same path are related, when neither of their characteristic covectors on Γ' coincides (Corollary 4.2.12). Finally, we need new conditions for overtwistedness (Proposition 4.2.13) and isotopies (Proposition 4.2.14), which will explain such behavior of full paths.

4.2.2 Characteristic covectors, tightness, and full paths

In Section 4.1.1 we have described the full path steps on the level of homology generators of $\mathrm{H}^2(R;\mathbb{Z})$. Here, we are mainly concerned with the associated change in $c|_\Gamma$, whether the new $c|_\Gamma$ comes from some presentation and when it leads to the end of the path. Moreover, we describe the first presentable $c|_\Gamma$ (or the end of the path) following any contact covector we have started with.

On presentability

We have reduced the study of the full path to its central steps. In the Algorithm 4.1.8, the central step is described up to reordering the legs. When we wish to emphasize according to which leg in the actual structure the central step is done, we will refer to it as a turn of L_i. Since the evaluation of characteristic covector on L_i-vertices other than x_i changes only by turns of L_i, we may separately study their influence.

Lemma 4.2.7. *Let c be a presentable non-initial characteristic covector. Assume that it evaluates on the vertices of some leg $L = (-a_0, -a_1, \ldots, -a_j, -a_{j+1}, \ldots, -a_k)$ as follows:*

$$\langle c, L\rangle = (a_0 - 2, a_1 - 2, \ldots, a_j - 2, a_{j+1} - 2 - 2n_{j+1}, \ldots, a_k - 2 - 2n_k)$$

where $k \geq j, n_{j+1}, \ldots, n_k \geq 0$ and $n_{j+1} > 0$.

The path runs into the next possibly presentable covector $\bar{c}$ only after

$$1 + 1 + (a_1 - 1) + (a_2 - 1)(a_1 - 1) + \cdots + (a_{j-1} - 1)\cdots(a_1 - 1) \text{ turns of } L,$$

in:

$$\langle \bar{c}, L\rangle = (-a_0, -a_1 + 2, \ldots, -a_j + 2, a_{j+1} - 2n_{j+1}, \ldots, a_k - 2 - 2n_k).$$

Proof. To be illustrative, we explicitly write out all the generators involved in the first few turns. Below are the two sides, L_1 and L_1', in homology generators; the $*$-symbol stands for truncation only.

$$\begin{array}{lllllllll}
L_1: & x_1 = h - e_1 - e_2 - e_5 - \cdots - e_{J-1} - & e_J & & & & & & \\
 & & e_J - & e_{J+1} & & & & & \\
 & & & e_{J+1} - & e_{J+2} & & & & \\
 & & & & \ddots & & & & \\
 & & & & e_{K-1} - e_K - e_{K+1} - * & & & & \\
L_1': & x_1' = e_2 - & e_5 & & & & & & \\
 & & \ddots & & & & & & \\
 & & e_{J-2} - & e_{J-1} & & & & & \\
 & & & e_{J-1} - e_J - e_{J+1} - \cdots - & e_K & & & & \\
 & & & & * & & & &
\end{array}$$

In this notation, the starting part of L_1 and the evaluation of c on it take values:

$$L_1 = (-J + 3, \underbrace{-2, \ldots, -2}_{K-J-1}, -T, -S, *) \text{ and } \langle c, L_1\rangle = (J - 5, 0, \ldots, 0, M, N, *).$$

By the first turn, according to the Algorithm, we change generators up to e_J – it does not influence further dual vertices, but a new vector can be presentable only when all the middle generators $e_J, ..., e_{K-1}$ are same-signed. Therefore, in order to (possibly) reach a presentable vector again we have to repeat turning of this particular leg $K - J$ times. The resulting manifold vector is of the form $(-J + 3, 0 \ldots, 0, M + 2, N, *)$, its presentability depends on the $(+2)$-changed manifold vertex $e_{K-1} - e_K - e_{K+1} - *$.

In terms of generators, we have reached another presentation exactly when the e_K-sign is negative. The positive e_K-sign, on the other hand, requires another turn, but this forces some further changes to preserve the dual. Namely, we

need to change signs on generators of the following chain of -2's, and one (without loss of generality, first) middle generator afterwards. The resulting vector is not necessarily presentable, provided the starting point was, it depends on presentability of the vertex starting in the (last changed) middle generator ($+2$ rotation change). But if it is, the new presentation is $(-J+3, 0, \ldots, 0, -T+2, N+2, *)$; for this, we need to turn this leg $K-J+1$ times.

Continuing in the same manner, we trace similar behavior at all levels. Concretely. We are successively turning fully positive vertices, which influences the evaluation on the following manifold vertex by $+2$. If the result is presentable, we have finished. Otherwise, the following vertex was also fully positive, at the moment its evaluation is minus self-intersection, and it will have turned under the influence of another turn of the previous vertex. For that we need to bring the previous vertex back to maximal rotation, using (again) influence of the previous vertices on the leg. But notice that each vertex is influenced only by turns of the vertex just before it. Therefore, to come from maximal rotation through minus self-intersection to minimal rotation on some vertex v_{k+1}, we need to influence it by two turns of its immediately previous vertex v_k. This in turn is obtained by $a_k - 1$ turns of its previous vertex v_{k-1}, first to get from minus self-intersection to minimal rotation, and then by the step of $+2$ to maximal rotation. This explains the number of steps and finishes the proof. □

Obviously, the leg (its vertices with self-intersections) together with the sign configuration (in presentable, rotation numbers) determine when the leg is turned. In particular, it specifies the gaps between the subsequent turnings of the same leg, when some other leg needs to be turned in order for the path to continue. Actually, the reverse also holds.

Lemma 4.2.8. *A form of a leg together with a distribution of signs on its generators is completely described by the sequence of its turns.*

Proof. As before, we separately state (and argue for) the first step.

Claim. *Between two subsequent turnings of the same leg L there are always either $a_0 - 2$ or $a_0 - 1$ turnings of other legs.*

Proof. Remember that all generators (except possibly the last) of the starting manifold vertex on the turning leg are positive. Since by each turn of other legs we change starting evaluation by $+2$ (through the change of h-sign from negative to positive), the gap is determined by the number of generators of the starting vertex. Its variation by one is due to whether the dual vertex following -2's is also fully negative after the L-turn. □

That said, given a turning sequence, we get a_0 out of the size of gap between subsequent turnings. If the gap is always the same $(a_0 - 1)$, this means that v_0 is the only vertex on L, and its self-intersection is $-a_0$.

Call this number of central turns between two turns of L, the (0^{th}) period of L. Let us define higher periods for a turning sequence:

1^{st} period: number of times the 0^{th} period is $a_0 - 2$ before it turns to $a_0 - 1$;

2^{nd} period: number of times the 1^{st} period is $a'_0 - 1$ before it turns to $a'_0 - 2$;

k^{th} period: number of times the $(k-1)^{\text{th}}$ period is $a'_{k-2} - 1$ before it turns to $a'_{k-2} - 2$.

The numbers should not be read from the first time round. As suggested by notation, they correspond to the self-intersections of dual vertices, hence they determine L', and by that L. The initial distribution of signs can be now recognized from the values of periods before the first change. □

Restrictions on the whole structure

We look at all possible (presentable) entries. For each we continue its path as long as it reaches another presentation, or otherwise it ends, either by a drop-out or a (non-presentable) initial vector. Throughout we assume that the (normalized) Seifert constants are ordered $r_1 \geq r_2 \geq r_3$. In order to reduce the possibilities we invoke the L-space condition.

L-space condition Recall the numerical condition for M to be an L-space: there are no coprime integers m, a such that $\frac{1}{r_1} > \frac{m}{a}, \frac{1}{r_2} > \frac{m}{m-a}, \frac{1}{r_3} > m$; we say that the coefficients (r_1, r_2, r_3) are not realizable. As a direct consequence of this condition we observe that:

(i) $r_1 \geq \frac{1}{2}$, equivalently one leg starts with -2 (otherwise the realizability condition is satisfied for coprime $m = 2, a = 1$),

(ii) if $L_1 = (\underbrace{-2, \ldots, -2}_{k}, *)$ (then $\frac{1}{r_1} > \frac{k+2}{k+1} = -(\underbrace{[2, \ldots, 2]}_{k+1})$), then $\frac{1}{r_2} \leq k + 2$, equivalently $x_2 \cdot x_2 \geq -k - 2$.

Dual configurations In the following arguments, there will frequently appear a pair of (truncated) legs which are dual to each other, that is, describing a lens space and its dual. Recall that the coefficients of the two are related as follows (here, $-2^{\times b_\iota}$ means a chain of b_ι-many -2's):

$$\begin{array}{rcl} L_i & = & (-b_1 - 2, \quad -2^{\times b_2}, \quad -b_3 - 3, \quad \ldots, \quad -b_m - 2) \\ L_j & = & (-2^{\times b_1}, \quad -b_2 - 3, \quad -2^{\times b_3}, \quad \ldots, \quad -2^{\times b_m}) \end{array} .$$

The inverses of the continued fractions they describe, add up to -1.

So, our starting point is a presentable characteristic covector, which does not present an initial end, or a drop-out. Thus, exactly one leg of the corresponding presentation starts in a fully positive vertex. We separate the cases: in Proposition 4.2.9 we gather presentations for which either v_0^1 or v_0^2 is stabilized fully positively, and in Proposition 4.2.11 we cover presentations for which v_0^3 is fully positively stabilized.

Proposition 4.2.9. *Let c be a presentable non-initial characteristic covector, associated to a presentation with fully positive starting vertex on L_i, either L_1 or L_2. This means that it evaluates on the vertices of*

$$L_i = (-a_0^i, -a_1^i, \dots, -a_j^i, -a_{j+1}^i, \dots, -a_{k_i}^i)$$

as in Lemma 4.2.7:

$$\langle c, L_i\rangle = (a_0^i - 2, a_1^i - 2, \dots, a_j^i - 2, a_{j+1}^i - 2 - 2n_{j+1}^i, \dots, a_{k_i}^i - 2 - 2n_{k_i}^i)$$

for some $0 \le j \le k_i, n_{j+1}^i, \dots, n_{k_i}^i \ge 0$ and $n_{j+1}^i > 0$.

Denote coefficients on other two legs by a_κ^λ, and let c evaluate as $\langle c, v_0^3\rangle = a_0^3 - 2 - 2n_0^3$ on the first vertex of the third leg L_3, and

$$\langle c, L_l\rangle = (-a_0^l, -a_1^l + 2, \dots, -a_k^l + 2, a_{k+1}^l - 2 - 2n_{k+1}^l, \dots, a_{k_l}^l - 2 - 2n_{k_l}^l)$$

on the leg L_l for $l \ne i, 3$, for some $-1 \le k \le k_l$, $n_{k+1}^l \le a_{k+1}^l - 3$.

Furthermore, define m and N_{m+1}^l as follows:

$$m := \max\{\kappa \le k;\ \text{denominator of } [a_0^l, \dots, a_\kappa^l, N] \le n_0^3 \text{ for some } N\}$$
$$N_{m+1}^l := \begin{cases} n_{k+1}^l + 1 & \text{if the denominator of } [a_0^l, \dots, a_k^l, n_{k+1}^l + 1]^{-1} \le n_0^3 \\ N & \text{otherwise.} \end{cases}$$

where $N \in [1, a_{m+1}^l)$ is such that the denominator of $[a_0^l, \dots, a_m^l, N]^{-1} \le n_0^3$ and the denominator of $[a_0^l, \dots, a_m^l, N+1]^{-1} > n_0^3$. Then the full path of c behaves as follows.

1. *If $-[a_0^i, \dots, a_{j-1}^i]^{-1} - [a_0^l, \dots, a_m^l, N_{m+1}^l]^{-1} < 1$, the full path drops out.*
2. *If $-[a_0^i, \dots, a_{j-1}^i]^{-1} - [a_0^l, \dots, a_m^l, N_{m+1}^l]^{-1} = 1$ and $m = k, N_{m+1}^l = n_{k+1}^l + 1$, we reach a new presentation $\bar{c}$ which on the three legs takes the following values:*

$$\begin{aligned} \langle \bar{c}, L_i\rangle &= (-a_0^i, -a_1^i + 2, \dots, -a_j^i + 2, a_{j+1}^i - 2n_{j+1}^i, \dots, a_{k_i}^i - 2 - 2n_{k_i}^i) \\ \langle \bar{c}, L_l\rangle &= (a_0^l - 2, a_1^l - 2, \dots, a_{k+1}^l - 2, a_{k+2}^l - 2n_{k+2}^l, \dots, a_{k_l}^l - 2 - 2n_{k_l}^l) \\ \langle \bar{c}, v_0^3\rangle &= a_0^3 - 2 - 2n_0^3 + 2D \end{aligned}$$

where D stands for the denominator of $[a_0^l, \dots, a_k^l, n_{k+1}^l + 1]^{-1}$, and the evaluations on the rest of L_3 remain the same as for c.

3. *Otherwise, the path continues in non-presentable and reaches the non-presentable initial end.*

Remark 4.2.10. Rewrite the coefficients up to a^i_j in the b-notation used for dual configurations above, so for appropriate $b_\iota \geq 0$ (notice $b_1 > 0$ on L_1):

$$L_i = (-2^{\times b_1}, -b_2 - 3, -2^{\times b_3}, \ldots, -2^{\times b_J}, -a^i_{j+1}, \ldots, -a^i_{k_i}).$$

Also for L_l, truncated as continued fractions in the Proposition, take

$$(a^l_0, \ldots, a^l_m, N^l_{m+1}) = (-b'_1 - 2, -2^{\times b'_2}, -b'_3 - 2, \ldots, -b'_J - 2).$$

Then the conditions, given in the Proposition in terms of continued fraction sums, can be restated as:

- the two continued fractions add up to 1 when $b'_k = b_k$ for all k;
- the sum is greater than 1 when for $K = \min\{k; b'_k \neq b_k\}$: $b'_K < b_K$ if K is odd, $b'_K > b_K$ if K is even;
- the sum is smaller than 1 when for $K = \min\{k; b'_k \neq b_k\}$: $b'_K > b_K$ if K is odd, $b'_K < b_K$ if K is even.

Proof of Proposition 4.2.9. We need to observe how specific behavior of the path restricts possible forms of a covector, and by that, of a presentation.

To meet another presentation, recall that we need to swap the signs of all generators forming the fully positive vertices $v^i_0, \ldots, v^i_j$ (Lemma 4.2.7). To achieve this, we need certain number of L_i-turns, which are arranged in the turning sequence, uniquely determined by the form of L_i. So, any turn of other two legs should appear at exactly specified non-turning stages of L_i.

Now notice that any turn of L_3 (before finishing the specified sequence) would immediately end the path (in non-presentable). Indeed, it has to appear after k (or $k+1$) turns of L_1 (which is, the 1^{st} period of L_1). So after it L_2 needs to be turned (its starting coefficient being $a^2_0 \leq k+2$, hence its 0^{th} period being at most $k+1$) and also L_1 needs to be turned (having 0^{th} period 0 or 1). But this already means we have arrived at the initial end, see Lemma 4.1.11.

Therefore, the turning sequence of L_i (up to its $(j+1)^{\text{th}}$ vertex) exactly specifies the turning sequence of L_l (needed to reach presentability on L_i again), its turns being in non-turning points of L_i, and vice versa. It is exactly the turning sequence of the dual leg with all evaluations fully negative. Rewritten in terms of relations between continued fractions, the two legs are of dual forms if and only if the corresponding continued fractions add up to one. In the dual (negative) leg for the last entry the significant information is the number of negative signs, as turning sequence depends only on whether we have reached maximal evaluation.

Taken together, we have obtained.

1. If not all gaps in the turning sequence of L_i are filled by turns of L_l, and at the same time, the sequence is not quit by the turn of L_3 before or at the time when first such non-filled gap appears, then the full path drops out.

2. If the two continued fractions add up to exactly one, this means the turning sequences of corresponding legs exactly fit together, and we reach another presentation – if and only if the evaluation on the starting vertex of the third leg is negative enough, not to quit the sequence of turnings interchanging between L_i and L_l. That is, there have to be more negative generators than there are turns of L_i and L_l, which equals the denominator of the corresponding continued fractions. The form of the new presentation is determined by Lemma 4.2.7.

3. Otherwise, either we hit into some turning point of L_l before reaching the next gap in the sequence of L_i, or we reach a turning point of L_3 at or before the time when the L_i-gap is not filled by the L_l-turn for the first time. As observed above, in these cases, the full path properly ends with the initial vector, but it is necessarily non-presentable because we have not yet reached the first possibly presentable stage as specified in Lemma 4.2.7. □

Proposition 4.2.11. *Throughout the path, there can be at most two non-initial characteristic covectors for which the starting vertex of L_3 is fully positive, that is $\langle c, v_0^3\rangle = a_0^3 - 2$.*

If $\langle c, v_1^3\rangle \neq a_1^3 - 2$ or $L_3 = (v_0^3)$, the turn of L_3 is presentable, the two presentations differ in: $\langle \bar{c}, v_0^3\rangle = -a_0^3$, $\langle \bar{c}, v_1^3\rangle = \langle c, v_1^3\rangle + 2$, and for $l = 1, 2$, also $\langle \bar{c}, v_0^l\rangle = \langle c, v_0^l\rangle + 2$.

If $\langle c, v_1^3\rangle = a_1^3 - 2$, and c is not terminal, the turn of L_3 necessarily makes the continuation of the path non-presentable, and ends it in a non-presentable initial end.

If $\langle c, v_1^3\rangle = a_1^3 - 2$, and c is terminal, let us write out the c-evaluations at the terminal end:

$$\langle c, L_1\rangle = (-a_0^1, -a_1^1 + 2, \dots, -a_j^1 + 2, a_{j+1}^1 - 2 - 2n_{j+1}^1, \dots, a_{k_1}^1 - 2 - 2n_{k_1}^1)$$
$$\langle c, L_2\rangle = (-a_0^2, -a_1^2 + 2, \dots, -a_k^2 + 2, a_{k+1}^2 - 2 - 2n_{k+1}^2, \dots, a_{k_2}^2 - 2 - 2n_{k_2}^2)$$

for some $0 \leq j \leq k_1$ and $0 \leq k \leq k_2$. Then:

1. *If for maximal $J \leq j, K \leq k$ such that $-[a_0^1, \dots, a_J^1, 3]^{-1} - [a_0^2, \dots, a_K^2, 2]^{-1} = 1$, the denominator of the two fractions is smaller than a_0^3, then the full path drops out.*

2. *If $\langle c, v_2^3\rangle \neq a_2^3 - 2$, and there exist $J \leq j, K \leq k$ such that*

$$-[a_0^1, \dots, a_J^1, 3]^{-1} - [a_0^2, \dots, a_K^2, 2]^{-1} = 1 \text{ and } \begin{array}{l} n_{J+1}^1 \geq 2 \text{ or } L^1 = (v_0^1, \dots, v_J^1) \\ n_{K+1}^2 \geq 1 \text{ or } L^2 = (v_0^2, \dots, v_K^2) \end{array},$$

and the denominator of the two fractions equals a_0^3, we reach a new presentation $\bar{c}$ which on the three legs takes the values:

$$\begin{aligned}\langle \bar{c}, L_1\rangle &= (a_0^1-2, a_1^2-2, \dots, a_J^1-2, \langle c, v_{J+1}^1\rangle + 4, \langle c, v_\iota^1\rangle_{\iota=J+2}^{k_1})\\ \langle \bar{c}, L_2\rangle &= (a_0^2-2, a_1^2-2, \dots, a_K^2-2, \langle c, v_{K+1}^2\rangle + 2, \langle c, v_\kappa^2\rangle_{\kappa=K+2}^{k_2})\\ \langle \bar{c}, L_3\rangle &= (-a_0^3, -a_1^3, \langle c, v_2^3\rangle + 2, \langle c, v_\mu^3\rangle_{\mu=3}^{k_3}).\end{aligned}$$

This $\bar{c}$ presents the initial end of the full path.

3. *Otherwise, the path continues in non-presentable and reaches the non-presentable initial end.*

Proof. As observed in the proof of Proposition 4.2.9, any time when the path runs into a presentation with fully positive v_0^3 (not at its terminal end), it reaches the initial vector, either before or after a turn of L_3. Therefore, if the characteristic vector before the L_3-turn is non-initial and presentable, the only other presentation, which can appear as we continue the path, can occur straight after this turn. The resulting vector is presentable if and only if $\langle c, v_1^3\rangle \neq a_1^3 - 2$ (when it exists). The relation between the two presentations is as always read from Lemma 4.2.7 (the simplest possible – one-turn – case).

The only remaining option is to have a presentable terminal end with $\langle c, v_0^3\rangle = a_0^3 - 2$. In that case the turn of L_3 does not end the path, and if this turn is not presentable itself, we need to look for any possible following presentation. Since presentability on L_3 can be recovered only by a turn of L_3, and since according to the above this turn ends the path, we might meet such a presentation (only) at the initial end. This in particular means that turns of L_1 and L_2 in between the two turns of L_3 should begin and end with a vector which is presentable on these two legs. The first turn after the L_3-turn, and the last turn before another L_3-turn are done according to L_1.

As before, we inductively determine that, in order for the turning sequences of L_1 and L_2 to fit together (being interchangeably turned until the second L_3-turn), the two legs need to have fully negative starting vertices, forming almost dual vectors. Almost in the sense that there is no "last pair", that is, the two vectors as given in the paragraph on dual configurations end with $-b_m - 3$ and $-2^{\times b_m}$ instead of $-b_m - 2$ and $-2^{\times b_m}$. In other words, they are dual when enlarged by 3 and 2, respectively.

The three possibilities are now given as before:

1. We have not reached the turning point of L_3 yet, but the sequence of turnings of L_1 and L_2 cannot continue.

2. The turn of L_3 appears exactly in the moment when neither L_1 nor L_2 can be turned, and the sign configuration on them is presentable. Additionally, we need that $\langle c, v_2^3\rangle \neq a_2^3 - 2$ to reach presentability of L_3 as well.

3. Otherwise, either the first two legs hit a common turning point, the third leg finishes the sequence early not having enough negative generators, or (simply) the terminal vector obtained as in (2) is not presentable because $\langle c, v_2^3\rangle = a_2^3 - 2$ (hence, after the L_3-turn, $\langle \bar{c}, v_2^3\rangle = a_2^3$). In all the cases, the path stops in a non-presentable initial end. □

Above we described how the successive presentations in the path are related to each other and indicate what property causes a drop-out. Any given presentation can now be either walked through these stages to the proper ends of the full path or it drops out. Joining results (taking into account also their analogues obtained by following the path in the terminal direction) we obtain the following picture. Here, the presentations are given as evaluations of characteristic covectors on generators of $\mathrm{H}_2(W_\Gamma)$, written as triples of vectors c^i whose entries are $c^i_j = \langle c, v^i_j\rangle$. Vectors are truncated – we write out only the relevant part and hide the rest into $*$.

Corollary 4.2.12 (Full path components)**.** *If a given presentation ξ does not admit both a fully positive and a fully negative starting vertex, its full path drops out at ξ. Moreover, a full path drops out when it runs into a presentation given by either of the following characteristic covectors $c|_\Gamma$, independently of how the three vectors continue in the hidden $*$-part.*
For some $(i,l) \in \{(1,2),(2,1)\}$:

$$c|_\Gamma = \left(\begin{array}{c|c|c} a_0^i - 2 & -a_0^l & \\ a_1^i - 2 & -a_1^l + 2 & \\ \vdots & \vdots & a_0^3 - 2 - 2n_0^3 \\ a_j^i - 2 & a_{k+1}^l - 2 - 2n_{k+1}^l & * \\ a_{j+1}^i - 2 - 2n_{j+1}^i & a_{k+2}^l - 2 - 2n_{k+2}^l & \\ * & * & \end{array}\right)$$

for which $-[a_0^i, \ldots, a_{j-1}^i]^{-1} - [a_0^l, \ldots, a_m^l, N_{m+1}^l]^{-1} < 1$ holds for N_{m+1}^l defined as in Proposition 4.2.9, or

$$c|_\Gamma = \left(\begin{array}{c|c|c} -a_0^1 & -a_0^2 & \\ -a_1^1 + 2 & -a_1^2 + 2 & \\ \vdots & \vdots & a_0^3 - 2 \\ -a_j^1 + 2 & -a_k^2 + 2 & a_1^3 - 2 \\ a_{j+1}^1 - 2 - 2n_{j+1}^1 & a_{k+1}^2 - 2 - 2n_{k+1}^2 & * \\ * & * & \end{array}\right)$$

such that for maximal $J \le j, K \le k$ with $-[a_0^1, \ldots, a_J^1, 3]^{-1} - [a_0^2, \ldots, a_K^2, 2]^{-1} = 1$, the denominator of the two fractions is smaller than a_0^3.

In the terminal direction, symmetrically, a drop-out occurs at presentations with oppositely stabilized surgery link (that is, surgery diagrams given by the same but reversely oriented link).

Any two presentations ξ_1 and ξ_2 whose associated characteristic vectors meet at the same path $\mathcal{P}_{\xi_1} = \mathcal{P}_{\xi_2}$ are related by the sequence of rotation number changes, each taking one of the following forms. The pairs are presented in the form of $c|_\Gamma$ and they have to be identical on all further generators, hidden in $*$.
Either for $(i,l) \in \{(1,2),(2,1)\}$:

$$\left(\begin{array}{c|c|c} a_0^i - 2 & -a_0^l & \\ a_1^i - 2 & -a_1^l + 2 & \\ \vdots & \vdots & a_0^3 - 2 - 2n_0^3 \\ a_j^i - 2 & a_{k+1}^l - 2 - 2n_{k+1}^l & * \\ a_{j+1}^i - 2 - 2n_{j+1}^i & a_{k+2}^l - 2 - 2n_{k+2}^l & \\ * & * & \end{array}\right) \simeq$$

$$\simeq \left(\begin{array}{c|c|c} -a_0^i & a_0^l - 2 & \\ -a_1^i + 2 & a_1^l - 2 & \\ \vdots & \vdots & a_0^3 - 2 - 2(n_0^3 - D) \\ -a_j^i + 2 & a_{k+1}^l - 2 & * \\ a_{j+1}^i - 2n_{j+1}^i & a_{k+2}^l - 2n_{k+2}^l & \\ * & * & \end{array}\right)$$

where D is the denominator of $[a_0^l, \ldots, a_k^l, n_{k+1}^l + 1]^{-1}$, and k, n_{k+1}^l satisfy

$$1 = -[a_0^i, \ldots, a_{j-1}^i]^{-1} - [a_0^l, \ldots, a_k^l, n_{k+1}^l + 1]^{-1},$$

or

$$\left(\begin{array}{c|c|c} a_0^1 - 2 - 2n_0^1 & a_0^2 - 2 - 2n_0^2 & a_0^3 - 2 \\ * & * & a_1^3 - 2 - 2n_1^3 \\ & & * \end{array}\right) \simeq$$

$$\simeq \left(\begin{array}{c|c|c} a_0^1 - 2n_0^1 & a_0^2 - 2n_0^2 & -a_0^3 \\ * & * & a_1^3 - 2n_1^3 \\ & & * \end{array}\right),$$

or

$$\left(\begin{array}{c|c|c} -a_0^1 & -a_0^2 & \\ -a_1^1+2 & -a_1^2+2 & \\ \vdots & \vdots & a_0^3-2 \\ -a_J^1+2 & -a_K^2+2 & a_1^3-2 \\ \vdots & \vdots & a_2^3-2-2n_2^3 \\ -a_j^1+2 & -a_k^2+2 & * \\ a_{j+1}^1-2-2n_{j+1}^1 & a_{k+1}^2-2-2n_{k+1}^2 & \\ * & * & \end{array}\right) \simeq$$

$$\simeq \left(\begin{array}{c|c|c} a_0^1-2 & a_0^2-2 & \\ \vdots & \vdots & -a_0^3 \\ a_J^1-2 & a_K^2-2 & -a_1^3+2 \\ a_{J+1}^1+2-2n_{J+1}^1 & a_{K+1}^2-2n_{K+1}^2 & a_2^3-2n_2^3 \\ * & * & * \end{array}\right)$$

where for $J \leq j, K \leq k$,

$$-[a_0^1,\dots,a_J^1,3]^{-1}-[a_0^2,\dots,a_K^2,2]^{-1}=1 \text{ and } \begin{array}{l} n_{J+1}^1 \geq 2 \text{ or } L^1=(v_0^1,\dots,v_J^1) \\ n_{K+1}^2 \geq 1 \text{ or } L^2=(v_0^2,\dots,v_K^2) \end{array},$$

and the denominator of the two fractions equals a_0^3. □

4.2.3 Convex surface theory, overtwistedness, and isotopies

To prove that the isotopic classification of tight structures is contained in the full paths of their dual covectors, we need to observe that presentations sharing the same path are indeed isotopic, and relate drop-outs to overtwistedness.

To begin with, remember two simple properties of full paths, which have a direct convex theoretic interpretation. The first is the shuffling property of basic slices within a single continued fraction block, which can be in the Heegaard Floer interpretation recovered by 2 PD steps on the consecutive dual vertices of square -2. The second is a necessary condition for tightness (see also Section 4.1.2), that the presentation contains both a leg starting in a fully positive vertex, and a leg starting in a fully negative vertex. In full paths, a fully positive starting vertex is required by Corollary 4.1.12, and a fully negative one by its analogue when following the path in the terminal direction. In convex surface theory, other presentations can be seen to fail the conditions of the Gluing Lemma, as in [30, Proposition 6.3], but can be also understood as a special case of overtwistedness proved below.

Let us now state the result as predicted from the Heegaard Floer picture, as in Corollary 4.2.12. We encode contact presentations into "matrices of negative signs", that is, triples of vectors q^i, possibly of different length, whose coefficients

are q^i_j, the number of negative basic slices in the j^{th} continued fraction block of the i^{th} singular fiber. The three vectors in the propositions are truncated, so that we write out only the relevant part (on which overtwistedness is decided, or which behaves non-trivially under isotopy moves) and hide the rest into $*$. Analogously, we can define "matrices of positive signs". Notice that the ones counting negative slices directly correspond to the relations obtained in the initial direction of the full path in Section 4.2.2. With positive slices they correspond to symmetric relations in the terminal direction. To describe isotopy moves it is enough to give only pairs of matrices of negative (or only positive) signs, while to encode conditions for overtwistedness, the two are different.

Proposition 4.2.13 (Overtwistedness conditions)**.** *Let a contact presentation be described by either of the following matrices of signs, negative or positive:*

O1. For some $(i,l) \in \{(1,2),(2,1)\}$*:*

$$(q^i|q^l|q^3) = \left(\begin{array}{c|c|c} 0 & a^l_0 - 1 & \\ 0 & a^l_1 - 2 & \\ \vdots & \vdots & n^3_0 \\ 0 & a^l_k - 2 & * \\ n^i_{j+1} & n^l_{k+1} & \\ * & n^l_{k+2} & \\ & * & \end{array}\right)$$

for which $-[a^i_0,\dots,a^i_{j-1}]^{-1} - [a^l_0,\dots,a^l_m,N^l_{m+1}]^{-1} < 1$ *holds for* N^l_{m+1} *defined as in Proposition 4.2.9.*

O2. Or

$$(q^1|q^2|q^3) = \left(\begin{array}{c|c|c} a^1_0 - 1 & a^2_0 - 1 & \\ a^1_1 - 2 & a^2_1 - 2 & \\ \vdots & \vdots & 0 \\ a^1_j - 2 & a^2_k - 2 & 0 \\ n^1_{j+1} & n^2_{k+1} & * \\ * & * & \end{array}\right)$$

such that for maximal $J \le j, K \le k$ *with* $-[a^1_0,\dots,a^1_J,3]^{-1} - [a^2_0,\dots,a^2_K,2]^{-1} = 1$*, the denominator of the two fractions is smaller than* a^3_0*.*

Then, independently of the basic slice decompositions of further continued fraction blocks (the $*$*-part of vectors), the corresponding contact structure is overtwisted.*

Proposition 4.2.14 (Isotopy conditions)**.** *The following pairs of matrices give isotopic contact structures, provided all coefficients are in the range* $n^i_j \in [0, a^i_j - 2], n^i_0 \in [0, a^i_0 - 1]$*, and the further basic slice decompositions (the* $*$*-parts) are the same.*

I1. On $(q^i|q^l|q^3)$ for $(i,l) \in \{(1,2),(2,1)\}$:

$$\left(\begin{array}{c|c|c} 0 & a_0^l - 1 & \\ 0 & a_1^l - 2 & \\ \vdots & \vdots & n_0^3 \\ 0 & a_k^l - 2 & * \\ n_{j+1}^i & n_{k+1}^l & \\ * & n_{k+2}^l & \\ & * & \end{array}\right) \simeq \left(\begin{array}{c|c|c} a_0^i - 1 & 0 & \\ a_1^i - 2 & 0 & \\ \vdots & \vdots & n_0^3 - D \\ a_j^i - 2 & 0 & * \\ n_{j+1}^i - 1 & 0 & \\ * & n_{k+2}^l - 1 & \\ & * & \end{array}\right)$$

where D is the denominator of $[a_0^l, \ldots, a_k^l, n_{k+1}^l + 1]^{-1}$, and k, n_{k+1}^l satisfy

$$1 = -[a_0^i, \ldots, a_{j-1}^i]^{-1} - [a_0^l, \ldots, a_k^l, n_{k+1}^l + 1]^{-1}.$$

I2. On $(q^1|q^2|q^3)$:

$$\left(\begin{array}{c|c|c} n_0^1 & n_0^2 & 0 \\ * & * & n_1^3 \\ & & * \end{array}\right) \simeq \left(\begin{array}{c|c|c} n_0^1 - 1 & n_0^2 - 1 & a_0^3 - 1 \\ * & * & n_1^3 - 1 \\ & & * \end{array}\right).$$

I3. On $(q^1|q^2|q^3)$:

$$\left(\begin{array}{c|c|c} a_0^1 - 1 & a_0^2 - 1 & \\ a_1^1 - 2 & a_1^2 - 2 & \\ \vdots & \vdots & 0 \\ a_J^1 - 2 & a_K^2 - 2 & 0 \\ \vdots & \vdots & n_2^3 \\ a_j^1 - 2 & a_k^2 - 2 & * \\ n_{j+1}^1 & n_{k+1}^2 & \\ * & * & \end{array}\right) \simeq \left(\begin{array}{c|c|c} 0 & 0 & \\ \vdots & \vdots & a_0^3 - 1 \\ 0 & 0 & a_1^3 - 2 \\ n_{J+1}^1 - 2 & n_{K+1}^2 - 1 & n_2^3 - 1 \\ * & * & * \end{array}\right)$$

where for $J \leq j, K \leq k$,

$$-[a_0^1, \ldots, a_J^1, 3]^{-1} - [a_0^2, \ldots, a_K^2, 2]^{-1} = 1 \text{ and } \begin{array}{l} n_{J+1}^1 \geq 2 \text{ or } L^1 = (v_0^1, \ldots, v_J^1) \\ n_{K+1}^2 \geq 1 \text{ or } L^2 = (v_0^2, \ldots, v_K^2) \end{array},$$

and the denominator of the two fractions equals a_0^3.

The proof of both Propositions is postponed till the end of the section, after a note on contact topological foundations of isotopies and some general computation of slopes.

State traversals and contact isotopies

Convex decomposition of the Seifert fibrations we are working with consists of the neighborhoods of the three singular fibers F_i and the background circle bundle over the pair of pants Σ. To ensure the product structure in the complement of F_i's we use non-normalized coefficients $M(0; r_1 - 1, r_2, r_3)$. The results here rely on Honda's classification of tight structures on separated pieces, namely solid tori and the product $\Sigma \times S^1$, see Section 2.2.1.

The isotopies can be described by the (state) transitions of toric annuli surrounding the three singular fibers. Concretely, the following lemma – due to Ghiggini and Schönenberger – enables us to relate certain pairs of toric annuli around two singular fibers to toric annuli around the remaining one.

Lemma 4.2.15. [31, Lemma 4.13] *Let Σ be a pair of pants and ξ a tight contact structure on $\Sigma \times S^1$ whose boundary $-\partial(\Sigma \times S^1) = T_1 \cup T_2 \cup T_3$ consists of tori in standard form with $\#\Gamma_{T_i} = 2$ for $i = 1, 2, 3$, and slopes $s(T_1) = -\frac{p_1}{q}, s(T_2) = -\frac{p_2}{q}, s(T_3) = \infty$. Suppose that there exists a pair of pants $\Sigma' \subset \Sigma$ such that $\Sigma \times S^1$ decomposes as $\Sigma \times S^1 = \Sigma' \times S^1 \cup C_1 \cup C_2$ where $C_i = T_i \times I$, with $\xi|_{C_i}$ minimally twisting and where $\xi|_{\Sigma' \times S^1}$ is a tight contact structure with infinite boundary slopes such that the section $\Sigma' \times \{\theta\}$ for some $\theta \in S^1$ is convex with dividing set consisting of arcs, each connecting two different boundary components.*

If $s(T_2) = -\frac{p_2}{q} < 0$ and both $\xi|_{C_i}$ decompose into basic slices of the same sign, there exists a convex annulus A bounded by the Legendrian rulings of T_1 and T_2, and without boundary parallel dividing curves.

Idea of the proof. The existence of an annulus A follows from the observation that $(\Sigma \times S^1, \xi)$ is isotopic to $(T^2 \times I, \xi|_{C_1})$ with removed $-\frac{p_2}{q}$-thickening of the standard neighborhood of a vertical ruling in the invariant neighborhood of T_1.

Alternatively, we notice that the dividing set on the vertical annuli A_i inside $C_i \backslash B_i$ (that is, C_i without the outermost basic slice B_i) consists of two arcs which cross the annulus and $q - 1$ boundary parallel arcs on T_i-side, which are (by assumption) all of the same sign (all in the same region with respect to the two crossing arcs). Additionally, there is a vertical annulus $A_\infty \subset \Sigma' \times S^1 \cup B_1 \cup B_2$ with boundary on ∂A_i, and a pair of dividing arcs crossing from ∂A_1 to ∂A_2. If we glue A_1, A_∞ and $-A_2$ along the common boundaries, we get an annulus A, whose dividing set consists of two arcs which cross the annulus and the same number $(q-1)$ of oppositely-signed boundary parallel arcs along the two boundary components. Since there are 0-twisting vertical curves in $\Sigma \times S^1$ (recall that the boundary of $\Sigma' \times S^1$ has ∞-slopes), we can alter Γ_A by adding bypasses:

Eventually, we get an annulus with dividing set consisting of $2q$ crossing arcs. $\square$

In our case, the decomposition $\Sigma \times S^1 = \Sigma' \times S^1 \cup C_1 \cup C_2$ always exists as we are dealing with the zero-twisting structures; both thickened tori are minimally twisting [38, Lemma 5.1]. The condition on the background structure, no boundary parallel dividing curves on the convex section, follows (as in [30, Lemma 5.4]) from the fact that ξ is appropriate on $\Sigma \times S^1$. And the latter is fulfilled by any $\Sigma \times S^1$, cut as a background out of tight small Seifert manifold [75, Lemma 2.4]. With the addition of [25, Section 3], Lemma 4.2.15 can be reformulated in the sense of [30, Lemmas 5.7, 5.8].

Lemma 4.2.16. *Let Σ be a pair of pants and let ξ be an appropriate contact structure on $\Sigma \times S^1$ with convex boundary $-\partial(\Sigma \times S^1) = T_1 \cup T_2 \cup T_3$ with $\#\Gamma_{T_i} = 2$ for $i = 1, 2, 3$, and boundary slopes $s(T_1) = -\frac{p_1}{q}, s(T_2) = -\frac{p_2}{q}, s(T_3) = \infty$.*

(L1) If there exists a collar neighborhood $C_3 \subset \Sigma \times S^1$ of T_3, which is minimally twisting with boundary slopes ∞ and $\frac{p_1+p_2-1}{q}$, whose basic slices are all same-signed, and for which $\xi|_{(\Sigma \times S^1)-C_3}$ coincides with the unique tight structure with boundary slopes $-\frac{p_1}{q}, -\frac{p_2}{q}, \frac{p_1+p_2-1}{q}$, and maximal twisting $-q$, then signs of basic slices in the decomposition of C_1 and C_2 are all opposite to C_3-signs.

(L2) And conversely, if C_1 and C_2 decompose into same-signed basic slices, then there exists C_3 composed of opposite-signed slices, with boundary slopes ∞ and $\frac{p_1+p_2-1}{q}$, and such that its complement is a unique tight structure as above.

Proof (following [30]). For (L1), uniqueness of a tight structure with given properties is stated in [25, Proposition 3.3]. The fact that the signs in the decomposition of collars are opposite, can be read from the relative Euler class evaluation on vertical annuli $A_i \subset C_i$, which have boundaries in vertical Legendrian divides on ∞-side and in Legendrian rulings on the other boundary. If we complete these annuli with annuli through the pair of pants up to T_3 for A_1, A_2, and up to T_1, T_2 for A_3, we get two pairs of homologically equivalent, but oppositely oriented, annuli. As the Euler class evaluation on all the extended parts is zero (the first having boundary in Legendrian divides, the second living inside $-q$-maximal twisting), the evaluation on A_1 and A_2 is opposite to that of A_3. Therefore, the collars C_1, C_2 decompose into basic slices all of the same sign, opposite to the signs in C_3.

For (L2), we take the unique tight $\Sigma'' \times S^1$ (as described in (L1)) and attach to it a thickened torus with slopes $\frac{p_1+p_2-1}{q}$, ∞, and slices signed oppositely to the ones in C_1. Then according to (L1) the signs on collars in decomposition $\Sigma' \times S^1 \cup C_1 \cup C_2$ are again opposite. And we have built up a contact structure, isotopic to the original in all three pieces ($\Sigma' \times S^1$ has the same dividing set on the pair of pants, while C_1 and C_2 have the same Euler class evaluations). $\square$

Slicing and continued fractions

We give a short reflection on the slopes of glued-up torus and its slicing. Denote by V_i the standard convex neighborhood of F_i with boundary $-\partial(M\backslash V_i)$ trivialized by $\binom{1}{0}$ the horizontal direction of $\Sigma\times 1$ and $\binom{0}{1}$ the direction of fiber, and from the other side ∂V_i by the meridian and some longitude, the last being chosen so that translation $A_i : \partial V_i \to -\partial(M\backslash V_i)$ is given by $A_i = \left(\begin{smallmatrix}\alpha_i & \alpha_i' \\ -\beta_i & -\beta_i'\end{smallmatrix}\right)$ where $\frac{\beta_i}{\alpha_i} = r_i$ (or $r_1 - 1$ for the first leg); in terms of the continued fraction expansion we have $-\frac{\alpha_i}{\beta_i} = [a_0^i, ..., a_{k_i}^i], -\frac{\alpha_i}{\alpha_i'} = [a_{k_i}^i, ..., a_0^i], -\frac{\beta_i}{\beta_i'} = [a_{k_i}^i, ..., a_1^i]$. Now, the ∞-slope of a thickened neighborhood U_i of a singular fiber corresponds to $[a_{k_i}^i, ..., a_0^i]$ in the torus basis, and the slopes of the factorization can be obtained in order (from outside in) by decreasing the last entry of this fraction.

We will be interested in slopes of tori, which peel off certain sequences of basic slices from thickened neighborhoods U_i, and their expression in the background basis. Notice the following general behavior.

Lemma 4.2.17. *The slope of a torus which peels off $\sum_0^{j-1}(a_\iota^i - 2) + m$ outer basic slices from U_i, as seen from $-\partial(M\backslash V_i)$, is independent of inner continued fraction blocks in the decomposition of U_i, that is, of vertices $a_j^i, \dots, a_{k_i}^i$, farther down the legs. It equals $[a_0^i, \dots, a_{j-1}^i, m]^{-1}$, or $[a_0^i, \dots, a_{j-1}^i, m]^{-1} + 1$ in the case $i = 1$.*

Proof. The slope of interest is in the torus basis expressed as $[a_{k_i}^i, ..., a_j^i - m]$.

Recall the matrix form of a negative continued fraction

$$[a_{k_i}^i, \dots, a_0^i] \leftrightarrow \left[\begin{pmatrix} -a_{k_i}^i & 1 \\ -1 & 0\end{pmatrix}^{-1} \cdots \begin{pmatrix} -a_0^i & 1 \\ -1 & 0\end{pmatrix}^{-1}\right]^2 = \left[\begin{pmatrix} -\beta_i' & -\alpha_i' \\ \beta_i & \alpha_i\end{pmatrix}\right]^2,$$

and notice that it is exactly the inverse of our identification $A : \partial V_i \to -\partial(M\backslash V_i)$.

Hence, we get the desired slope in the second column of:

$$\begin{pmatrix} -a_0^i & 1 \\ -1 & 0\end{pmatrix} \cdots \underbrace{\begin{pmatrix} -a_{j+1}^i & 1 \\ -1 & 0\end{pmatrix} \cdots \begin{pmatrix} -a_{k_i}^i & 1 \\ -1 & 0\end{pmatrix} \begin{pmatrix} -a_{k_i}^i & 1 \\ -1 & 0\end{pmatrix}^{-1} \cdots \begin{pmatrix} -a_{j+1}^i & 1 \\ -1 & 0\end{pmatrix}^{-1}}_{I} \begin{pmatrix} -a_j^i + m & 1 \\ -1 & 0\end{pmatrix}^{-1} =$$

$$= \begin{pmatrix} -a_0^i & 1 \\ -1 & 0\end{pmatrix} \cdots \begin{pmatrix} -a_j^i & 1 \\ -1 & 0\end{pmatrix} \begin{pmatrix} 0 & -1 \\ 1 & -a_j^i + m\end{pmatrix} = \begin{pmatrix} -a_0^i & 1 \\ -1 & 0\end{pmatrix} \cdots \begin{pmatrix} -a_{j-1}^i & 1 \\ -1 & 0\end{pmatrix} \begin{pmatrix} 1 & m \\ 0 & 1\end{pmatrix}$$

Indeed, this is independent of a_ι^i for $\iota \geq j$.

Now, comparing the second columns:

$$\left[\begin{pmatrix} -a_0^i & 1 \\ -1 & 0\end{pmatrix} \cdots \begin{pmatrix} -a_{j-1}^i & 1 \\ -1 & 0\end{pmatrix} \begin{pmatrix} 1 & m \\ 0 & 1\end{pmatrix}\right]^2 =: \begin{pmatrix} A \\ B\end{pmatrix} \leftrightarrow \begin{pmatrix} -B \\ -A\end{pmatrix} =: \left[\begin{pmatrix} 0 & -1 \\ 1 & -a_0^i\end{pmatrix} \cdots \begin{pmatrix} 0 & -1 \\ 1 & -a_{j-1}^i\end{pmatrix} \begin{pmatrix} 0 & -1 \\ 1 & -m\end{pmatrix}\right]^2,$$

we express the slope as $[a_0^i, \dots, a_{j-1}^i, m]^{-1}$ ($[a_0^i, \dots, a_{j-1}^i, m]^{-1} + 1$ for $i = 1$). □

This independence of inner layers, allows us to compute the background-basis slope of any sequence of slices (from outside in) on a truncated leg. In the opposite

direction, if the slope of peeled-off slices is $[a^i_0,\dots,a^i_{j-1},m]^{-1}$ ($[a^i_0,\dots,a^i_{j-1},m]^{-1}+1$ if $i=1$), this in the torus basis corresponds to $[a^i_k,\dots,a^i_j-m]$ when $m\le a^i_j-1$. When $m=a^i_j$, we get $[a^i_k,\dots,a^i_{j+1},0]$, undefined as a continued fraction, but in terms of the chain of surgeries, the 0-framed meridian cancels a_{j+1} which results in $[a^i_k,\dots,a^i_{j+2}]$.

Proofs

The proofs of Propositions 4.2.13 and 4.2.14 are stated for matrices of negative signs, but they can be verbatim repeated for positive ones. Without loss of generality, basic slices within each continued fraction block are shuffled so that the negative slices are outer.

Proof of Proposition 4.2.13. The guiding principle is as follows. Look at the two singular tori U_μ, U_ν whose outermost slices are negative. If we can peel such sequences of negative basic slices from U_μ, U_ν that their inner boundary tori T_μ, T_ν have slopes with the same denominator, say $-\frac{p_\mu}{q}, -\frac{p_\nu}{q}$, we can use Lemma 4.2.15 to find a torus parallel to ∂U_λ of slope $\frac{p_\mu+p_\nu-1}{q}$, call it T. Whenever this slope is not greater than the critical slope of the singular fiber, $\mathrm{Crit}(F_\lambda)$ (that is, the slope of meridian of the glued-up torus in the background basis), there exists a torus of critical slope between ∂U_λ and T, which proves overtwistedness (see also [50, Section 2]). Furthermore, if the slope of T is such that the thickened torus between ∂U_λ and T (whose basic slices are all positive by (L2)) forms a basic slice together with some of the slices in the original decomposition of U_λ, any negative basic slice in this glued-together basic slice implies overtwistedness by the Gluing Lemma. Below we analyze the slopes in each of the cases separately.

O1. Consider first the structures of the first kind with $(i,l)=(1,2)$. Around F_2 there are only negative slices in the first $k+1$ continued fraction blocks and n^2_{k+1} of them in the block corresponding to the vertex v^2_{k+1} (here we shuffle them to be its outer). Around F_3, on the other hand, we have n^3_0 negative slices (again, shuffled so that they are the outer). Thus, peeling off from U_2 basic slices up to the $(N^2_{m+1})^{\text{th}}$ slice of the $-a^2_{m+1}$-block, we obtain the slope $[a^2_0,\dots,a^2_m,N^2_{m+1}]^{-1}$ (in the background basis), which can be joined by cutting annulus to the torus with slope $-\frac{1}{D}$ around F_3 (peeling off D slices from U_3, where D is the denominator of $[a^2_0,\dots,a^2_m,N^2_{m+1}]^{-1}$, which is at most n^3_0 by assumption). That way, we have found a torus T parallel to T_1 of slope $-[a^2_0,\dots,a^2_m,N^2_{m+1}]^{-1}$.

Now, observe that the critical slope of F_1 satisfies

$$[a^1_0,\dots,a^1_{j-1}-1]^{-1}+1\le \mathrm{Crit}(F_1)=[a^1_0,\dots,a^1_{k_1}]^{-1}+1\le [a^1_0,\dots,a^1_{j-1}]^{-1}+1.$$

Our assumed condition gives $-[a^2_0,\dots,a^2_m,N^2_{m+1}]^{-1}<[a^1_0,\dots,a^1_{j-1}]^{-1}+1$. If also a bit more holds true, namely $-[a^2_0,\dots,a^2_m,N^2_{m+1}]^{-1}\le \mathrm{Crit}(F_1)$, the torus T embraces the critical one. Otherwise, we have $-[a^1_0,\dots,a^1_{k_1}]^{-1}-$

$[a^2_0,\dots,a^2_m,N^2_{m+1}]^{-1}\geq 1$ and we can truncate both fractions so that the truncations add up to exactly one [46, Lemma 3.2]. So, $-[a^1_0,\dots,a^1_J]^{-1}-[a^2_0,\dots,b^2_M]^{-1}=1$ for some $J\in\{j,\dots,k_1\}$ and $M\in\{0,\dots,m+1\}$, and $b^2_M=a^2_M$ for $M\leq m$ or $b^2_M=N^2_{m+1}$ for $M=m+1$. Peeling off from U_2 only slices of the first $M+1$ outer blocks and corresponding (as many as the denominator of $[a^2_0,\dots,b^2_M]^{-1}$, which is certainly less than or equal to $D\leq n^3_0$) slices in U_3, the slope of T is $[a^1_0,\dots,a^1_J]^{-1}+1$ in the background basis. By the text under Lemma 4.2.17 this equals $[a^1_{k_1},\dots,a^1_{J+2}]$ in torus basis, and T bounds a basic slice with a torus T_1 of slope $[a^1_{k_1},\dots,a^1_{J+2}-1]$. For tightness, the conditions of the Gluing Lemma require for all the subslices of a glued-together basic slice to be positive, but this is not satisfied as the toric annulus bounded by T_1 and T contains the $(j+1)^{\text{th}}$ continued fraction block ($J\geq j$) and $n^1_{j+1}>0$ by assumption.

For $(i,l)=(2,1)$, the arguments are the same, but here the induced slope of T (built from peeling-off tori in U_1 and U_3) equals $[a^1_0,\dots,a^1_m,N^1_{m+1}]^{-1}+1$, while the critical slope is given by

$$[a^2_0,\dots,a^2_{j-1}-1]^{-1}\leq \mathrm{Crit}(F_2)=[a^2_0,\dots,a^2_{k_2}]^{-1}\leq[a^2_0,\dots,a^2_{j-1}]^{-1}.$$

O2. Structures of the second kind admit negative basic slices in the outer layers of U_1 and U_2. The background-basis slopes $[a^1_0,\dots,a^1_J,3]^{-1}+1$ on T_1 around F_1 and $[a^2_0,\dots,a^2_K,2]^{-1}$ on T_2 around F_2 – which add up to zero – are reached by peeling off the corresponding sequences of (negative) basic slices when v^1_{J+1},v^2_{K+1} exist, and by decreasing the twisting number of the Legendrian singular fibers F_1 or F_2 by stabilizing when $L_1=(v^1_0,\dots,v^1_J)$ or $L_2=(v^2_0,\dots,v^2_K)$. Joining the two tori T_1 and T_2 by an annulus interpolating between the rulings, and edge-rounding, we obtain a torus T around F_3 of slope $-\frac{1}{D}$ where D is the denominator of $[a^1_0,\dots,a^1_J,3]^{-1}$. By assumption, the denominator D is not greater than a^3_0-1, hence the obtained slope $-\frac{1}{D}$ is smaller than or equal to $-\frac{1}{a^3_0-1}<\mathrm{Crit}(F_3)$, that is, T embraces the critical torus. □

Proof of Proposition 4.2.14. Recognition of isotopies, in all cases, follows the same steps. First, we apply (L2) to get an additional thickened torus C around the singular torus U_λ with positive outermost slices – traverse outer layers, whose basic slices are all negative, from U_μ and U_ν. This new collar together with some, say n, continued fraction blocks around F_λ join into a thicker basic slice, separated into positive basic subslices. The isotopy is now given by reversing all these signs. In case we have used all continued fraction blocks of U_λ, it is interpreted in destabilization followed by opposite stabilization of a core knot. Otherwise, C together with $n+1$ outermost continued fraction blocks in U_λ builds a continued fraction block. Its signs can be shuffled, resulting in the $+2$-change in its innermost $(n+1)^{\text{th}}$ block (one negative slice replaced by positive) and turn of sign on all basic slices that form C and the first n continued fraction blocks

(from positive to negative). The basic slices around the other two fibers, F_μ and F_ν, are then adapted according to (L1) – the peeled off ones change their signs from negative to positive, others remain untouched. The relevant slopes for the three isotopy moves are analyzed below.

I1. Since the equality $-[a^i_0,\dots,a^i_{j-1}]^{-1}-[a^l_0,\dots,a^l_k,n^l_{k+1}+1]^{-1}=1$ holds and n^3_0 is at least as much as the denominator of the two fractions, we can peel off from U_l and U_3 as many negative slices that the slope of the torus T we get around F_i via (L2) equals $[a^i_{k_i},\dots,a^i_{j+1}]$ in the torus basis. The torus T bounds a basic slice with the torus of slope $[a^i_{k_i},\dots,a^i_{j+1}-1]$ which cuts off the positive outermost slices from U_i. The torus of slope $[a^i_{k_1},\dots,a^i_{j+2}]$ then gives a continued fraction block with the torus T.

I2. These are essentially isotopies from [30, Proposition 6.4]. Peeling off a single (negative outermost) basic slice from U_1 and U_2, we obtain a torus of slope 0, expressed in the background basis, around F_3. It corresponds to the slope $[a^3_{k_3},\dots,a^3_1]$, and forms a glued-together basic slice with the outermost continued fraction block (with inner slope $[a^3_{k_3},\dots,a^3_1-1]$), and hence, a continued fraction block with $[a^3_{k_3},\dots,a^3_2]$.

I3. In the proof of Proposition 4.2.13, for structures of the second kind (O2.), we have obtained that the slope of the torus T built via (L2) from the two tori of slopes $[a^1_0,\dots,a^1_J,3]^{-1}+1$ around F_1 and $[a^2_0,\dots,a^2_K,2]^{-1}$ around F_2, which sum up to zero, equals $-\frac{1}{D}$ for D the denominator of $[a^1_0,\dots,a^1_J,3]^{-1}$. By assumption, D equals a^3_0, moreover, $-\frac{1}{a^3_0}$ is in the torus basis expressed as $[a^3_{k_3},\dots,a^3_2]$. Thus, the torus T bounds a basic slice with the torus of slope $[a^3_{k_3},\dots,a^3_2-1]$ and a continued fraction block with the torus of slope $[a^3_{k_3},\dots,a^3_3]$ in the slicing of U_3. □

Proof of Theorem 4.2.1. In the outline of the proof we have reduced Theorem 4.2.1 to Theorem 4.2.3.

Suppose we are given a contact surgery presentation ξ as in Figure 4.1, whose full path $\mathcal{P}_\xi$ properly ends. By Theorem 4.1.2, such a presentation describes a tight structure with non-vanishing contact invariant; furthermore, all presentations which share this same path define the same element in $\widehat{\mathrm{HF}}(-M)$, hence they induce the same Spin^c structure and have the same 3-dimensional invariant. In Corollary 4.2.12 we identify how presentations in the same path are related to each other, and in Proposition 4.2.14 we realize all these relations by contact isotopies. Any further isotopies are, of course, excluded by the fact that different paths present different elements in $\widehat{\mathrm{HF}}(-M)$.

On the other hand, if the path $\mathcal{P}_\xi$ drops out (fails the tightness criterion), the corresponding structure ξ admits one of the features recognized in Corollary 4.2.12 or it can be walked through presentations, related by the above isotopy moves, to some presentation which admits such a feature. Finally, for these

structures either the existence of a torus with critical slope or the Gluing Lemma argument proves their overtwistedness, in Proposition 4.2.13.

This finishes the proof of Theorem 4.2.3, originally stated as Theorem 4.2.1. □

5

Fillable contact structures on $M(-1; r_1, r_2, r_3)$

Seifert fibered 3-manifolds not carrying (Stein) fillable contact structures has been characterized by Lecuona and Lisca [46], they call them manifolds of special type. Here, we address the question which exactly are the fillable contact structures on small Seifert fibered spaces.

Let us summarize from Chapter 4: Tight contact structures on small Seifert fibered spaces $M(e_0; r_1, r_2, r_3)$ whenever $e_0 \neq -1$ or -2, and on L-spaces with $e_0 = -2$ are completely classified – they are all Stein fillable. On $M(-1; r_1, r_2, r_3)$ there are essentially two types of tight contact structures, distinguished by the maximal twisting of the regular fiber. The negative twisting structures are related to the transverse contact structures, and they are expected to be all at least symplectically fillable. On the other hand, zero-twisting tight contact structures share a common contact surgery description (of Figure 4.1) and are (at least, when L-spaces) characterized by non-vanishing of the Ozsváth-Szabó contact invariant $c(M, \xi) \in \widehat{\mathrm{HF}}(-M, \mathbf{t}_\xi)$.

The zero-twisting structures are all supported by planar open books, as shown in Section 2.3.1. But in contrast to contact structures on small Seifert spaces with $e_0 \neq -1$ not all tight ones are Stein fillable. Relying on a theorem of Wendl [74] about fillings of planar contact structures, non-Stein fillable structures are not fillable at all. Non-fillability was first observed by Ghiggini, Lisca and Stipsicz in [30] for a particular structure on $M(-1; \frac{1}{2}, \frac{1}{2}, \frac{1}{p})$. Based on their classification [30] of tight structures on $M(-1; r_1, r_2, r_3)$ for $r_1 \geq r_2 \geq \frac{1}{2}$, Plamenevskaya and Van Horn-Morris [67] then recognized exactly which of those manifolds admit non-fillable tight structures using Wendl's work and obstructing existence of positive factorizations in (abelianization of) standardly associated (planar) open books. On the other hand, Lecuona and Lisca [46] showed that for $M(-1; r_1, r_2, r_3)$ of special type, that is, when it is L-space and $r_i + r_j < 1$ for all pairs i, j, topology (the diagonalization argument) prevents existence of Stein fillings.

Here, we show that all fillable zero-twisting structures on $M(-1; r_1, r_2, r_3)$ arise as Legendrian surgeries on tight $S^1 \times S^2$. For L-spaces this covers all fillable structures, and hence implies the result of Lecuona and Lisca that small Seifert

fibered manifolds of special type do not admit any fillable structure.

More specifically, we obtain the following.

Proposition 5.0.1. *Contact surgery diagram as in Figure 4.1 with $r_1 + r_2 = 1$ and $r_3 = 0$ describes the tight contact $S^1 \times S^2$ if and only if $\mathrm{rot}_j^1 = -\mathrm{tb}_j^1 - 1$ for the Legendrian unknots in L_1 and $\mathrm{rot}_j^2 = \mathrm{tb}_j^2 + 1$ for the Legendrian unknots in L_2.*

Theorem 5.0.2. *Assume that a contact structure ξ on $M(-1; r_1, r_2, r_3)$ is given by some surgery diagram of Figure 4.1. For each pair i, j for which $r_i + r_j \geq 1$, form a sublink L_{ij} of the surgery link consisting of two unknots with $+1$-coefficient and two truncated chains such that rational numbers $-\frac{1}{s_i}$ they present satisfy $s_i \leq r_i, s_j \leq r_j$, and $s_i + s_j = 1$. Then ξ is fillable if and only if there exists L_{ij} which describes the tight $S^1 \times S^2$.*

In words, fillability of a given surgery presentation is completely decided on specific sublinks representing $S^1 \times S^2$, whose tightness is in turn met by a unique choice of rotation numbers for this sublink.

This chapter is dedicated to the study of planar open books supporting our contact manifolds. To prove fillability, we find an explicit positive factorization of the monodromy. For negative results, we study abelianization of the mapping class group of the planar page (following the approach of Plamenevskaya and Van Horn-Morris).

5.1 Abelianized planar monodromy

Planar monodromy Since our contact structures are all planar, the following theorem of Wendl ensures that to prove non-fillability, it suffices to study positive factorizations of the given monodromy.

Theorem 5.1.1. [74, Corollary 2] *A planar contact manifold is strongly symplectically (and thus Stein) fillable if and only if every supporting planar open book has monodromy isotopic to a product of positive Dehn twists.*

Let us briefly review the characteristic features of the abelianized planar mapping classes, as used by Plamenevskaya and Van Horn-Morris in [67].

The mapping class group of a planar surface (in the presentation of Margalit and McCammond) is described (geometrically) on a disk, $\mathbf{D}_n$, with n holes arranged in the roots of unity. The group $\mathrm{Map}\,\mathbf{D}_n$ is generated by all convex Dehn twists (that is, the twists whose core is the boundary of the convex hull of a set of holes), and factored by commutators of disjoint twists and all lantern relations. Then, up to conjugation – as an element of $\mathrm{AbMap}\,\mathbf{D}_n$ – a Dehn twist is determined by the set of holes it encircles. Furthermore, any monodromy ϕ factors into a product of Dehn twists, and each Dehn twist can be, using the

lantern relations, decomposed into pairwise (around a pair of holes) and boundary (around a single hole) Dehn twists; when a positive Dehn twist encircles r holes, it can be factorized so that for every hole there are exactly $r-1$ positive pairwise twists and $r-2$ negative boundary twists around it. Hence, ϕ as an element of $\mathrm{AbMap}\,\mathbf{D}_n$ is uniquely determined by a collection of multiplicities $\{m_\alpha, m_{\alpha\beta}\}$, defined as the number of twists (counted with signs) on the disk with all but one hole α, or a pair of holes α and β, capped off. Finally, being interested only in positive factorization, the number of its non-boundary twists around every hole is bounded from above by the number of all twists encircling this hole in any given presentation [67, Lemma 3.1].

Nonfillability result Look at the monodromies as translated from the surgery presentations (Section 2.3.1).

Notation 5.1.2 (see Figure 5.1)**.** Given the continued fraction expansion

$$-\frac{1}{r_i} = -a_0^i - \cfrac{1}{\ddots - \frac{1}{-a_{k_i}^i}} = [a_0^i, \dots, a_{k_i}^i],\ a_j^i \geq 2,$$

denote by ν_j^i and π_j^i any of the stabilization holes which correspond to, respectively, negative and positive stabilizations of the a_j^i-unknot (that is, the stabilization holes which are additionally encircled, respectively left out, by the positive Dehn twist corresponding to the a_j^i-unknot in comparison to the a_{j-1}^i-unknot or the core in the case $j=0$). Using $|\cdot|$ for the number of respective holes, we see $2+|\nu_j^i|+|\pi_j^i| = a_j^i$ (or a_0^i+1 when $j=0$), $-1-|\nu_j^i|-|\pi_j^i| = \mathrm{tb}_j^i$ and $|\pi_j^i|-|\nu_j^i| = \mathrm{rot}_j^i$. Additionally, write π^{in} and ν^{out} for the inner and the outer boundary of the annulus. When grouped into certain types, we use ν^i for any of $\cup_j \nu_j^i$, similarly $\nu_{\geq j}^i$ for any of $\cup_{J\geq j}\nu_J^i$, and ν to denote any of $\nu^{out}\cup\nu^i$; and analogously for π-type holes.

Notation 5.1.3. We number the first unknot of the i^{th} leg whose stabilizations are not all of the same sign as the stabilizations of a_0^i-unknot, by n_i; when the a_0^i-unknot admits positive and negative stabilizations, we choose $n_i = 0$. We name the corresponding continued fraction by $-\frac{1}{q_i} := [a_0^i, \dots, a_{n_i-1}^i]$, or $-\frac{1}{q_i} := -\infty$ when $n_i = 0$.

Proposition 5.1.4. *When there is no pair of legs i and j for which a_0^i- and a_0^j-unknot are stabilized oppositely, with $\mathrm{rot}_0^i = -a_0^i+1$ and $\mathrm{rot}_0^j = a_0^j-1$, and $q_i+q_j \geq 1$, the corresponding monodromy does not admit any positive factorization.*

Proof. We start with the factorization Φ of the monodromy ϕ as being read from the surgery presentation, and we try to build a positive factorization of ϕ, at

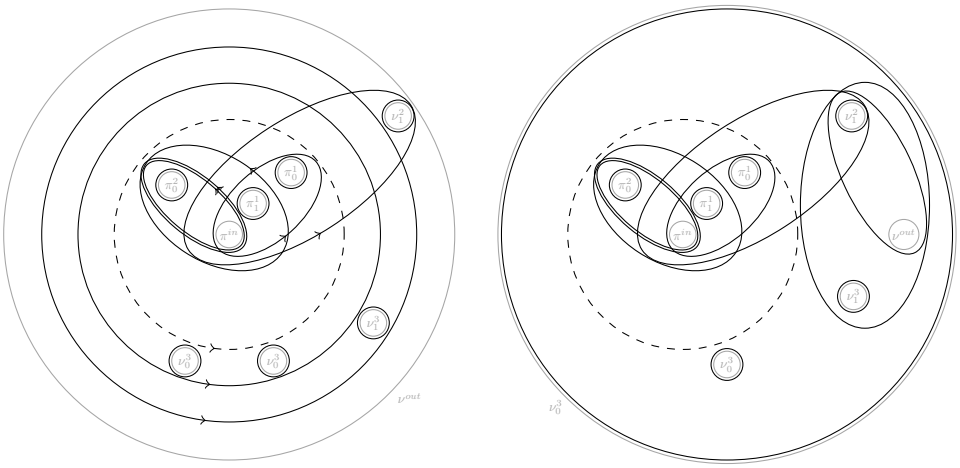

Figure 5.1: Illustration of our notation conventions on an example: $L_1 = (-2,-3,-2)$ and $\mathrm{rot}^1 = (1,1,0)$, $L_2 = (-2,-3)$ and $\mathrm{rot}^2 = (1,-1)$, $L_3 = (-3,-3)$ and $\mathrm{rot}^3 = (-2,-1)$. In gray are boundary components of the punctured disk, full curves correspond to positive Dehn twists, and dashed curves to negative Dehn twists. The page is shown in two perspectives: with initial outer boundary (left) and with outer boundary in one ν_0^3-hole (right).

least on the level of abelianization. Abusing the notation, we use same names in AbMap, and in fact, throughout the proof we are interested in Dehn twists only up to conjugation.

Without loss of generality (due to Proposition 4.1.13), we may assume that there is only one leg, say the 3rd, whose starting unknot is stabilized fully negatively, otherwise we turn our perspective interchanging the outer and the inner boundary of the annulus.

We will interchangeably use three perspectives: initial with ν^{out} as the outer boundary of the disk, turned-over with π^{in} as the outer boundary, and finally, call it $\mathbf{D} = \mathbf{D}_{\pi\cup\nu}$, the punctured disk obtained by setting one of the ν_0^3-holes to be the outer boundary. The multiplicities with respect to each viewpoint will be denoted by m for the initial disk, by m' for the turned-over one, and by capital M in $\mathbf{D}$. Let $\mathbf{D}$ be our preferred viewpoint if not stated otherwise. When some of its holes are capped off, we denote this by putting the remaining holes in the index; so, the notation $\mathbf{D}_\chi$ means the page $\mathbf{D}$ with all but χ-type holes capped off. Notice that all the multiplicities remain the same, and we keep the notation.

To begin with, let us study how possible positive factorizations behave with respect to π-holes.

Lemma 5.1.5. *By capping off all ν-holes, except the outer boundary of $\mathbf{D}$, we descend from* $\mathrm{AbMap}\,\mathbf{D}_{\pi\cup\nu}$ *to* $\mathrm{AbMap}\,\mathbf{D}_\pi$*, $\phi \mapsto \overline{\phi}$, which maps the given factorization $\Phi \mapsto \overline{\Phi}$. This $\overline{\Phi}$ is a composition $\overline{\Phi}_1\overline{\Phi}_2\overline{\Phi}_3$, where $\overline{\Phi}_i$ is a product of*

Dehn twists coming from a^i-unknots and boundary twists around π^i-holes. Every positive factorization $\overline{\Psi}$ of $\overline{\phi}$ splits into subfactorizations $\overline{\Psi} = \overline{\Psi}_1\overline{\Psi}_2\overline{\Psi}_3$ so that $\overline{\Psi}_i$ and $\overline{\Phi}_i$ describe the same element in $\mathrm{AbMap}\,\mathbf{D}_\pi$.

Proof. The $\overline{\Phi}$ itself presents a positive factorization of restricted monodromy $\overline{\phi}$. Indeed, the only negative twist of Φ cancels with the boundary twist of the outer ν_0^3 after capping-off ν-holes.

Now, set π^{in} as the outer boundary and consider the capped-off page $\mathbf{D}_\pi$ in the turned-over perspective. Here, no π^i-hole is encircled together with any π^j-hole for $i \neq j$, in symbols $m'_{\pi^i\pi^j} = 0$, and the only remaining ν_0^3 is in at most $k_1 + k_2 + 2$ twists (the number of twists around it in $\overline{\Phi}$). On the other hand, the pairwise multiplicity of ν_0^3 with π_0^i is exactly $m'_{\nu_0^3\pi_0^i} = k_i + 1$. So, there are exactly $k_i + 1$ twists encircling ν_0^3 together with only π^i-holes. Therefore, since there are no twists containing π^i and π^j together, we can consider the whole (abelianized) monodromy $\overline{\phi}$ as a product of three monodromies $\overline{\phi}_i$, uniquely determined by multiplicities: the π^i-multiplicities are the same as in $\overline{\Phi}$, and the twists around ν_0^3 are distributed so that ν_0^3-multiplicity with π^i-holes is $k_1 + 1, k_2 + 1$, and 0, respectively. Thus, any positive factorization splits as $\overline{\Psi}_1\overline{\Psi}_2\overline{\Psi}_3$ with $\overline{\Psi}_i$ describing $\overline{\phi}_i$. □

Lemma 5.1.6. *In the notation of Lemma 5.1.5, let us write out positive factorizations as $\overline{\Phi}_i = f_0^i \cdots f_{k_i}^i \cdots f_{l_i}^i$ and $\overline{\Psi}_i = p_0^i \cdots p_{k_i}^i \cdots p_{l'_i}^i$ for $i = 1, 2$, where we order the Dehn twist factors with the ones containing π^{in} first and in the decreasing order of the number of holes they include. Then for $K_i := \min\{k; f_k^i \neq p_k^i\}$, $p_{K_i}^i$ is a strict subset of $f_{K_i}^i$, and neither of π^i-holes not in $f_{K_i}^i$ are encircled by any non-boundary twist $p_k^i, k \geq K_i$.*

Proof. Look at the capped-off page $\mathbf{D}_\pi$ in the turned-over perspective, with π^{in} as outer boundary. We first notice that K_i always occurs among twists containing ν_0^3, thus $K_i \leq k_i$, as otherwise all pairwise multiplicities are reached within $\{p_k^i; 0 \leq k \leq k_i\}$, and the factorization agrees with $\overline{\Phi}$. Now, if $p_{K_i}^i$ did not contain some $f_{K_i}^i$-hole χ, the pairwise multiplicity of χ with ν_0^3 in $\overline{\Psi}$ would be strictly smaller than in $\overline{\Phi}$, in symbols $m'_{\chi\nu_0^3}(\overline{\Psi}) < m'_{\chi\nu_0^3}(\overline{\Phi})$. Indeed, the number of twists containing ν_0^3 is fixed and equal to k_i, and f_k^i for $k \geq K_i$ all contain χ, while f_k^i for $k < K_i$ contains χ if and only if p_k^i does. Finally, as (in $\mathbf{D}$) pairwise M-multiplicities of holes out of $f_{K_i}^i$ with any other hole are exactly as many as there are twists from $\{p_k^i = f_k^i; k < K_i\}$ around them, neither can be encircled together with any other hole additionally. □

We have reduced the problem of finding a positive factorization to whether any factorization $\overline{\Psi}$ (maybe $\overline{\Phi}$) from Lemma 5.1.5 can be lifted to a positive factorization of $\phi \in \mathrm{AbMap}\,\mathbf{D}$.

In the following, we investigate possible lifts of $\overline{\Psi}$-twists, in particular, which of the ν-holes they include.

Lemma 5.1.7. *If there exists a positive factorization of ϕ lifting $\overline{\Psi}$, then for $i = 1, 2$, the last $k_i - n_i + 1$ twists containing π^{in} in $\overline{\Psi}_i$ (that is, the ones which avoid all π^i_k with $k < n_i$) lift to the twists which additionally contain only ν^i-holes.*

Proof. Recall that on the disk with the initial outer boundary all multiplicities $m_{\nu^i\nu^j}, i \neq j$, vanish. On $\mathbf{D}$ this means that whenever some ν^i is encircled together with any of ν^j, the twist needs to contain also the initial outer boundary, the hole ν^{out}. But the $\pi^{in}\nu^1$- and $\pi^{in}\nu^2$-multiplicities are greater than $M_{\pi^{in}\nu^{out}} = 1$, specifically, for ν^i_j-hole the multiplicity is exactly $M_{\pi^{in}\nu^i_j} = k_i - j + 2$. Thus (at least) $k_i - n_i + 1$ Dehn twists which contain π^{in} need to lift into twists which include only ν^i-type ν-holes. Moreover, as $m_{\pi^i_k\nu^i} = 0$ for $k < n_i$, whenever such π^i_k is encircled together with ν^i, the twist contains also ν^{out} – hence the $k_i - n_i + 1$ twists mentioned above are the last $k_i - n_i + 1$ twists from $\overline{\Psi}_i$ which contain π^{in} (and avoid all π^i_k for $k < n_i$). □

Remark 5.1.8. Considering m'-multiplicities in the turned-over perspective, the same (with interchanged role of ν- and π-holes) can be concluded for the $k_3 - n_3 + 1$ twists containing ν^{out} and avoiding ν^3_k for $k < n_3$.

Let us list some properties of encircling $\nu^{out} \cup \nu^3$-holes (viewed in $\mathbf{D}$):

1. Their pairwise multiplicity with any of $\pi^{in} \cup \pi^1 \cup \pi^2$ is one (and with any of π^3 one plus the number of twists mentioned in Remark 5.1.8).
2. Each of ν^3_j-holes is encircled by at most $j + 2$ non-boundary Dehn twists, ν^{out} by at most $k_3 + 2$ (the number of twists around them in Φ); for $j \geq n_3$, $j - n_3 + 1$ of them are described by Remark 5.1.8.
3. Pairwise multiplicity of each ν^3_j with any $\nu^3_{\geq j}$ is exactly $j + 1$.
4. According to Lemma 5.1.7, lifts of the twists $p^i_{n_i}, \ldots, p^i_{k_i}$ for $i = 1, 2$, never encircle any of $\nu^{out} \cup \nu^3$; denote $\overline{\Psi}^* := \overline{\Psi} \setminus \{p^i_{n_i}, \ldots, p^i_{k_i}; i = 1, 2\}$ and $\overline{\Psi}^*_i = \overline{\Psi}_i \cap \overline{\Psi}^*$.

So, since we need to enclose each $\nu^{out} \cup \nu^3$ with all of π-holes once (1) and by the bounded number of twists (2), we look (in every factorization $\overline{\Psi}$) for partitions of π-holes by the $\overline{\Psi}^*$-twists, which have appropriate number of parts. If two sets of $\overline{\Psi}^*$-twists define set-wise the same partition, we say they are parallel as the twists of the two sets need to be parallel (or equal), the equal twists are referred to as shared.

Let us proceed successively, focusing on ν^3_j for every j in $0, 1, \ldots, k_3 + 1$, here we denote $\nu^3_{k_3+1} := \nu^{out}$. We say that $\overline{\Psi}$ lifts over $\nu^3_{\leq j}$, if $\overline{\Psi}^*$-twists can be lifted to a positive factorization in $\mathrm{AbMap}\,\mathbf{D}_{\pi \cup \nu^3_{\leq j}}$ which satisfies the listed properties.

Recursively define $J_0 = -1$ and

$$J_l := \min\{j; j > J_{l-1} \text{ and } |\nu^3_j| \geq 1 \text{ and if } j = 0 : |\nu^3_0| > 1\}.$$

Lemma 5.1.9. *If $\overline{\Psi}$ lifts over $\nu^{out} \cup \nu^3$-holes, the $\overline{\Psi}^*$-twists whose lifts encircle $\nu^{out} \cup \nu^3$-holes, can all (apart from the ones from Remark 5.1.8) be chosen from a single $\overline{\Psi}^*_i$ for either $i = 1$ or 2. Furthermore, if any factorization $\overline{\Psi}_i$ lifts over $\nu^3_{\leq j}$, so does $\overline{\Phi}_i$.*

Proof. The first property (1) states that the set of all twists whose lifts encircle a $\nu^{out} \cup \nu^3$-hole forms a partition of $\pi^{in} \cup \pi^1 \cup \pi^2$-holes. In particular, every partition needs a twist which contains π^{in}. If a partition is defined by $\overline{\Psi}^*$-twists, it consists of some $p^I_K \in \{p^i_k; k < n_i, i \in \{1, 2\}\}$ and some twists covering all π^I-holes which are not in p^I_K. Now, if there is a partition of less than $J_0 + 2$ parts, we can extend all its defining twists over all $\nu^{out} \cup \nu^3$. Indeed, this choice satisfies the second (2) and the third (3) property (when completed by some twists which do not contain any π-holes), and the lifted twists obviously come from a single $\overline{\Psi}^*_I$. If all partitions have more than $J_0 + 2$ parts, the second (2) property can never be satisfied and there is no positive factorization. Finally, if there is a partition of exactly $J_0 + 2$ parts, J_0 of them are necessarily shared by all $\nu^{out} \cup \nu^3$, to fulfill the third (3) property. Since around each π-hole there can be only one twist which does not contain π^{in}, the twists other than p^I_K are always shared by all $\nu^{out} \cup \nu^3$ and the partitions corresponding to different $\nu^3_{J_l}$-levels arise from splitting the p^I_K-part, which is possible only by $\overline{\Psi}^*_I$-twists.

Suppose now we are lifting $\overline{\Psi}_i \neq \overline{\Phi}_i$. At each level we are looking for partitions with the least possible parts (which has not yet been used at the previous levels). As long as the twists used in $\overline{\Psi}^*_i$-partitions agree with some $\overline{\Phi}^*_i$-twists, the two factorizations lift simultaneously. Otherwise, as soon as we need the largest (as a set) $p^i_k \neq f^i_k, k < k_i$, Lemma 5.1.6 tells that $\overline{\Phi}^*_i$ admits at least one more partition of at least one less part. Since by assumption $\overline{\Psi}_i$ lifts over $\nu^3_{\leq j}$, this $\overline{\Phi}^*_i$-partition has less than $j + 2$ parts, and can be used for all $\nu^3_{\geq j}$, fulfilling the properties. □

Remark 5.1.10. The concluding statement in Lemma 5.1.9 essentially means that we can focus only on $\overline{\Phi}$ as the most liftable among $\overline{\phi}$-factorizations, when looking for obstructions of positive factorization. Moreover, if we number the legs so that $-\frac{1}{q_1} > -\frac{1}{q_2}$, the $\overline{\Psi}_i$ in Lemma 5.1.9 can be $\overline{\Phi}_1$ (it lifts whenever any of $\overline{\Psi}_i$ lifts).

Lemma 5.1.11. *At the l^{th} level when $J_l < n_3$:*

(i) If there is a (not-yet-used) $\overline{\Phi}^*_1$-partition into less than $J_l + 2$ parts, the assumptions of the proposition are not satisfied.

(ii) If there is no (not-yet-used) $\overline{\Phi}_1^*$-partition into less than J_l+2 parts, and there are less than $|\nu^3_{J_l}|$ (or $|\nu^3_0|-1$ for $J_1=0$) of parallel $\overline{\Phi}_1^*$-partitions into J_l+2 parts, there is no positive factorization of ϕ.

(iii) Otherwise, we proceed to the next level.

Proof. Suppose that $\overline{\Phi}_1^*$ falls under (iii) for all levels up to l^{th}. At the l^{th} level, if there are only partitions of more than J_l+2 twists or there are less than $|\nu^3_{J_l}|$ of J_l+2-part partitions, there is no positive factorization; because we cannot satisfy the first (1) and the second (2) listed property simultaneously. On the other hand, when we can partition π-holes into less than J_l+2 parts, the structure does not fulfill our assumptions. Indeed, in Remark 5.2.2 we write out how the coefficients of two legs need to be related in order for corresponding rational numbers to add up to one. In our case, the J_l is the index of the unknot on L_3 with surgery coefficient less than -2, J_l-J_{l-1} counts the number of parallel twists, which is one more than number of -2-unknots preceding $-a^3_{J_l}$-unknot. For the levels up to l^{th}, the conditions of (iii) mean that the number of left-out holes exactly agrees with J_l-J_{l-1}, corresponding on L_1 to an unknot of coefficient $-J_l+J_{l-1}-2$, which is followed by exactly $|\nu^3_{J_l}|$ of -2-unknots. But condition (i) at the l^{th} level quit this sequence, having J_l-J_{l-1} parallel twists (so, $J_l-J_{l-1}-1$ of -2's on L_3) but leaving out less than J_l-J_{l-1} holes by the next a^1-unknot (its coefficient being at least $-J_l+J_{l-1}-1$). Since $J_l<n_3$ and we are considering only $\overline{\Phi}_1^*$-partitions, the two truncated chains correspond to rational numbers smaller than or equal to $-\frac{1}{q_i}$. □

The process eventually stops as we run into an obstruction for positive factorization (ii) or we leave the assumed conditions (i). If not before when we cross the n_3-level, as over that holes we are not allowed to extend more than n_3+2 twists – so, the only possible positive factorizations would arise from partitions into $n_3+2<J_l+2$ twists, which as before implies that the assumptions of the proposition are not satisfied. □

5.2 Surgery links of tight $S^1\times S^2$

Lemma 5.2.1. *Whenever $r_i+r_j\geq 1$, there is a sublink L_{ij} of the surgery presentation, as in Theorem 5.0.2, surgery along it smoothly describes $S^1\times S^2$.*

Proof. By basic calculus of continued fractions there exist truncated continued fractions $-\frac{1}{s_i}=[a^i_0,\dots,a^i_{m_i}]<[a^i_0,\dots,a^i_{k_i}]=-\frac{1}{r_i}$ $(m_i\leq k_i)$ such that $s_i+s_j=1$ (see [46, Lemma 3.2]).

The framed link L_{ij} smoothly consists of four -1-linked unknots with framing coefficients $0,0,-\frac{s_i+1}{s_i},-\frac{s_j+1}{s_j}$. Blowing-up once and applying inverse slam-dunks to rationally framed unknots, we obtain a chain of unknots with coefficients

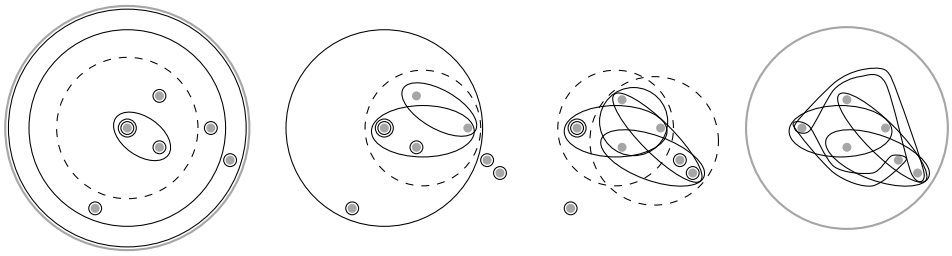

Figure 5.2: Example of positive factorization: $L_i = (-3,-3)$ and $L_j = (-2,-3,-2)$. On the first and the last picture the page is presented as a punctured disk with outer boundary in ν^{out} and one of ν_0^i, respectively. Intermediate steps are presented as punctured spheres.

$(-a^i_{m_i},\dots,-a^i_0,-1,-a^j_0,\dots,-a^j_{m_j})$, which can be successively, starting with the middle -1-surgery, blown-down ending in a 0-framed unknot. □

Remark 5.2.2. Notice that the two chains forming the two legs of L_{ij} need to be dual to each other (that is, describing a lens space and its orientation reversal). Explicitly, the coefficients of the two are related as follows (here, $-2^{\times b}$ means a chain of b-many -2-unknots):

$$\begin{array}{rcl} L_i & = & (-b_1-2, \quad -2^{\times b_2}, \quad -b_3-3, \quad \dots, \quad -b_m-2) \\ L_j & = & (-2^{\times b_1}, \quad -b_2-3, \quad -2^{\times b_3}, \quad \dots, \quad -2^{\times b_m}) \end{array} .$$

When looked in the presentation of Figure 4.1 middle, the first unknots of both chains are framed one lower, so $-b_1-3$ and -3 respectively.

Proposition 5.2.3 (Proposition 5.0.1)**.** *Contact surgery presentation by Legendrian link L_{ij} corresponds to the tight $S^1\times S^2$ if and only if all stabilizations on one leg are positive and all stabilizations on the other leg are negative.*

Proof. Necessity of the condition is a special case of Proposition 5.1.4. We prove here that it is also sufficient, describing concrete factorization.

Considering Legendrian link L_{ij} with all stabilizations on the i^{th} leg $L_i = (-a^i_0,\dots,-a^i_{m_i})$ negative and all stabilizations on the j^{th} leg $L_j = (-a^j_0,\dots,-a^j_{m_j})$ positive, all Dehn twists corresponding to the a^i-unknots lie outside the core circle N (along which the negative Dehn twist is performed) and the ones from the a^j-unknots lie inside. We can rewrite this monodromy by iterative use of the lantern relation as follows (look also at the example given by Figure 5.2).

In the following we use the b-notation in the sense of Remark 5.2.2.

One of the two legs, say L_j, starts in -2-unknots, say b_1 of them. In the first step we consider the associated b_1 parallel Dehn twists, a Dehn twist around the hole π_0^j responsible for stabilization of the first unknot in this chain, and b_1 stabilizations ν_0^i of a_0^i-unknot (one less than all if we have not reached the end

of L_i). We apply daisy relation on them (that is, a repeated lantern relation as described in [67, Lemma 3.5]). This pushes the negative twist N over b_1 stabilizations (the ν_0^i-holes) of a_0^i, and gives additional positive Dehn twist D_1 around all considered stabilization holes (the one π_0^j from a_0^j and b_1 of ν_0^i from a_0^i).

From now on, imagine the remaining ν_0^i-hole as the outer boundary of the disk. Now we take positive Dehn twist coming from the a_0^i and all of its parallel push-offs, there are b_2+1 of them where b_2 is the number of -2-unknots following a_0^i-unknot on L_i. Further, we take positive Dehn twist D_1 and all b_2+1 stabilization holes $\pi_{b_1}^j$ of $a_{b_1}^j$. We apply the daisy relation on them, resulting in a new negative twist N' around all considered holes, and a positive twist D_2 around considered holes which are not initially encircled by a_0^i. Concretely, the twist N' goes around the initial outer boundary ν^{out}, all stabilization holes ν^i of L_i (except one ν_0^i), and the first two levels stabilization holes of L_j (this is, $\pi_0^j \cup \pi_{b_1}^j$), while D_2 enlarges D_1 over the second level stabilization holes of L_j (containing $\pi_0^j \cup \nu_0^i \cup \pi_{b_1}^j$).

We continue by interchangeably applying daisy relation from inside (involving some a_k^j-twist) and from outside (involving some a_k^i-twist), interchangeably "pushing" the two negative twists N and N' over always the next level of L_i- or L_j-holes, respectively. (For the negative twist which arises through a single application of daisy relation we use the name of the negative twist which has been canceled through the same process.) At the same time, each application of daisy relation "enlarges" D_{l-1} into D_l, additionally encircling the next level of L_i- (for l odd) or L_j-holes (when l even). After the l^{th} application of daisy relation, the twists contain:

$$
\begin{aligned}
l = 2l'+1: \quad & D_l = \{\pi_0^j \cup \nu_0^i \cup \cdots \cup \pi^j_{\sum_{k=1}^{l'} b_{2k-1}+l'-1} \cup \nu^i_{\sum_{k=1}^{l'} b_{2k}+l'}\} \\
& N = \{\pi^{in} \cup \pi^j \cup \nu_0^i \cup \cdots \cup \nu^i_{\sum_{k=1}^{l'} b_{2k}+l'}\} \\
& N' = N' \text{ after } (l-1)^{\text{th}} \text{ step} \\
\\
l = 2l': \quad & D_l = \{\pi_0^j \cup \nu_0^i \cup \cdots \cup \nu^i_{\sum_{k=1}^{l'-1} b_{2k}+l'-1} \cup \pi^j_{\sum_{k=1}^{l'} b_{2k-1}+l'-1}\} \\
& N' = \{\nu^{out} \cup \nu^i \cup \pi_0^j \cdots \cup \pi^j_{\sum_{k=1}^{l'} b_{2k-1}+l'-1}\} \\
& N = N \text{ after } (l-1)^{\text{th}} \text{ step}
\end{aligned}
$$

In the last level there is one less stabilization hole of the a^j- (a^i-) unknot in comparison to the number of parallel twists from -2's ending L_i (L_j); when applying daisy relation we include also the initial outer (inner) boundary hole. So after the last step, D_m contains also the initial outer (inner) boundary and it cancels with the negative twist N' (N). While the other negative twist, N, N' respectively, encircles all the holes and it cancels with the positive Dehn twist along the current outer boundary. □

Proof of Theorem 5.0.2. Joining Proposition 5.1.4 and Proposition 5.2.3 we obtain the theorem. Indeed, Legendrian surgeries on tight $S^1 \times S^2$ (from Proposition 5.2.3) give Stein fillable structures, while all other presentations fall under the conditions of Proposition 5.1.4, thus they do not admit positive factorization of associated planar monodromy, and by that, do not admit any Stein filling. $\square$

Bibliography

[1] S. Akbulut, and B. Özbağcı, *Lefschetz fibrations on compact Stein surfaces*, Geom Topol. **5** (2001) 319–334.

[2] K. Baker, J. Etnyre, J. Van Horn-Morris, *Cabling, contact structures and mapping class monoids*, J. Differential Geom. **90** (2012) 1–80.

[3] J. Baldwin, *Capping off open books and the Ozsváth-Szabó contact invariant*, J. Symplectic Geom. **11** (2013) 525–561.

[4] I. Baykur, N. Monden, and J. Van Horn-Morris, *Positive factorizations of mapping classes*, Algebr. Geom. Topol. **17** (2017) 1527–1555.

[5] H. Choi, and J. Park, *A Lefschetz fibration structure on minimal symplectic fillings of a quotient surface singularity*, arXiv:1802.03304 [math.GT].

[6] V. Colin, E. Giroux, and K. Honda, *On the coarse classification of tight contact structures*, in Geometry and Topology of Manifolds, 109–120, Proc. Sympos. Pure Math. 71, Amer. Math. Soc., Providence, RI, 2003.

[7] F. Ding, and H. Geiges, *A Legendrian surgery presentation of contact 3-manifolds*, Proc. Cambridge Philos. Soc. **136** (2004) 583–598.

[8] F. Ding, and H. Geiges, *A unique decomposition theorem for tight contact 3-manifolds*, Enseign. Math. (2) **53** (2007) 333–345.

[9] F. Ding, and H. Geiges, *Handle moves in contact surgery diagrams*, J. Topol. **2** (2009) 105–122.

[10] F. Ding, H. Geiges, and A. Stipsicz, *Surgery diagrams for contact 3-manifolds*, Turkish J. Math. **28** (2004) 41–74.

[11] Y. Eliashberg, *Classification of overtwisted contact structures on 3-manifolds*, Invent. Math. **98** (1989) 623–637.

[12] Y. Eliashberg, *Filling by holomorphic disks and its applications*, Geometry of Low-Dimensional Manifolds: 2, Proc. Durham Symp. 1989, London Math. Soc. Lecture Notes, **151**, Cambridge Univ. Press, 1990, 45–67.

[13] Y. Eliashberg, *Topological characterization of Stein manifolds of dimension* > 2, International J. of Math. **1** (1990) 29–46.

[14] Y. Eliashberg, *Contact 3-manifolds twenty years since J. Martinet's work*, Ann. Inst. Fourier **42** (1992) 165–192.

[15] Y. Eliashberg, *Unique holomorphically fillable contact structure on the 3-torus*, Int. Math. Res. Not. **2** (1996) 77–82.

[16] Y. Eliashberg, *Few remarks about symplectic filling*, Geom. Topol. **8** (2004) 277–293.

[17] J. Epstein, D. Fuchs, and M. Meyer, *Chekanov-Eliashberg invariants and transverse approximate of Legendrian knots*, Pacific J. Math. **201** (2001), 89–106.

[18] J. Etnyre, *On symplectic fillings*, Algebr. Geom. Topol. **4** (2004) 73–80.

[19] J. Etnyre, *Planar open book decompositions and contact structures*, Int. Math. Res. Not **79** (2004) 4255–4267.

[20] J. Etnyre, and K. Honda, *Knots and contact geometry I. Torus knots and the figure-eight knot*, J. Symplectic Geom. **1** (2001), 63–120.

[21] J. Etnyre, and K. Honda, *Tight contact structures with no symplectic fillings*, Invent. Math. **148** (2002) 609–626.

[22] J. Etnyre, and J. Li, *The arc complex and contact geometry, non-destabilizable planar open book decompositions of the tight contact 3-sphere*, Int. Math. Res. Not. **2015** (2015) 1401–1420.

[23] J. Etnyre, and B. Özbağcı, *Invariants of contact structures from open books* Trans. Amer. Math. Soc. **360** (2008) 3133–3151.

[24] P. Ghiggini, *Strongly fillable contact 3-manifolds without Stein fillings*, Geom. Topol. **9** (2005) 1677–1687.

[25] P. Ghiggini, *Ozsváth-Szabó invariants and fillability of contact structures*, Math. Z. **253** (2006) 159–175.

[26] P. Ghiggini, *On tight contact structures with negative maximal twisting number on small Seifert manifolds*, Algebr. Geom. Topol. **8** (2008) 381–396.

[27] P. Ghiggini, M. Golla, and O. Plamenevskaya, *An obstruction to planarity of contact 3-manifolds*, arXiv:1708.04108 [math.SG].

[28] P. Ghiggini, K. Honda, and J. Van Horn-Morris, *The vanishing of the contact invariant in the presence of torsion*, arXiv:0706.1602 [math.GT].

[29] P. Ghiggini, P. Lisca, and A. Stipsicz, *Classification of tight contact structures on small Seifert 3-manifolds with $e_0 \geq 0$*, Proc. Amer. Math. Soc. **134** (2006) 909–916.

[30] P. Ghiggini, P. Lisca, and A. Stipsicz, *Tight contact structures on some small Seifert fibered 3-manifolds*, Amer. J. Math. **129**(**5**) (2007) 1403–1447.

[31] P. Ghiggini, and S. Schönenberger, *On the classification of tight contact structures*, in Geometry and Topology of Manifolds, 121–151, Proc. of Sympos. Pure Math. 71, Amer. Math. Soc., Providence, RI, 2003.

[32] P. Ghiggini, and J. Van Horn-Morris, *Tight contact structures on the Brieskorn spheres $-\Sigma(2,3,6n-1)$ and contact invariants*, J. Reine Angew. Math. **718** (2016) 1–24.

[33] E. Giroux, *Convexité en topologie de contact*, Comment. Math. Helv. **66** (1991) 637–677.

[34] E. Giroux, *Contact geometry: from dimension three to higher dimensions*, Proceedings of the International Congress of Mathematicians (Beijing 2002) 405–414.

[35] R. Gompf, *Handlebody construction of Stein surfaces*, Ann. of Math. **148** (1998) 619–693.

[36] R. Gompf, and A. Stipsicz, *4-manifolds and Kirby calculus*, Graduate Studies in Mathematics, vol. 20, American Math. Society, Providence 1999.

[37] K. Honda, *On the classification of tight contact structures I*, Geom. Topol. **4** (2000) 309–368.

[38] K. Honda, *On the classification of tight contact structures II*, J. Differential Geom. **55** (2000) 83–143.

[39] K. Honda, *Gluing tight contact structures*, Duke Math. J. **115**(**3**) (2002) 435–478.

[40] K. Honda, W. Kazez, and G. Matić, *Right-veering diffeomorphisms of compact surfaces with boundary*, Invent. Math. **169** (2007) 427–449.

[41] K. Honda, W. Kazez, and G. Matić, *On the contact class in Heegaard Floer homology*, J. Differential Geom. **83** (2009) 289–311.

[42] A. Juhász, *A survey of Heegaard Floer homology*, New Ideas in Low Dimensional Topology, World Scientific, 2014, 237–296.

[43] Y. Kanda, *The classification of tight contact structures on the 3-torus*, Comm. Anal. Geom. **5** (1997) 413–438.

[44] Ç. Karakurt, *Contact structures on plumbed 3-manifolds*, Kyoto J. Math. **54**(**2**) (2014) 271–294.

[45] Ç. Kutluhan, G. Matić, J. Van Horn-Morris, and A. Wand, *Filtering the Heegaard Floer contact invariant*, arXiv:1603.02673 [math.GT].

[46] A. Lecuona, and P. Lisca, *Stein fillable Seifert fibered 3–manifolds*, Algebr. Geom. Topol. **11** (2011) 625–642.

[47] T.-J. Li, and C. Y. Mak, *The Kodaira dimension of contact 3-manifolds and geography of symplectic fillings*, arXiv:1610.06870 [math.SG].

[48] P. Lisca, and G. Matić, *Tight contact structures and Seiberg-Witten invariants*, Invent. Math. **129** (1997) 509–525.

[49] P. Lisca, and A. Stipsicz, *Ozsváth-Szabó invariants and tight contact 3-manifolds I*, Geom. Topol. **8** (2004) 925–945.

[50] P. Lisca, and A. Stipsicz, *Ozsváth-Szabó invariants and tight contact 3-manifolds II*, J. Differential Geom. **75** (2007) 109–141.

[51] P. Lisca, and A. Stipsicz, *Ozsváth-Szabó invariants and tight contact 3-manifolds III*, J. Symplectic Geom. **5**(**4**) (2007) 357–384.

[52] P. Lisca, and A. Stipsicz, *On the existence of tight contact structures on Seifert fibered 3-manifolds*, Duke Math. J. **148**(**2**) (2009) 175–209.

[53] A. Loi, and R. Piergallini, *Compact Stein surfaces with boundary as branched covers of B^4*, Invent. Math. **143** (2001) 325–348.

[54] I. Matkovič, *Classification of tight contact structures on small Seifert fibered L-spaces*, Algebr. Geom. Topol. **18** (2018) 111–152.

[55] I. Matkovič, *Fillability of small Seifert fibered spaces*, arXiv:1608.00543 [math.GT].

[56] A. Némethi, *On the Ozsváth-Szabó invariant of nagative definite plumbed 3-manifolds*, Geom Topol. **9** (2005) 991–1042.

[57] A. Némethi, *Lattice cohomology of normal surface singularities*, Publ. of RIMS, Kyoto Univ. **44**(**2**) (2008), 507–543.

[58] B. Özbağcı, and A. Stipsicz, *Surgery on Contact 3-Manifolds and Stein Surfaces*, Bolyai Society Mathematical Studies **13**, Springer-Verlag, Berlin, 2004.

[59] P. Ozsváth, A. Stipsicz, and Z. Szabó, *Planar open books and Floer homology*, Int. Math. Res. Not. **54** (2005) 3385–3401.

[60] P. Ozsváth, and Z. Szabó, *On the Floer homology of plumbed three-manifolds*, Geom. Topol. **7** (2003) 185–224.

[61] P. Ozsváth, and Z. Szabó, *Holomorphic disks and topological invariants for closed three-manifolds*, Ann. of Math. **159** (2004), 1027–1158.

[62] P. Ozsváth, and Z. Szabó, *Holomorphic disks and three-manifold invariants: properties and applications*, Ann. of Math. **159** (2004), 1159–1245.

[63] P. Ozsváth, and Z. Szabó, *Holomorphic triangle invariants and the topology of symplectic four-manifolds*, Duke Math. J.**121** (2004) 1–34.

[64] P. Ozsváth, and Z. Szabó, *Heegaard Floer homologies and contact structures*, Duke Math. J. **129** (2005) 39–61.

[65] P. Ozsváth, and Z. Szabó, *Holomorphic triangles and invariants of smooth 4-manifolds*, Adv. Math. **202** (2006) 326–400.

[66] O. Plamenevskaya, *Contact structures with distinct Heegaard Floer invariants*, Math. Res. Lett. **11** (2004) 547–561.

[67] O. Plamenevskaya, and J. Van Horn-Morris, *Planar open books, monodromy factorizations and symplectic fillings*, Geom. Topol. **14** (2010) 2077–2101.

[68] S. Schönenberger, *Planar open books and symplectic fillings*, PhD thesis, University of Pennsylvania, 2005.

[69] A. Stipsicz, *Ozsváth-Szabó invariants and 3-dimensional contact topology*, Proceedings of the International Congress of Mathematicians, Hyderabad 2010, vol II, 1159–1178.

[70] W. Thurston, and H. Winkelnkemper, *On the existence of contact forms*, Proc. Amer. Math. Soc. **52** (1975), 345–347.

[71] I. Torisu, *Convex contact structures and fibered links in 3-manifolds*, Int. Math. Res. Not. **9** (2000) 441–454.

[72] A. Wand, *Tightness is preserved by Legendrian surgery*, Ann. of Math. **182** (2015) 723–738.

[73] A. Wand, *Factorizations of diffeomorphisms of compact surfaces with boundary*, Geom. Topol. **19** (2015) 2407–2464.

[74] C. Wendl, *Strongly fillable contact manifolds and J-holomorphic foliations*, Duke Math. J. **151** (2010) 337–384.

[75] H. Wu, *Legendrian vertical circles in small Seifert spaces*, Commun. Contemp. Math. **8** (2006) 219–246.

$$\infty = 0$$